MOLECULAR DOCKING ASSESSMENT OF THE ANTICANCER POTENTIAL OF PHYTOCONSTITUENTS OF *MORINGA OLEIFERA*, *OLEA EUROPAEA, BRASSICA OLERACEA, AND VITIS VINIFERA* AGAINST COLORECTAL CANCER

BY

NOSA-EDEGBE PRISCILLIA UWA

PHA1908541

DEPARTMENT OF PHARMACEUTICAL CHEMISTRY

FACULTY OF PHARMACY

UNIVERISTY OF BENIN

BENIN CITY

NOVEMBER 2025

MOLECULAR DOCKING ASSESSMENT OF THE ANTICANCER POTENTIAL OF PHYTOCONSTITUENTS OF *MORINGA OLEIFERA*, *OLEA EUROPAEA, BRASSICA OLERACEA,* AND *VITIS VINIFERA* AGAINST COLORECTAL CANCER.

BY

NOSA-EDEGBE PRISCILLIA UWA

PHA1908541

A DISSERTATION SUBMITTED TO THE DEPARTMENT OF PHARMACEUTICAL CHEMISTRY, FACULTY OF PHARMACY, UNIVERSITY OF BENIN, BENIN CITY IN PARTIAL FULFILMENT OF THE REQUIREMENT FOR THE AWARD OF DOCTOR OF PHARMACY DEGREE HONOURS IN PHARMACY

NOVEMBER 2025

CERTIFICATION

This is to certify that this work was done by Nosa-Edegbe Priscillia Uwa in the Department of Pharmaceutical Chemistry, Faculty of Pharmacy, University of Benin, Benin City, Nigeria in partial fulfilment of the requirement of the award of the Doctor of Pharmacy Degree (Pharm D)

_____ _____

Dr. U.M. OGBEIDE **Date**

Supervisor

_____ _____

Dr. Vincent Imieje **Date**

Head of Department

DEDICATION

This work is dedicated to God almighty, for His unfailing love and continuous supply of strength throughout my sojourn in this great citadel of learning, to the great friends I made along the way, and to my parents Pharm Dr. Nosa Edegbe and Mrs. Glory Edegbe for their support and care.

ACKNOWLEDGEMENT

My sincere gratitude goes to God almighty for His grace, mercies, love, provision and strength throughout the period of my project work.

I am also very grateful to my supervisor, Dr. U.M. Ogbeide whose understanding, patience, benevolence, friendliness, experience and wise decisions made the entire work a huge success. Words can never be enough to express my heartfelt gratitude to you sir, thank you and to my colleagues during this project work- Rock, Isaac, Regina and Kluvet, thanks for your support in making the work a success.

My special appreciation goes to every member of my family who supported, encouraged and provided for me; Pharm Dr. Nosa Edegbe and Mrs. Glory Edegbe, my siblings, my aunt, Dr. Gladys Agharese, for her unwavering support and my friends who have always been supportive through school.

I want to specially appreciate Pharm Dr. Paul Ijomah, Chief of the Oncology Pharmacy department, UBTH, for igniting my passion for cancer pharmacy and striving to provide healthcare solutions for this global and increasingly significant illness.

TABLE OF CONTENT

LIST OF TABLES

LIST OF FIGURES

LIST OF ABBREVIATIONS

2D: Two-dimensional

3D: Three-dimensional

ADME: Absorption, Distribution, Metabolism and Excretion

ADMET: Absorption, Distribution, Metabolism, Excretion and Toxicity

ASN: Asparagine

ASP: Aspartic acid

cAMP: Cyclic Adenosine Monophosphate

CSD: Cambridge Structural Database

DNA: Deoxyribonucleic Acid

FTDock: Fourier Transform Dock

GC-MS: Gas Chromatography- Mass Spectrometry

LD_{50}: Lethal Dose, 50%

PDB: Protein Data Bank

QSAR: Quantitative Structure Activity Relationship

RCSB: Research Collaboratory for Structural Bioinformatics

RNA: Ribonucleic Acid

SDF: Structure Data File

SER: Serine

THR: Threonine

TYR: Tyrosine

VAL: Valine

ABSTRACT

Colorectal cancer (CRC) remains a major global health challenge characterized by high incidence and mortality rates. Emerging evidence supports the use of plant-derived bioactive compounds as promising agents in cancer therapeutics. This study aimed to assess the anticancer potential of phytoconstituents from *Moringa oleifera*, *Olea europaea*, *Brassica oleracea*, and *Vitis vinifera* against key colorectal cancer protein targets using *in silico* methods. Phytochemical constituents from these plants were compiled from literature and chemical databases, with their three-dimensional structures retrieved from PubChem. Target proteins implicated in colorectal carcinogenesis, including Human Thymidylate Synthase enzyme, 1HVY, and epidermal growth factor receptor (EGFR), 1XKK, were prepared for docking using Biovia discovery studio. Molecular docking simulations were performed with AutoDock Vina in PyRx, evaluating binding affinities and ligand interactions at active sites. Post-docking analysis and ADMET predictions were done using Biovia discovery studio and ADMETLAB, respectively. This study reveals that *Moringa oleifera*, *Olea europaea*, *Brassica oleracea*, and *Vitis vinifera* had 18, 3, 18, 10 compounds respectively that has comparable binding affinities with the standards; regorafenib (-9 and -9.7 Kcal/mol), tipifarnib (-7 and -9 kcal/mol), osimertinib (-7.4 and -8.4 Kcal/mol),

capecitabine (-7.5 and -7.8 Kcal/mol) and tipiracil (-7.7 and -7.2 Kcal/mol) against 1XKK and 1HVY respectively. kaempferol, apigenin, genistein, flavonol, and pinosylvin demonstrated good ADME properties and low toxicity profiles. These compounds can serve as potential leads for anticancer agents and more *in silico* study as well as wet laboratory experiments are needed.

CHAPTER ONE

INTRODUCTION AND LITERATURE REVIEW

1.0 Colorectal Cancer

Colorectal cancer (CRC) is among the leading causes of cancer-related morbidity and mortality worldwide. It originates from the epithelial cells lining the colon or rectum and is characterized by uncontrolled cellular proliferation that can invade surrounding tissues and metastasize distant organs (Siegel *et al*., 2020). CRC accounts for approximately 10% of all cancer cases globally and ranks third in incidence and second in cancer-related deaths (Bray *et al*., 2018).

The pathogenesis of colorectal cancer is multifactorial, involving interactions between genetic predispositions, environmental factors such as diet and lifestyle, and molecular changes within cells, including mutations in oncogenes and tumor suppressor genes (Fearon & Vogelstein, 1990). The conventional therapeutic strategies for colorectal cancer include surgical resection, chemotherapy, radiotherapy, and targeted biological agents, yet challenges remain due to resistance, toxicity, and recurrence (Dekker *et al*., 2019).

1.1 Antineoplastics

Antineoplastic drugs, also known as anticancer agents, are medications used in the treatment of cancer by inhibiting the growth and spread of malignant tumors. The primary goal of antineoplastics is to kill or control cancer cells while minimizing damage to normal cells. These

drugs can be classified broadly into chemotherapy agents, targeted therapies, immunotherapies, and hormonal therapies.

In colorectal cancer treatment, chemotherapy remains a foundational approach, often involving drugs such as 5-fluorouracil (5-FU), capecitabine (an oral prodrug of 5-FU), irinotecan, and oxaliplatin. These drugs interfere with DNA synthesis, repair, or mitosis, thereby inhibiting cancer cell proliferation. Combination regimens—like FOLFOX (5-FU, leucovorin, oxaliplatin) and FOLFIRI (5-FU, leucovorin, irinotecan)—are routinely used to enhance therapeutic efficacy.

1.2 Mechanism of Antineoplastics

Antineoplastic drugs are commonly classified based on their mechanism of action.

1. Alkylating Agents

   These drugs form covalent bonds with DNA bases, particularly guanine, causing DNA cross-linking and strand breakage. This damages the DNA, impairs replication and transcription, and induces apoptosis. Examples include nitrogen mustards (cyclophosphamide), platinum compounds (cisplatin, oxaliplatin), and nitrosoureas. Alkylating agents are cell-cycles and can affect cells in all phases.

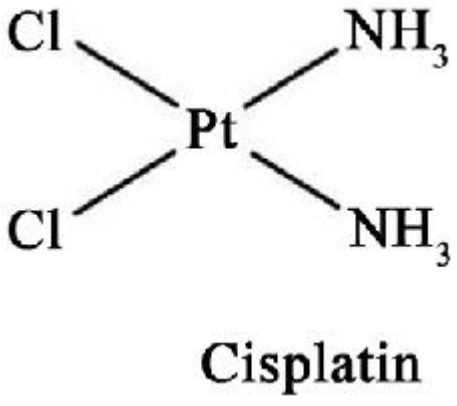

Fig. 1.1: Cisplatin.

2. Antimetabolites

Antimetabolites structurally resemble natural nucleotides or cofactors and interfere with DNA and RNA synthesis by inhibiting key enzymes or becoming incorporated into nucleic acids causing faulty replication. For instance, folate analogs like methotrexate inhibit dihydrofolate reductase, and pyrimidine analogs like 5-fluorouracil inhibit thymidylate synthase. These agents are mostly S-phase specific.

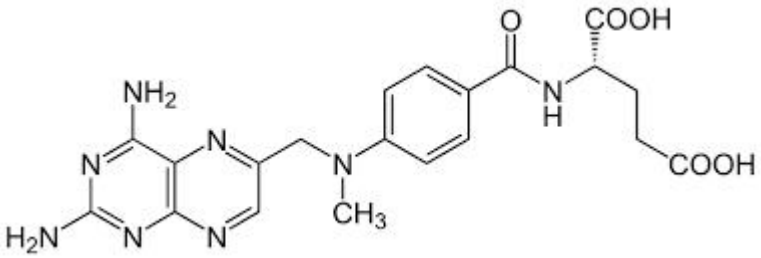

Fig 1.2: Methotrexate.

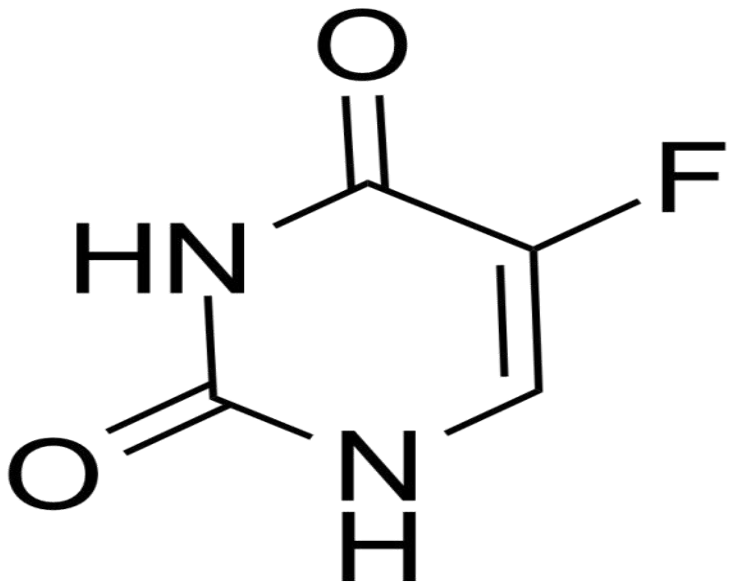

Fig 1.3: 5-fluorouracil.

3. Topoisomerase Inhibitors

These interfere with topoisomerase enzymes needed for DNA unwinding, which is vital for replication and transcription. Topoisomerase I inhibitors (irinotecan, topotecan) and II inhibitors (etoposide) stabilize the DNA-enzyme complex after strand cleavage, preventing re-ligation and causing DNA breaks.

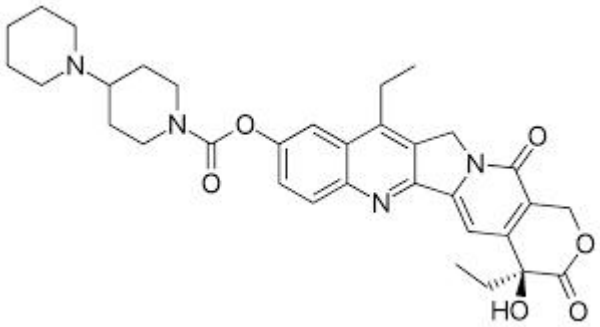

Fig 1.4: Irinotecan.

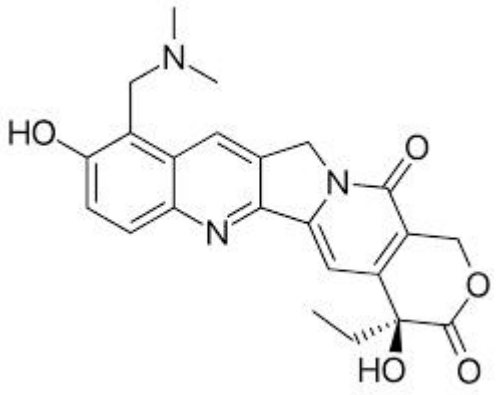

Fig 1.5: Topotecan.

4. Antitumor Antibiotics

Derived from microorganisms, these intercalate into DNA, generate free radicals, or inhibit DNA/RNA synthesis, leading to DNA damage and apoptosis. Doxorubicin and bleomycin are examples. Effects can include cardiotoxicity or pulmonary toxicity.

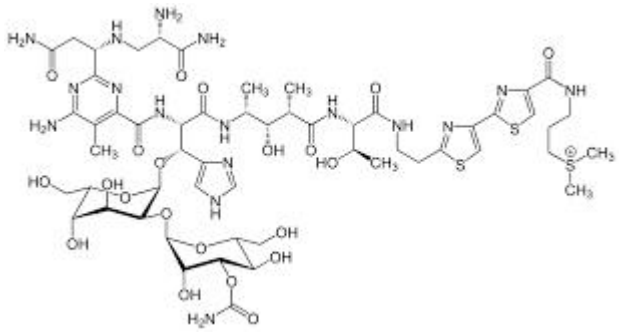

Fig 1.6: Bleomycin.

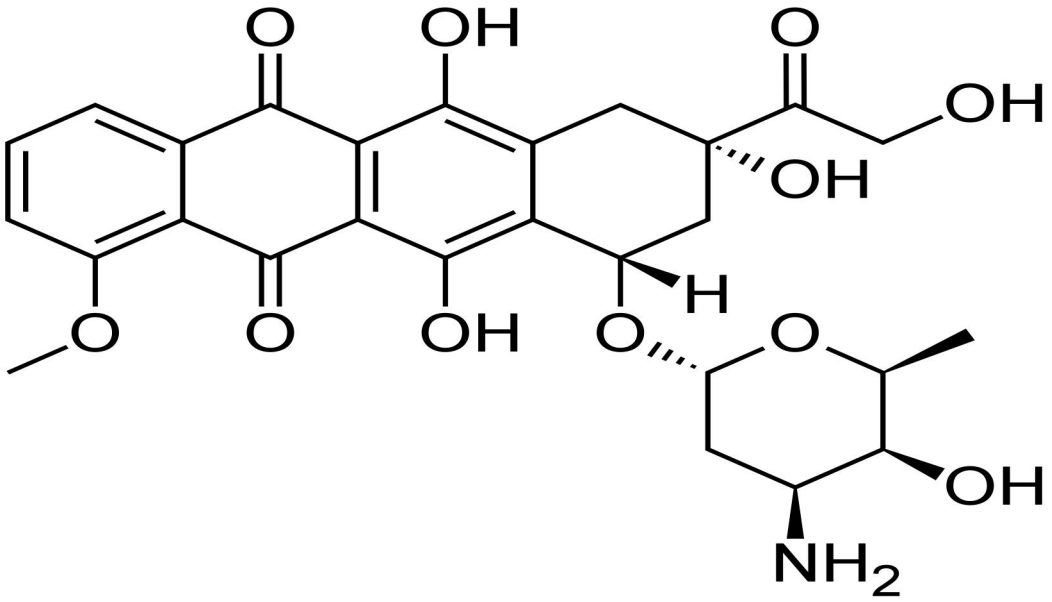

Fig 1.7: Doxorubicin.

5. Mitotic Inhibitors (Plant Alkaloids)

Drugs like vincristine and paclitaxel target microtubules, essential for chromosome segregation during mitosis. Vincristine disrupts microtubule polymerization leading to metaphase arrest, while paclitaxel stabilizes microtubules, preventing their disassem**bly.**

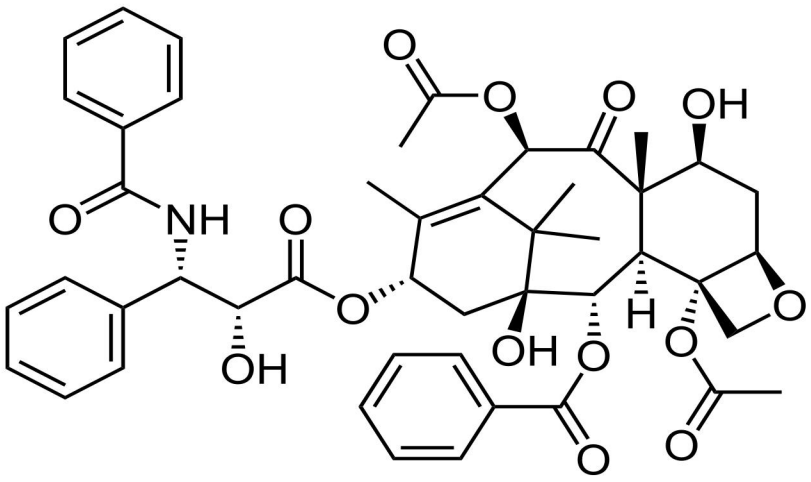

Fig 1.8: Paclitaxel.

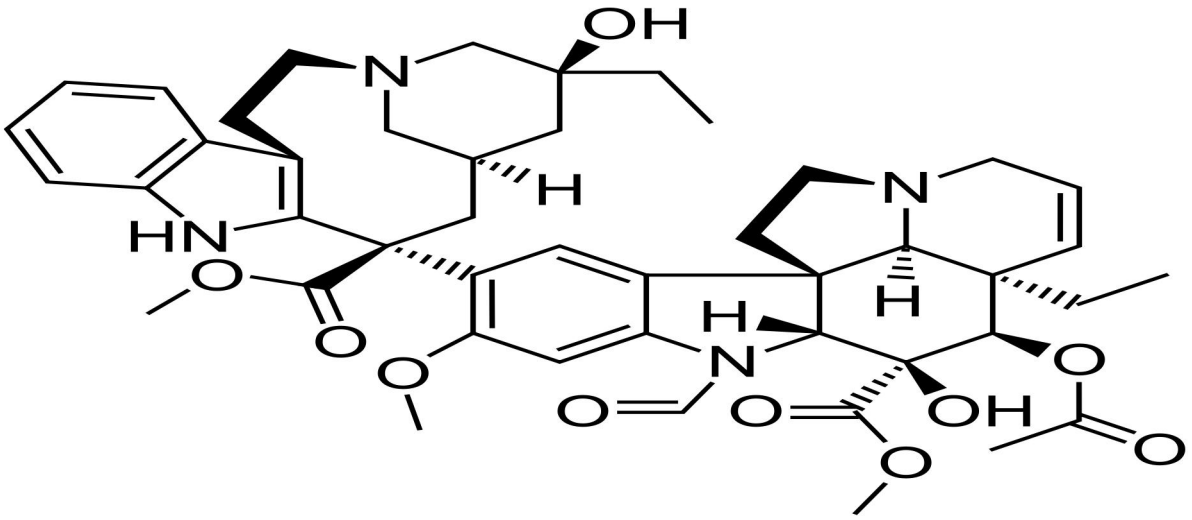

Fig 1.9: Vincristine.

6. Hormonal Agents

   Used mainly in hormone-sensitive cancers, they block hormone receptors or inhibit synthesis of hormones essential for tumor growth (e.g., tamoxifen as an estrogen receptor antagonist).

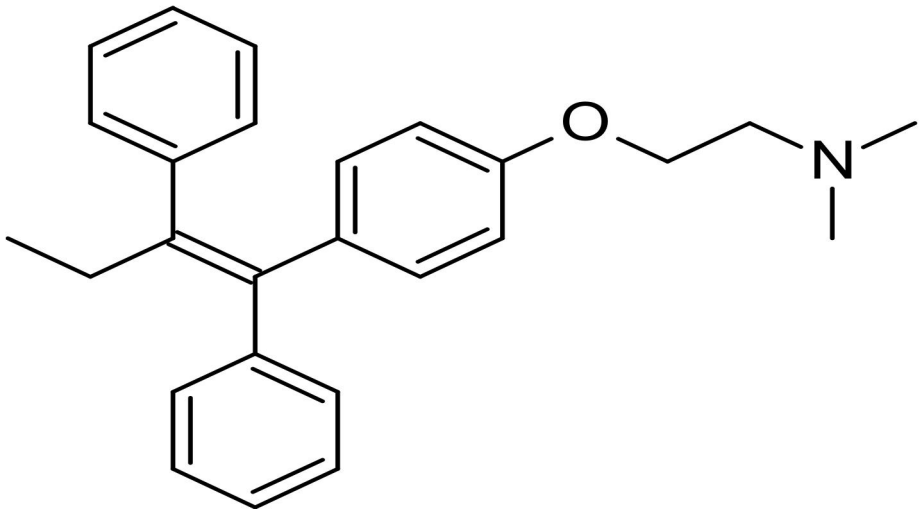

Fig 1.10: Tamoxifen.

7. Signal Transduction Inhibitors and Targeted Therapies

   These inhibit overexpressed or mutated receptors (e.g., EGFR, VEGFR), kinases or other proteins involved in growth signaling, angiogenesis, or cell survival pathways. Examples include tyrosine kinase inhibitors and monoclonal antibodies.

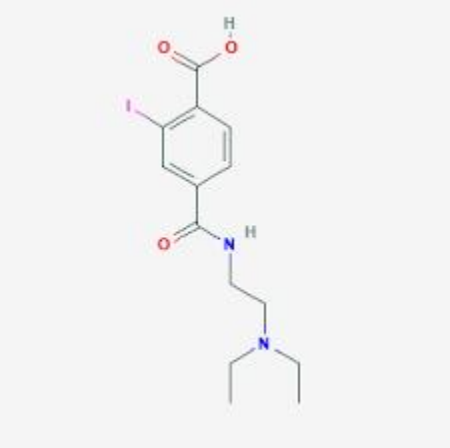

Fig 1.11: Bevacizumab, a monoclonal antibody.

The cell cycle specificity divides drugs into phase-specific agents (targeting S or M phase) and phase-nonspecific agents (acting throughout cell cycle). This classification helps optimize combination regimens for maximum cancer cell kill.

1.3 Role of Natural Products in Colorectal Cancer Management

Natural products, particularly those derived from plants, have gained significant attention as potential sources of novel anticancer compounds due to their structural diversity and bioactivity (Newman & Cragg, 2020). Phytochemicals exhibit varied mechanisms including induction of apoptosis, inhibition of cell proliferation, angiogenesis modulation, and antioxidative effects (Kwak *et al*., 2011). Recent research has emphasized identifying bioactive compounds in medicinal plants that can serve as lead molecules for anticancer drug development.

1.4 In Silico Approaches in Drug Discovery for Colorectal Cancer

In silico drug discovery, including molecular docking, virtual screening, and ADMET prediction, has revolutionized the early stages of drug development (Sliwoski *et al*., 2014). Molecular

docking evaluates the binding affinity of potential ligands with target proteins crucial to disease progression, enabling high-throughput screening and rational drug design (Meng *et al*., 2011). *In silico* studies reduces cost and time, guiding experimental validation and optimization of candidate molecules (Lionta *et al*., 2014).

1.5 Selected Medicinal Plants with Potential Anti-Colorectal Cancer Activity

This study focuses on five medicinal plants that possess promising bioactive compounds with potential anticancer effects against colorectal cancer: *Moringa oleifera*, *Olea europaea* (common olive), *Brassica oleracea* (wild cabbage), *Musa acuminata* (dwarf banana), and *Vitis vinifera* (wine grape). The botanical names are used throughout for scientific precision.

1.5.1 *Moringa oleifera* (Lam) Fabaceae

Moringa is a fast-growing tree native to the Indian subcontinent widely cultivated for its nutritional and medicinal properties (Leone *et al*., 2015). It is known as 'Barambo' in Hausa, 'Odudu Oyibo' in Igbo and 'Ewele' in Yoruba. The plant is utilized widely among these different ethnic groups in Nigeria; the leaf, seed, flowers and the stem and root barks of Moringa are used as food, tea and medicine. The moringa tree is a fast-growing, drought-resistant tree with feathery, compound leaves, scented white flowers, and long, angled, drumstick-like fruits. Its leaves, seeds, and roots have been extensively studied for anticancer activities, showing promise due to phytoconstituents such as glucosinolates, isothiocyanates, flavonoids, and phenolic acids (Sreelatha & Padma, 2011). Reports highlight its capacity to induce apoptosis and inhibit proliferation in colon cancer cell lines (Tiloke *et al*., 2013).

Fig 1.12: Moringa Pods

Fig 1.13: Moringa Leaves

Fig 1.14: Moringa Roots

Fig 1.15: Moringa Stem

1.5.1.1 Trado Medicinal Uses *of Moringa oleifera*

The abundant bioactive and nutritional properties of this plant make it useful in many and diverse areas of life, including the health, cosmetic, agricultural, and food industries to mention but a few. Research has found that the presence of proteins, carbohydrates, lipids, vitamins, minerals, flavonoids, phenols, alkaloids, fatty acids, saponins, essential oils, folate, aromatic hydrocarbons, sterols, glucosinolates, and glycosides, among others, characterize the moringa nutrient profile and, as a result, give rise to its remedial effects on ailments such as wounds, stomach and duodenal ulcers, allergies, obesity, diabetes, inflammation, asthma (Great Iruoghene Edo *et al*. 2023).

Table 1.1 Trado Medicinal Uses of *Moringa oleifera*

PLANT PARTS	USES	REFERENCE
Leaves	Used for treating asthma, bronchitis, hyperglycemia, dyslipidemia, flu, heart burn, syphilis, malaria, pneumonia, diarrhea, headaches, scurvy, skin diseases, eye and ear infections; reduces blood pressure and cholesterol; anticancer, antimicrobial, antioxidant, antidiabetic, antiatherosclerotic; neuroprotectant; beneficial for digestion, bone health, and wound healing	Abalaka M.E. *et al*. The antibacterial evaluation of *Moringa oleifera* leaf extracts on selected bacterial pathogens. Journal of Microbiology Research. 2012;2(2):1–4. .

Seeds	Treat hyperthyroidism, Crohn's disease, antiherpes virus, arthritis, rheumatism, gout, cramp, epilepsy, sexually transmitted diseases; antimicrobial, anti-inflammatory; boost immunity, regulate blood sugar, aid digestion	Abd Rani N. Z. *et al*. Moringa genus: a review of phytochemistry and pharmacology. Frontiers in Pharmacology. 2018
Root bark	Cardiac stimulant, antiulcer, anti-inflammatory; treat kidney stones, liver diseases, inflammation, ulcers, ear and tooth pain; antibiotic properties	Gopalakrishnan L.*et al*, Moringa oleifera: A review on nutritive importance and its medicinal application. Food Science and Human Wellness. 2016;5(2):49–56.
Seed oil	Used for skin wounds healing, hair health improvement, antioxidant	Olagbemide P. *et al*, Proximate analysis and chemical composition of raw and defatted *Moringa oleifera* kernel. Advances in Life Science and Technology. 2014;24:92–99.
Bark	Treat wounds, skin infections; antibiotic properties; used in animal fodder and fencing	Rani N. *et al*. Moringa genus: a review of phytochemistry and pharmacology. Frontiers in Pharmacology. 2018

Moringa oleifera holds significant traditional medicinal value around the world, often referred to as the "miracle tree" or "tree of life" due to its wide-ranging therapeutic uses in folk medicine and Ayurveda. Nearly all parts of the plant—leaves, pods, seeds, bark, roots, flowers, gum, and seed oil—have been used to treat various ailments. Its leaves are used to improve general health, treat insomnia, wounds, and inflammatory conditions such as glandular inflammation, headaches, and bronchitis.

They have been used to improve nutrition for infants and lactating mothers and as a remedy for diabetes and infections. The pods are traditionally employed to treat hepatitis, relieve joint pain, and manage digestive issues like diarrhea. The seeds are **u**sed as a laxative and treatment for tumors, prostate and bladder problems, arthritis, and to purify water. The bark is applied to treat ulcers, wounds, skin infections, hypertension, and toothache. The roots are used for kidney stones, liver diseases, inflammation, ulcers, ear and tooth pain, and even paralysis. The flowers are used traditionally to treat ulcers, splenic enlargement, and serve as an aphrodisiac. Gum from the tree bark is used for fever reduction and to induce abortion in traditional medicine. The seed oil is utilized for skin wound healing, skin and hair care.

Ancient Ayurvedic texts such as Charaka Samhita and Ashtanga Hridaya mention moringa for treating worms, headaches, asthma, ear conditions, puerperal disorders, and conjunctivitis.

1.5.1.2 Phytochemical Constituents of *Moringa oleifera*

Moringa oleifera is rich in diverse phytochemical constituents that contribute to its nutritional and medicinal properties. Major phytochemical constituents include**;**

Table 1.2 Phytochemical Constituents of *Moringa oleifera*

Plant Part	Phytochemical Constituents	Specific Compounds	Biological Significance
Leaves	Flavonoids, phenolic acids, alkaloids, saponins, tannins, glucosinolates, isothiocyanates, carotenoids, vitamins	Quercetin, kaempferol, apigenin, luteolin, myricetin, chlorogenic acid, gallic acid, ferulic acid, coumaric acid, β-carotene, vitamin A, vitamin C	Antioxidant, anti-inflammatory, antimicrobial, antidiabetic, anticancer, hepatoprotective, nutritional source of vitamins and minerals
Seeds	Proteins, antimicrobial peptides, essential and nonessential amino acids	Chitin-binding proteins, flocculant proteins	Antimicrobial, water purification, antioxidant
Roots & Bark	Terpenoids, alkaloids, tannins, steroidal aglycones, reducing sugars	Various bioactive compounds	Anti-fertility, anti-urolithiatic, traditional medicine uses

Plant Part	Phytochemical Constituents	Specific Compounds	Biological Significance
Flowers & Fruits	Flavonoids, antioxidants	Not specified	Anti-inflammatory, antimicrobial

1.5.2 *Olea europaea* (Linn) Oleaceae

Olea europaea commonly called common olive is an evergreen tree native to the Eastern Mediterranean region, with its origin likely in the area of modern-day Turkey and Syria, or the broader Levant region. Common characteristics include silvery-green, lance-shaped foliage, a gnarled trunk, and the production of small, creamy-white flowers and green to purplish-black olives, which are botanically drupes. The tree has evergreen, silvery-green to gray-green leaves that are lance-shaped and typically 2-3 inches long. The underside of the leaves is silvery. Olive trees are slow-growing and can develop into either a tree or a shrub, with a gnarled trunk and a rounded crown as they mature. It has small, fragrant, creamy-white flowers which appear in clusters on the tree. The fruits, known as olives, start green and ripen to a dark purple or black. Botanically, the olive is a drupe. The young olive tree bark is smooth and gray, becoming rougher, more textured, and darker with age.

The plant has well-documented antioxidant and anticancer effects, largely attributed to polyphenolic compounds like oleuropein, hydroxytyrosol, and oleocanthal (Gonçalves *et al*., 2015). These compounds are known to modulate pathways involved in carcinogenesis, including inflammation and oxidative stress, with studies demonstrating inhibition of colorectal cancer cell growth (Benavente-García & Castillo, 2008).

Fig 1.16: Olive tree

Fig 1.17: Fruit

Fig 1.18: Leaves and fruit

1.5.2.1 Trado Medicinal Uses *of Olea europaea*

The olive tree (*Olea europaea*) has extensive traditional medicinal uses across various cultures. Its leaves, fruits, seeds, bark, and oil are used to treat a wide range of ailments. Leaves and fruit infusions are taken to manage diabetes, hypertension, diarrhea, and respiratory as well as urinary tract infections. Olive oil mixed with lemon juice is traditionally used to treat gallstones. Olive leaf extracts serve as hypotensive, diuretic, and anti-inflammatory agents, while the seed oil is used as a laxative and for inflammation relief. The oil is also applied externally to prevent hair loss, soothe fractured limbs, and heal skin conditions. Additionally, the bark is utilized in some African traditional medicines for urinary problems and parasitic infections. Overall, *Olea europaea* holds significant value in traditional medicine for its antimicrobial, anti-inflammatory, antihypertensive, hypoglycemic, and wound-healing properties.

Table 1.3 **Trado Medicinal Uses of *Olea europaea***

PLANT PART	USES	REFERENCES
Leaves and Fruits (infusions, decoctions)	Hypoglycemic, hypotensive, antidiabetic, anti-inflammatory, tonic, antibacterial, used for respiratory and urinary infections, diarrhea, eye infections, sore throat, gout, hemorrhoids, rheumatism, vasodilator, antipyretic	De Oliveira *et al*. (2025) [Frontiers Microbiology]
Olive oil	Laxative, treatment for gallstones (with lemon juice), skin emollient, wound healing, burn and rheumatism treatment, hair loss prevention, applied on fractured limbs	Gagour J. *et al*. A Review of Recent Progresses on Olive Oil Chemical Profiling, Extraction Technology, Shelf-Life, and Quality Control. Chem. Biodivers. 2024;21:e202301697
Bark	Febrifuge, astringent, used for tapeworm infestation, eye illnesses, itchy rashes, headache, bladder	Trigui *et al*. (2023)

	infections, bone setting (fractures)	
Seeds and seed oil	Laxative (oral), anti-inflammatory balm (topical)	Ghanbari R. *et al*. Valuable nutrients and functional bioactives in different parts of olive (*Olea europaea* L.)—a review. International Journal of Molecular Sciences. 2012;13(3):3291–3340.
Fresh leaves (boiled extracts)	Treatment of asthma, hypertension, diuresis	Nicolì F. *et al*. Evaluation of Phytochemical and Antioxidant Properties of 15 Italian *Olea europaea* L. Cultivar Leaves. Molecules. 2019;24:1998.
Leaf infusions	Diuretic, antipyretic, anti-inflammatory, eye infection treatment, sore throat relief	Hannachi H *et al*. Chemical Profiles and Antioxidant Activities of Leaf, Pulp, and Stone of Cultivated and Wild Olive Trees (*Olea europaea* L.) Int. J. Fruit Sci. 2020;20:350–370.
Roots	Treatment of malaria, helminthiasis, retained afterbirth, mental illness, cancer (root bark)	Mahmoud A. *et al*. Overall *in vitro, in vivo*, and *in silico* evaluation of *Olea europaea* and *Ficus carica* leaf extracts for antimicrobial activity against multidrug-resistant pathogens. [Frontiers Microbiology] 2025.
Fruit infusion	Treatment of bloody diarrhea, skin cleanser	Muhammad H.*et al*. Traditional Uses, Phytochemistry, and

1.5.2.2 Phytochemical Constituents of *Olea europaea*

Olea europaea (olive tree) contains rich polyphenols, secoiridoids, flavonoids, phenolic acids, lignans, and triterpenoids mainly found in leaves, fruits, seeds, bark, stems, and flowers. Oleuropein and hydroxytyrosol are key compounds known for their antioxidant, anti-inflammatory, antimicrobial, cardioprotective, antidiabetic, and anticancer activities. Olive fruits contribute important fatty acids and vitamins supporting heart and skin health. The diverse phytochemicals in *Olea europaea* promote overall health by protecting against oxidative damage, inflammation, infections, and chronic diseases. Major phytochemical constituents include;

Table 1.4 Phytochemical Constituents of *Olea europaea*

Plant Part	Phytochemical Constituents	Specific Compounds	Biological Significance
Leaves	Polyphenols, secoiridoids, flavonoids, phenolic acids, lignans, triterpenoids, essential oils	Oleuropein, hydroxytyrosol, tyrosol, luteolin, apigenin, quercetin, verbascoside, ursolic acid, maslinic acid, oleanolic acid	Antioxidant, anti-inflammatory, antimicrobial, cardioprotective, antidiabetic, anticancer, immunomodulatory
Fruits	Phenolic compounds, fatty acids, tocopherols, carotenoids, volatile compounds	Oleuropein, hydroxytyrosol, tyrosol, oleocanthal, caffeic acid, gallic acid, linoleic acid, oleic acid, β-carotene, δ/γ/α-tocopherol	Anti-inflammatory, antioxidant, antimicrobial, cardiovascular benefits, skin protective
Seeds	Proteins, minerals, fatty acids	Albumin, globulin, oleuropein, ligstroside	Nutritional source of fatty acids, antioxidant, antimicrobial effects
Bark	Lignans, coumarins, phenolic compounds	Oleuropein, olivil, pinoresinol, esculetin, scopoletin	Antimicrobial, anti-inflammatory, antioxidant activities

Plant Part	Phytochemical Constituents	Specific Compounds	Biological Significance
Stems & Branches	Phenolic compounds, triterpenoids	Oleuropein, erythrodiol, maslinic acid, oleanolic acid, taxifolin	Antioxidant, anti-inflammatory, antimicrobial
Flowers	Polyphenols	Various phenolics	Contribute to antioxidant and antimicrobial properties

1.5.3 *Brassica oleracea* (Linn) Brassicaceae

Brassica oleracea is a herbaceous plant originating from wild plants on the rocky coastal cliffs of the Mediterranean and Atlantic coasts of Europe, including Southern Britain. This wild ancestor, also known as wild cabbage, is a perennial herb found in cool, damp coastal habitats and was domesticated by ancient civilizations into the numerous vegetable forms we know today, such as cabbage, kale, and broccoli. It has fleshy, glaucous leaves that are usually petiolate and lobed with a large terminal segment. The flowers are bright yellow and grow in racemes. It grows on coastal cliffs, particularly limestone cliffs, and is salt-tolerant. Over thousands of years, humans selected and propagated these wild plants for different traits, leading to the vast diversity of modern cultivars like cabbage, kale, broccoli, and cauliflower.

Evidence suggests domestication began in ancient Egypt and the Roman Empire, with the earliest records describing various types used for medicinal purposes before becoming established as garden vegetables. It is known locally in Nigeria as "kabeji". The plant contains metabolites such as glucosinolates and isothiocyanates known for their chemopreventive potential (Traka & Mithen, 2009). These metabolites can induce phase II detoxification enzymes and apoptosis in cancer cells, including colorectal tumor cells (Herr & Büchler, 2010). Wild cabbage phytochemicals hold promise as modulators of carcinogen metabolism.

Fig 1.19:*Brassica oleracaea* leaves

Fig 1.20: *Brassica oleracaea* fruit

1.5.3.1 Trado Medicinal Uses of *Brassica oleracea*

The plant has been traditionally used in medicine for a variety of health benefits. Different parts of the plant, including leaves, seeds, and whole plant extracts, contain important phytochemicals such as flavonoids, glucosinolates, phenolics, and anthocyanins. These compounds contribute to its well-documented biological activities, including anti-inflammatory, antioxidant, anticancer, antibacterial, and hepatoprotective effects. Brassica vegetables are valued for their roles in immune stimulation, cancer chemoprevention, and metabolic health, making *Brassica oleracea* both a nutritious food and a medicinal resource with extensive applications. These tradomedicinal uses are outlined below.

Table 1.5 Trado Medicinal Uses of *Brassica oleracea*

Plant Part	Traditional Medicinal Uses	References
Leaves	Used topically to treat minor skin infections, mastitis, edema, and as anti-inflammatory for wounds; also used to soothe swollen feet, relieve fevers, and reduce childhood croup symptoms.	Kapusta-Duch *et al*., 2025. "The compositions, characteristics, health benefits and applications of Brassica crops." Frontiers in Plant Science.
Juice (Leaf juice)	Used for alleviating constipation, as a laxative, and to treat mushroom poisoning.	Kapusta-Duch *et al*., 2025. "The compositions, characteristics, health benefits and applications of Brassica crops." Frontiers in Plant Science.
Whole plant extract	Used for anti-inflammatory, analgesic, antioxidant purposes; taken orally or applied topically to reduce inflammation and pain.	Kapusta-Duch *et al*., 2025. "The compositions, characteristics, health benefits and applications of Brassica crops." Frontiers in Plant Science.
Cabbage leaves	Applied to the skin to accelerate healing of wounds and reduce inflammation and pain.	Kapusta-Duch *et al*., 2025. "The compositions, characteristics, health benefits and applications of

Plant Part	Traditional Medicinal Uses	References
(wraps)		Brassica crops." Frontiers in Plant Science.
Seeds	Traditionally used for their antioxidant properties and possible anticancer benefits.	Kapusta-Duch *et al*., 2025. "The compositions, characteristics, health benefits and applications of Brassica crops." Frontiers in Plant Science.

1.5.3.2 Phytochemical Constituents of *Brassica oleracea*

The plant is rich in diverse phytochemicals that contribute to its significant health benefits. Key constituents include flavonoids (such as kaempferol and quercetin), phenolic acids (like gallic acid and chlorogenic acid), glucosinolates, alkaloids, saponins, terpenoids, and tannins. These compounds exhibit potent antioxidant, anti-inflammatory, antimicrobial, and anticancer properties. The various phytochemical constituents, plant parts in which they are found, as well as their biological significance are outlined below.

Table 1.6 Phytochemical Constituents of *Brassica oleracea*

Plant Part	Phytochemical Constituents	Specific Compounds	Biological Significance
Leaves	Flavonoids, phenols, tannins, glucosinolates, alkaloids, saponins	Quercetin, kaempferol derivatives, sinapoylgentiobiose isomers, sinapoylglucose isomers, sinapoylcholine	Antioxidant, anti-inflammatory, antimicrobial, UV protection, anticancer
Florets	Flavonoids, polyphenols, glucosinolates	Sulforaphane, sinigrin, chlorogenic acid, caffeic acid	Antioxidant, antiproliferative, anticancer
Seeds	Fatty acids, flavonoids, glucosinolates, alkaloids	9-Octadecenamide, hexadecane, glucosinolates	Antimicrobial, antioxidant, cytotoxic effects

1.5.4 *Vitis vinifera* (Wine Grape)

Vitis vinifera L., Vitaceae family, also known as the common grape vine, is a vigorous, woody, deciduous tendril climber native to the Mediterranean Region, Central Europe, and Southwestern Asia. It is characterized by lobed bright green leaves, and bears clusters of small fruits (grapes) in the summer which can be eaten fresh or dried into raisins, sultanas, and currants.

. The species is known for its wide diversity of cultivated varieties, which are the basis for most of the world's wines. The wild ancestor, Vitis sylvestris, also called the wild grapevine, is found in the same regions. The plant is cultivated globally for grapes used in wine and for fresh consumption. It is rich in resveratrol, flavonoids, and anthocyanins that exhibit antioxidant, anti-inflammatory, and anticancer activities (Baur & Sinclair, 2006). Resveratrol, notably, has demonstrated the ability to inhibit proliferation of colorectal cancer cells and modulate signaling pathways such as Wnt/β-catenin involved in tumorigenesis (Popat *et al*., 2013).

Fig 1.21: *Vitis vinifera* Leaves and stem

Fig 1.22: *Vitis vinifera* Leaves

Fig 1.23: *Vitis vinifera* Leaves and fruit

1.5.4.1 Trado Medicinal Uses of *Vitis vinifera*

Vitis vinifera has a long-established role in traditional medicine across many cultures, primarily for vascular conditions like varicose veins and haemorrhoids, respiratory ailments, digestive disorders, and skin health. Preparations made from leaves, fruits, seeds, and flowers are widely used, exhibiting mainly antioxidant, anti-inflammatory, diuretic, and circulatory benefits. These tradomedicinal uses are outlined below**.**

Table 1.7 Trado Medicinal Uses of *Vitis vinifera*

Plant Part / Preparation	Traditional Medicinal Uses	References
Leaves	Used for venous diseases including varicose veins, haemorrhoids; astringent, diuretic, vasoprotective; relief of heavy legs, calf cramps	Valli Kanagarla *et al*., 2013. Traditional use of grape leaves and seeds in herbal medicine for antioxidant, antimicrobial, and antiviral activities.
Fruits (grape)	Laxative, diuretic, restorative, treatment for anemia, cough, respiratory infections, cold and flu; antioxidant and anti-inflammatory	Kalem *et al*., 2021. Review covering traditional uses of grapes for blood disorders, respiratory illnesses, allergy, wound care, digestive issues, varicose

Plant Part / Preparation	Traditional Medicinal Uses	References
		veins, and antiseptic properties.
Seeds	Hypolipidemic, antioxidant, anti-inflammatory, antimicrobial; used for skin disorders and as cosmetic raw material	Valli Kanagarla *et al*., 2013. Traditional use of grape leaves and seeds in herbal medicine for antioxidant, antimicrobial, and antiviral activities.
Flowers	Used as expectorant, haematinic; treatment for bronchitis and other respiratory ailments	Valli Kanagarla *et al*., 2013, A review on benefits and uses of Vitis vinifera (Grape)

Plant Part / Preparation	Traditional Medicinal Uses	References
Stem ashes	Used in traditional remedies for joint pain, swelling, piles	Jose Gilberto *et al*. 2025, A recent review on the traditional use, phytochemical constituents, and pharmacological activity of Vitis vinifera L. (Vitaceae)
Leaves juice	Eye bath, diuretic	Valli Kanagarla *et al*., 2013. Traditional use of grape leaves and seeds in herbal medicine for antioxidant, antimicrobial, and antiviral activities

1.5.4.2 Phytochemical Constituents of *Vitis vinifera*

Vitis vinifera (grapes) contain a rich array of phytochemicals, most notably polyphenols, which include flavonoids (such as anthocyanins, catechins, and flavanols), stilbenes (like resveratrol), and tannins. Other significant constituents are phenolic acids, proanthocyanidins, fatty acids, and vitamins. These compounds, the plant parts in which they are found and their biological significance are outlined below.

Table 1.8 Trado Medicinal Uses of *Vitis vinifera*

Plant Part(s)	Phytochemical Constituents	Specific Compounds	Biological Significance
Seeds	Flavonoids, phenolic acids, tannins, proanthocyanidins	Catechin, epicatechin, gallic acid, quercetin, resveratrol	Antioxidant, antimicrobial, cardioprotective, anti-inflammatory, anticancer, neuroprotective
Skins	Flavonoids, anthocyanins, stilbenes, tannins	Malvidin, quercetin, kaempferol, myricetin, resveratrol	Antioxidant, anti-inflammatory, UV-protection, anticancer
Leaves	Flavonoids (glycosides), hydroxybenzoic acids, stilbenes	Quercetin-3-O-glucuronide, rutin, caftaric acid, caffeic acid, gallocatechin, procyanidins	Antioxidant, hepatoprotective, anti-inflammatory
Grape Pomace	Flavonoids, phenolic acids	Quercetin, vanillic acid, kaempferol, syringic acid, gallic acid	Antioxidant, anti-inflammatory

Stems	Flavonoids, stilbenes, phenolic acids	Gallic acid, syringic acid, caffeic acid, epicatechin, catechin gallate, ampelopsins, resveratrol	Antioxidant, antifungal, anti-inflammatory

Vitis vinifera (grapes) contain a rich array of phytochemicals, most notably polyphenols, which include flavonoids (such as anthocyanins, catechins, and flavanols), stilbenes (like resveratrol), and tannins. Other significant constituents are phenolic acids, proanthocyanidins, fatty acids, and vitamins. These compounds, the plant parts in which they are found and their biological significance are outlined below.

1.6 MOLECULAR DOCKING STUDIES

Molecular docking is usually the first step in finding active compounds from existing chemicals in a drug discovery project and it classifies biomolecules into ligands, proteins and nucleic acids; types of docking systems therefore are: Protein-ligand, Protein-protein, Nucleic acid-protein (Wang and Zhu, 2016).

Molecular docking approaches are used in understanding drug-biomolecular interactions to facilitate rational drug design and discovery as well as to facilitate mechanistic study by placing a molecule (ligand) into the preferred binding site of the target specific region of the DNA/protein (receptor) mainly in a non-covalent fashion to form a stable complex of potential efficacy and more specificity (Dar and Mir, 2017). In molecular docking technique, knowledge of the binding site before docking can increase significantly the docking efficiency, and this information can be obtained from proteins co-crystallized with similar ligands (Meng *et al.*, 2012).

The result obtained from the docking studies can be used to predict the binding energy and stability of complexes which can in turn be used to predict the binding affinity between a ligand and a protein and the structure of the protein-ligand complex formed, the activity of the ligand can also be predicted (Prakash, 2010; Wang and Zhu, 2016; Dar and Mir, 2017).

The structures of various compounds used in molecular docking can be obtained from compound databases such as: Drug Bank, ZINC, Chem ID, ChemBank, PDB Bind, PubChem, Asinax, CSD (Cambridge Structural Database) (Hwa, Chaudhary and Mishra, 2016; Dar and Mir, 2017).

1.6.1 Molecular Docking Models

Various molecular docking models have been introduced and they include:

- Lock and Key Model- This was introduced in 1890 by Emil Fischer; the substrate here is expected to fit into the reactive site of the macromolecule (receptor/protein) just like a key fits in a lock. It is also known as the rigid model (Tripathi and Misra, 2020).
- Induced Fit Model- This model was introduced by Daniel Koshland in 1958, also known as flexible docking. Here, both ligand and protein target are to mutually adapt to each other using small conformational changes till an optimal fit is achieved; both ligand and receptor are flexible thus the ligand binds flexibly to the active site of the receptor (Tripathi and Misra, 2020).
- Conformation Ensemble Model- This model recognizes that proteins may undergo larger conformational changes due to its nature of plasticity which allows it to change from one state to another.

1.6.2 Docking Methods According to Flexibility Modelling

- Rigid ligand and rigid receptor docking- Here, the receptor and ligand are treated as inflexible bodies; examples of docking programs used include FTDOCK and FLOG (Meng *et al.*, 2012).

- Flexible ligand and rigid receptor docking- The ligand used here is flexible while the receptor is kept rigid during docking; docking programs used here include AutoDock, FlexX and Autodock Vina (Meng *et al.*, 2012).
- Flexible ligand and flexible receptor docking- Glide can be used as a docking program here (Meng *et al.*, 2012).

1.6.3 Docking Process

Docking involves 3 processes namely:

- Ligand preparation; where duplicate structures are removed (Roy, Kar and Das, 2015).
- Protein preparation; where hydrogen atoms are added, protein minimized, charges and atoms are set properly and other modifications done (Roy, Kar and Das, 2015).
- Ligand-protein docking- A grid box can be generated at the centroid of the ligand bound to the receptor's active site or the active pockets of the protein can be found to dock the prepared ligand. The interaction energy is then compared with that of the bound ligand of the crystallized protein structure so as to assess the degree of fit into the receptor (Roy, Kar and Das, 2015).

1.6.4 Docking Software

Examples of docking software include (Roy, Kar and Das, 2015):

- Autodock- A suite which predicts the way small molecules(that is, drug candidates or substrates) bind to a receptor of a known 3-dimensional structure.
- Discovery Studio

- Dock- A program which examines possible binding orientations of protein-protein and protein-DNA complexes.
- Glide- A fast and accurate docking program.
- Q Site- Docking program with very accurate calculations of the energy of protein-ligand interactions in the active site.

Molecular docking can be applied in lead optimization, hit identification, prediction of Drug-DNA interaction, protein engineering and binding site prediction (Hwa, Chaudhary and Mishra, 2016; Dar and Mir, 2017). Currently marketed drugs using the structure based drug design-docking study include Captopril and Indinavir (Roy, Kar and Das, 2015).

For the purpose of this research, molecular docking approaches will be used in evaluating and determining the mode of action of the phytochemical constituents present in these medicinal plants which have been reported to possess tocolytic effect by screening these phytochemicals against known targets.

1.7 Molecular Docking in Colorectal Cancer Research

Molecular docking studies have emerged as a pivotal in silico method to predict the interaction and binding affinity of phytochemicals with cancer-related protein targets (Wadood *et al*., 2017). Docking simulations assist in understanding the binding modes of ligands and rationalizing their inhibitory potential against proteins such as EGFR (epidermal growth factor receptor), FGFR4 (Fibroblast Growth Factor Receptor 4), Thymidylate synthase, Farnesyltransferase, and Thymidine phosphorylase, which play roles in colorectal carcinogenesis and progression (Wadood *et al*., 2017; Singh *et al*., 2020).

1.8 Aim and Objectives

The aim of this study was to assess the anticancer potential of the phytoconstituents of *Moringa oleifera*, *Olea europaea, Brassica oleracea, and Vitis vinifera* against colorectal cancer.

1.8.1 Specific Objectives

The specific objectives were to:

1. obtain phytoconstituents of the plants from literature.
2. carry out molecular docking studies of the phytoconstituents obtained against key colorectal cancer target proteins.
3. carry out post-docking analysis.
4. determine the ADMET properties of selected ligands.

CHAPTER 2

MATERIALS AND METHODS

2.0 MATERIALS

2.0.1 RCSB PDB

The Research Collaboratory for Structural Bioinformatics Protein Data Bank (RCSB PDB) is a resource for experimental data needed for scientific discoveries. It provides access to 3-Dimensional structure data for large biological molecules (RNA, proteins and DNA). Knowledge of the 3D structure of a biological molecule is central in basic and applied research in biomedicine and useful for the proper understanding of the role of the molecule in health and disease of both humans and animals (Burley *et al.*, 2021).

2.0.2 PyRx

PyRx is a software that carries out virtual screening and is used for computational drug discovery. PyRx can be used for screening compound libraries against potential drug targets, thus being a valuable Computer-Aided Drug Design (CADD) tool.

PyRx uses various plug-in softwares such as:

- AutoDock Vina, used as a docking software; for docking several ligands against one macromolecule.
- Open Babel, used for importing Structure Data Format (SDF) files such as ligands, energy minimization and converting ligands to a dockable format [Protein Data Bank, Partial Charge(Q) & Atom Type(T) (pdbqt)]

- Python, used as a programming language

2.0.3 PyMOL

PyMOL is a molecular software for 3D visualization of proteins, nucleic acids and other macromolecules; and by introduction of various plugins, can be used for macromolecular analysis, pharmacophore and homology modeling, protein-ligand docking and other simulations (Yuan, Chan and Hu, 2017). The PyMOL software was used in the identification of the binding/active amino acid residues to be able to carry out target-directed docking.

2.0.4 Biovia Discovery Studio 2020

This is a software program used for analyses and modeling of molecular structure, pharmacophore modeling, Quantitative Structure Activity Relationship (QSAR) and other simulations. Discovery studio was used to view and analyze the active/ binding site and the ligand and visualize various binding models of each ligand.

2.0.5 Swiss ADME

Swiss ADME is a website that allows computation of physicochemical descriptors, prediction of ADME (Absorption, Distribution, Metabolism, Excretion) parameters, pharmacokinetic properties and drug-like nature of molecules in the advancement of drug discovery (Daina, Michielin and Zoete, 2017). Points such as acute toxicity, organ toxicity (hepatotoxicity, cytotoxicity, carcinogenicity, mutagenicity and immunotoxicity), adverse outcomes and toxicity targets (Banerjee *et al.*, 2018).

2.1 METHODS

2.1.1 Identification and Preparation of Protein Target

The target proteins were identified using the RCSB PDB (https://rcsb.org)(Berman *et al.*, 2000). Editing of the target protein was done on Biovia Discovery Studio Visualizer 2020 to remove all non-standard residues, water molecules and other chains that are not useful for molecular docking. Hydrogen ions and charges were added to the protein. The prepared protein was thereafter saved in the PDB format.

2.1.2 Identification and Preparation of Ligands

Compounds which have been isolated from these plants and identified using GC-MS were downloaded from PubChem as SDF files and imported into PyRx software using the Open Babel plug-in. The compounds were then minimized and converted to pdbqt format to be used as ligands for molecular docking.

2.1.3 Identification of Binding Site

The active/binding amino acids were identified using PyMOL, this was possible because the protein is co-crystallized with capecitabine which is a known ligand.

2.1.4 Molecular Docking and Post-docking Analysis

The protein target which was previously prepared and saved in the PDB format, was loaded into PyRx and made a macromolecule; all the ligands were also imported into PyRx. The binding amino acids on the macromolecule was then labelled and the Autodock Vina plug-in was used for docking while the grid box was placed on the binding amino acids, this was carried out at an exhaustiveness of 8.

Upon completion of docking, the binding affinities were obtained for all ligands and those with a binding affinity ≤ -7 were selected for analysis of receptor-ligand interaction. The various binding conformation of each ligand against the protein was saved from PyRx in the PDB format.

The binding site and ligand interaction between the identified binding amino acid residues and the ligands were then analyzed using Biovia Discovery Studio Visualizer 2020. 3-dimensional and 2-dimensional analysis were done to visualize the various binding models of each ligand and determine the ligands with higher potential of antineoplastic activity.

2.1.5 ADMET Profiling

Some ligands were selected for ADMET profiling based on higher hydrogen bond interaction and highest binding affinity. The ADME properties of these ligands were then obtained using the Swiss ADME web server and the ligands which failed to violate any of the Lipinski rule of five were then selected and their toxicity checked using the ADMETLAB.

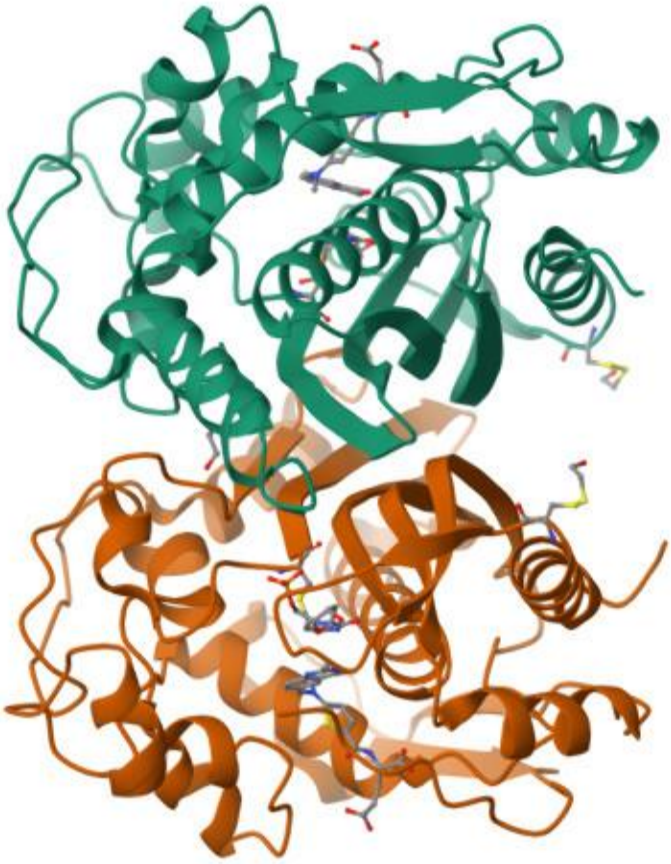

Fig. 2.1: Cryo-EM structure of Human thymidylate synthase complexed with dUMP and Raltitrexed, an antifolate drug, in the closed conformation (1HVY).

CHAPTER THREE

RESULT

3.0 Binding Site Amino Acids

The binding site amino acids identified with the aid of PyMOL are:

1XKK

- LYS 745
- ASP 855

1HVY

- ARG 50
- ASP 218
- ASN 226
- ALA 312

3.1 Molecular Docking Analysis

Compounds from *Moringa oleifera, Olea europaea, Brassica oleracaea,* and *Vitis vinifera* all showed varying degrees of binding affinities for the protein targets (1XKK and 1HVY); this is shown in **Tables 3.1 – 3.4**.

3.1.1 *Moringa oleifera*

Twenty-three (23) and twenty-two (22) compounds including the standard/control ligands (regorafenib, tipifarnib, osimertinib, tipiracil and capecitabine) bound with different affinities to the target proteins, 1XKK and 1HVY, respectively as can be seen in **Tables 3.1**. The various

binding models/ interaction with the binding site amino acids in 3D and 2D views can also be seen in **Figures 3.1** and **3.2**.

3.1.2 *Olea europaea*

Six (6) compounds including the standard/control ligands (regorafenib, capecitabine and tipiracil) bound with different affinities to each target protein as can be seen in **Table 3.2.** The various binding interaction of each ligand with the binding site amino acids in 3D and 2D views can be seen in **Figures 3.3** and **3.4**.

3.1.3 *Brassica oleracaea*

Sixteen (16) and twenty-three (23) compounds including the standard/control ligands (Regorafenib, Tipifarnib, Osimertinib, Tipiracil and Capecitabine) bound with different affinities to the target proteins, 1XKK and 1HVY, respectively, as can be seen in **Tables 3.3** The various binding interactions of each ligand with the binding site amino acids in 3D and 2D views can be seen in **Figure 3.5** and **3.6**.

3.1.4 *Vitis vinifera*

Fifteen (15) and twelve (12) compounds including the standard/control ligands (regorafenib, tipifarnib, osimertinib, tipiracil and capecitabine) bound with different affinities to the target proteins, 1XKK and 1HVY, respectively, as can be seen in **Tables 3.4.** The various binding interaction of each ligand with the binding site amino acids in 3D and 2D views can be seen in **Figure 3.7** and **3.8**

Table 3.1: Binding affinities of *M. oleifera* compounds

S/N	Compounds	PubChem CID	ΔG Energy (Kcal/mol) for 1XKK	ΔG Energy (Kcal/mol) for 1HVY
1	Regorafenib	11167602	-9	-9.7
2	Tipifarnib	159324	-7	-9
3	Osimertinib	71496458	-7.4	-8.4
4	Capecitabine	60953	-7.5	-7.8
5	Tipiracil	6323266	-7.7	-7.2
6	Niazicin A	10068657	-7.8	-7.7
7	Niazicinin A	101920262	-8.3	-7.9
8	O-Ethyl-N-((4-((6-deoxy-alpha-L-mannopyranosyl)oxy)phenyl)methyl)carbamothioate	10247749	-7.9	-
9	Niazidin	11792427	-7.9	-
10	[(2S,3R,4R,5S,6S)-2-[4-(cyanomethyl)phenoxy]-3,5-dihydroxy-6-methyloxan-4-yl] acetate	165350865	-8.3	-
11	Niazirin	129556	-7.6	-
12	Apigenin	5280443	-8.6	-8.2
13	Luteolin	5280445	-8.9	-8.6
14	Kaempferol	5280863	-8.7	-7.9
15	Genistein	5280961	-8	-7.8
16	Isorhamnetin	5281654	-8.9	-8.3
17	Myricetin	5281672	-9.2	-8.5
18	Rhamnetin	5281691	-8.2	-8.2
19	Diadzein	5281708	-7.9	-7.6
20	Ellagic acid	5281855	-8.2	-9.5
21	O-Coumaric acid	637540	-7.1	-
22	Carbonimidothioic acid, [[4-[(4-O-acetyl-6-	85095594	-7.6	-7.4

	deoxy-I+/--L-mannopyranosyl)oxy]phenyl]methyl]-, O-ethyl ester, (E)-			
23	O-methyl N-[[4-(3,4,5-trihydroxy-6-methyloxan-2-yl)oxyphenyl]methyl]carbamothioate	89812211	-7.7	-
24	Carbonimidothioic acid, [[4-[(4-O-acetyl-6-deoxy-I+/--L-mannopyranosyl)oxy]phenyl]methyl]-, O-ethyl ester, (E)-	165350865	-	-7.4
25	4-[(3-O-Acetyl-6-deoxy-I+/--L-mannopyranosyl)oxy]benzeneacetonitrile	165356002	-	7.8
26	Dehydrodieugenol	165225	-	-7.2
27	(2S)-2-acetamido-3-[(Z,4Z)-4-cyclopenta[b]pyridin-5-ylidenebut-2-en-2-yl]sulfanylpropanoic acid	163112956	-	-7.7
28	(6Z,10E,14E,18E)-2,6,10,15,19,23-hexamethyltetracosa-2,6,10,14,18,22-hexaene	11975273	-	-7.6

Table 3.2: Binding affinities of compounds from *O. europaea*

S/N	Compounds	PubChem CID	ΔG Energy (Kcal/mol) for 1XKK	ΔG Energy (Kcal/mol) for 1XKK
1	Regorafenib	11167602	-8.5	-9.8
2	Capecitabine	60953	-7.1	-7.8
3		6323266	-7.7	-7.7
4	Tipiracil	11630759	-8.6	-7.9
5	HYDROCINCHONINE	11652416	-7.5	-7.8
6	Oleocanthal	23624475	-8	-7.9
	Oleacin 90%			

Table 3.3: Binding affinities of compounds from *Brassica oleracaea*

S/N	Compounds	PubChem ID	ΔG Energy (Kcal/mol) For 1XKK	ΔG Energy (Kcal/mol) For 1HVY
1	Regorafenib	11167602	-8.1	-9.6
2	Tipifarnib	159324	-7.1	-9.3
3	Osimertinib	71496458	-7.4	-8.8
4	Capecitabine	60953	-7.7	-7.8
5	Tipiracil	6323266	-7.8	-7.3
6	4-Phenyl-1H,3H-naphtho(1,8-cd)pyran-1,3-dione	11818168	-7.1	-8.9
7	Cyanidin	128861	-7.1	-8.2
8	2-(3,4-Dihydroxyphenyl)naphthalic anhydride	163183898	-7.2	-9.4
9	2-hydroxy-4-phenylphenalen-1-one	46906667	-7.5	-

10	2-methoxyphenalen-1-one	5027250	-7.5	-7.9
11	Quercetin	5280343	-7	-
12	Kaempferol	5280863	-7.4	-8.5
13	Myricetin	5281672	-7.3	-9
14	3-Flavanol	3707243	-8.2	-
15	Phenalenone	11050	-8	-
16	(2R,3S)-2,3-dihydroxy-9-(4-hydroxyphenyl)-2,3-dihydrophenalen-1-one	10881321	-	-9
17	(2S,3S)-2,3-dihydroxy-4-(4-methoxyphenyl)-2,3-dihydrophenalen-1-one	10958179	-	-9.4
18	Flavonol	11349		-7.8
19	Dephinidin	128853	-	-8
20	(2R,3S)-2,3-dihydroxy-9-(4-hydroxy-3-methoxyphenyl)-2,3-dihydrophenalen-1-one	162968764	-	-8.6
21	2-(3,4-Dihydroxyphenyl)naphthalic anhydride	163183898	-	-9.4

22	9-(4-methoxyphenyl)phenalen-1-one	2754648	-	-8.5
23	Anigofurone	636472	-	-9
24	2,3-Dihydro-4-(4-methoxyphenyl)-1H-phenalene-1,2,3-triol	74027046	-	-8.4
25	2-hydroxy-9-(4-methoxyphenyl)phenalen-1-one	46906619	-	-8.8

Table 3.4: Binding affinities of compounds from *Vitis vinifera*

S/N	Compounds	PubChem ID	ΔG Energy (Kcal/mol) For 1XKK	ΔG Energy (Kcal/mol) For 1HVY
1	Regorafenib	11167602	-8.3	-9.7
2	Tipifarnib	159324	-8	-9.3
3	Osimertinib	71496458	-7.4	-8.7
4	Capecitabine	60953	-7.8	-7.7
5	Tipiracil	6323266	-7.7	-7.3
6	Cis-Astringin	16040016	-9.1	-8.7
7	Acuminoside	14194083	-8.1	-8.6
8	Cyanidin	128861	-8.7	-8
9	4-Hydroxy-3-(3-methylbut-3-en-1-ynyl)benzoic acid	14394291	-7.4	
10	Icariside B8	14539953	-7.4	-7.8

11	(3E)-3-[2-[(1S,4R,4aS,8aR)-4-hydroxy-5,5,8a-trimethyl-2-methylidene-3,4,4a,6,7,8-hexahydro-1H-naphthalen-1-yl]ethylidene]oxolan-2-one	16038718	-8.6	-7.9
12	Pinosylvin	5280457	-8.3	-
13	Naringenin chalcone	5280960	-8.5	-
14	Pinocembrin chalcone	6474295	-8.5	-7.4
15	2-Phenylethyl beta-D-galactopyranoside	84675	-7.9	-7.4

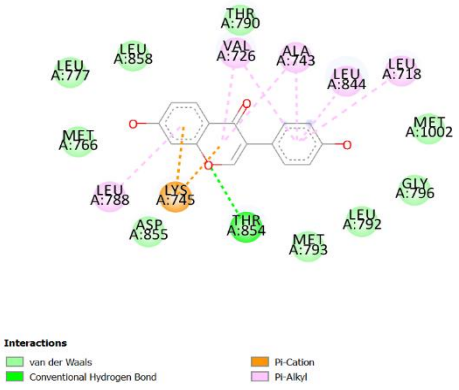
THR A:790
LEU A:858
VAL A:726
ALA A:743
LEU A:844
LEU A:718
LEU A:777
MET A:1002
MET A:766
GLY A:796
LEU A:788
LYS A:745
LEU A:792
ASP A:855
THR A:854
MET A:793
Interactions
van der Waals
Conventional Hydrogen Bond
Pi-Cation
Pi-Alkyl

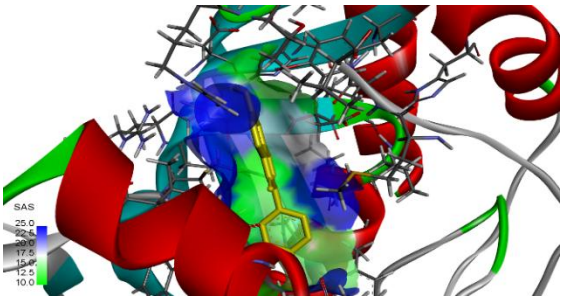
SAS

A

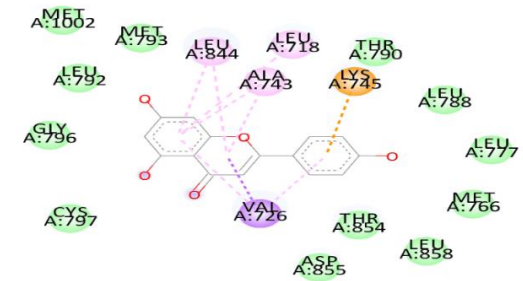
MET A:1002
MET A:793
LEU A:844
LEU A:718
THR A:790
LEU A:792
ALA A:743
LYS A:745
LEU A:788
GLY A:796
LEU A:777
CYS A:797
VAL A:726
THR A:854
MET A:766
LEU A:858
ASP A:855
Interactions
van der Waals
Pi-Cation
Pi-Sigma
Pi-Alkyl

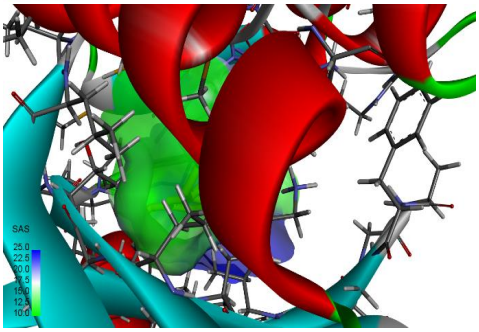
SAS

B

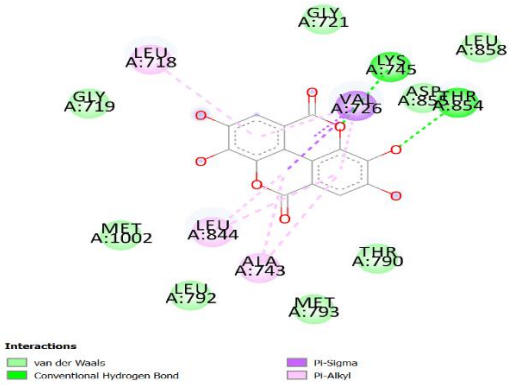
GLY A:721
LEU A:858
LEU A:718
LYS A:745
GLY A:719
VAL A:726
ASP A:854
THR A:854
MET A:1002
LEU A:844
THR A:790
ALA A:743
LEU A:792
MET A:793
Interactions
van der Waals
Conventional Hydrogen Bond
Pi-Sigma
Pi-Alkyl

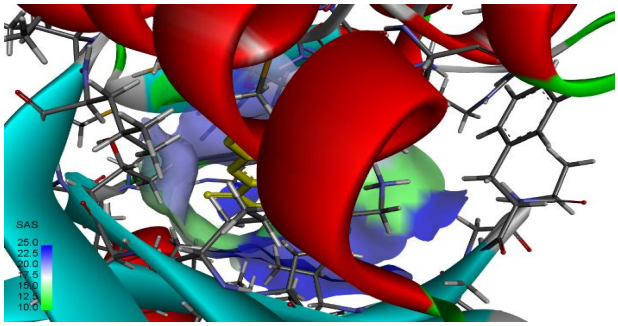
SAS
25.0
22.5
20.0
17.5
15.0
12.5
10.0

C

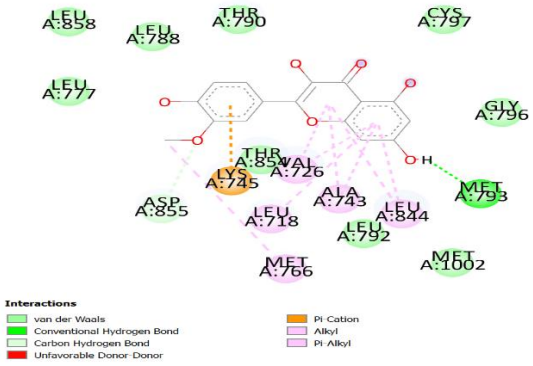
LEU A:858
LEU A:788
THR A:790
CYS A:797
LEU A:777
GLY A:796
THR A:854
VAL A:726
LYS A:745
MET A:793
ASP A:855
ALA A:743
LEU A:718
LEU A:844
LEU A:792
MET A:766
MET A:1002
Interactions
van der Waals
Conventional Hydrogen Bond
Carbon Hydrogen Bond
Unfavorable Donor-Donor
Pi-Cation
Alkyl
Pi-Alkyl

D

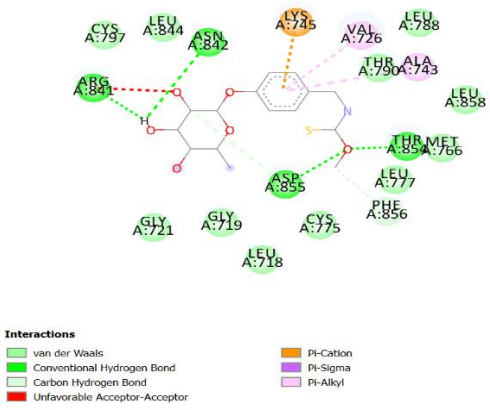
CYS A:797
LEU A:844
ASN A:842
LYS A:745
VAL A:726
LEU A:788
THR A:790
ALA A:743
ARG A:841
LEU A:858
THR A:854
MET A:766
ASP A:855
LEU A:777
PHE A:856
GLY A:721
GLY A:719
CYS A:775
LEU A:718
Interactions
van der Waals
Conventional Hydrogen Bond
Carbon Hydrogen Bond
Unfavorable Acceptor-Acceptor
Pi-Cation
Pi-Sigma
Pi-Alkyl

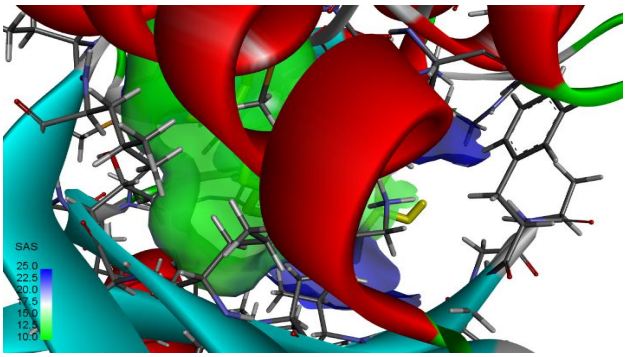
SAS
25.0
22.5
20.0
17.5
15.0
12.5
10.0

E

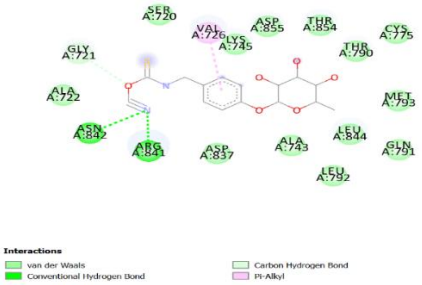
SER A:720
VAL A:726
ASP A:855
THR A:854
CYS A:775
GLY A:721
LYS A:745
THR A:790
ALA A:722
MET A:793
ASN A:842
LEU A:844
ARG A:841
ASP A:837
ALA A:743
GLN A:791
LEU A:792
Interactions
van der Waals
Conventional Hydrogen Bond
Carbon Hydrogen Bond
Pi-Alkyl

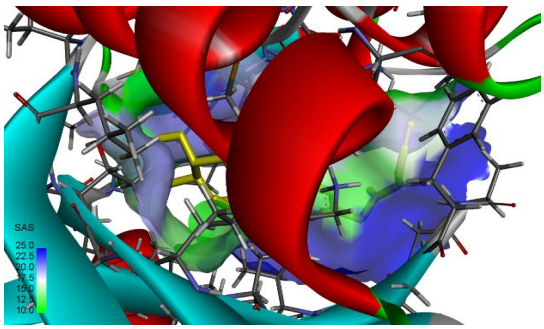
SAS
26.0
22.5
20.0
17.5
15.0
12.5
10.0

F

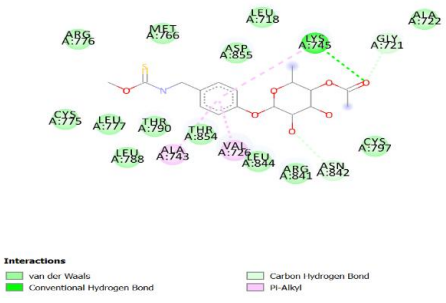
Interactions
van der Waals
Conventional Hydrogen Bond
Carbon Hydrogen Bond
Pi-Alkyl

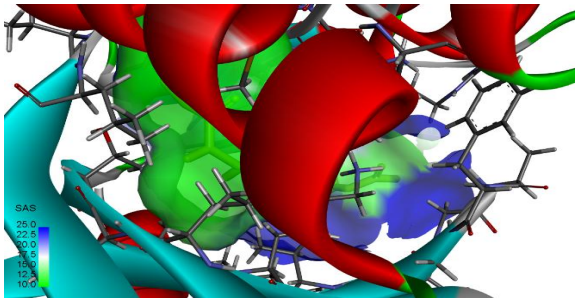
SAS

G

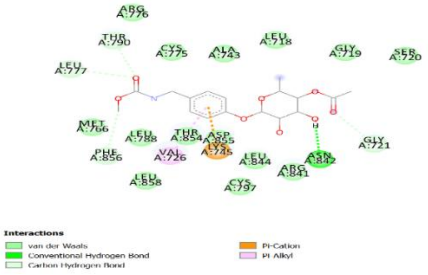
Interactions
van der Waals
Conventional Hydrogen Bond
Carbon Hydrogen Bond
Pi-Cation
Pi Alkyl

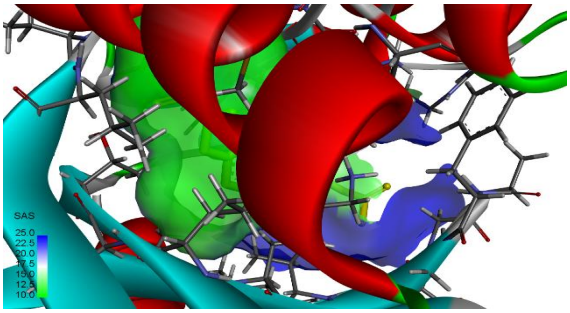
SAS

H

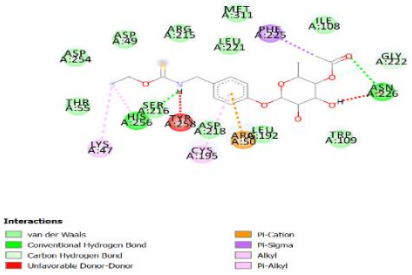
Interactions
van der Waals
Conventional Hydrogen Bond
Carbon Hydrogen Bond
Unfavorable Donor-Donor
Pi-Cation
Pi-Sigma
Alkyl
Pi-Alkyl

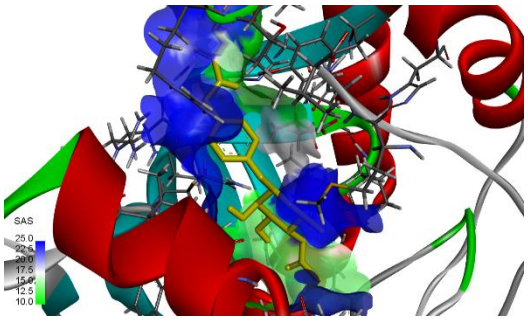
SAS

I

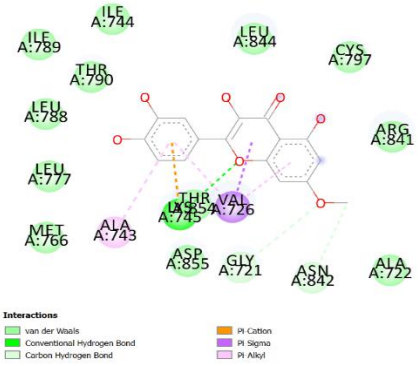
Interactions
van der Waals
Conventional Hydrogen Bond
Carbon Hydrogen Bond
Pi-Cation
Pi Sigma
Pi Alkyl

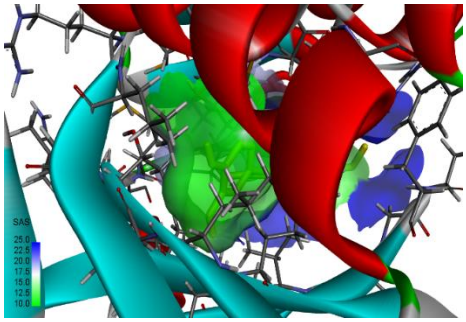
SAS

J

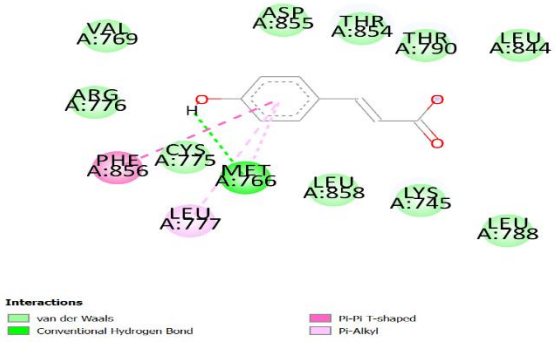
VAL A:769
ASP A:855
THR A:854
THR A:790
LEU A:844
ARG A:776
CYS A:775
PHE A:856
MET A:766
LEU A:858
LYS A:745
LEU A:777
LEU A:788
Interactions
van der Waals
Conventional Hydrogen Bond
Pi-Pi T-shaped
Pi-Alkyl

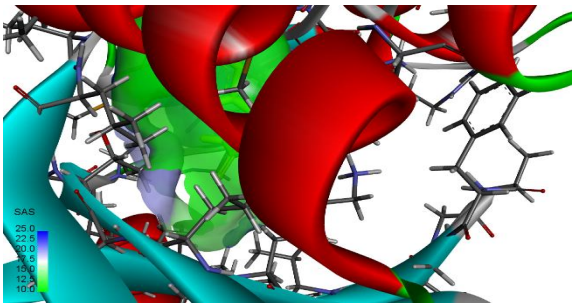
SAS

K

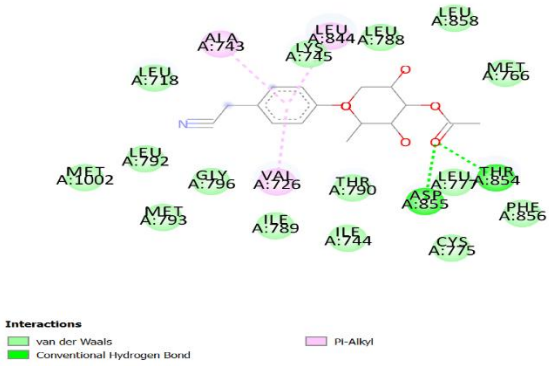
LEU A:858
ALA A:743
LEU A:844
LEU A:788
LYS A:745
LEU A:718
MET A:766
LEU A:792
MET A:1002
GLY A:796
VAL A:726
THR A:790
LEU A:777
THR A:854
ASP A:855
PHE A:856
MET A:793
ILE A:789
ILE A:744
CYS A:775
Interactions
van der Waals
Conventional Hydrogen Bond
Pi-Alkyl

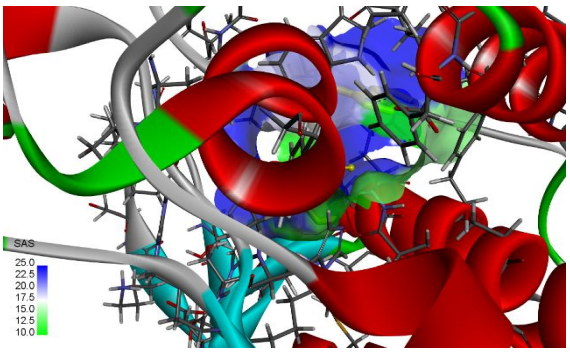
SAS

L

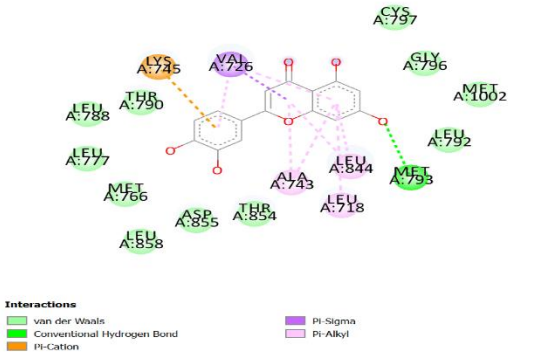
CYS A:797
LYS A:745
VAL A:726
GLY A:796
MET A:1002
THR A:790
LEU A:788
LEU A:792
LEU A:777
LEU A:844
MET A:793
ALA A:743
MET A:766
LEU A:718
ASP A:855
THR A:854
LEU A:858
Interactions
van der Waals
Conventional Hydrogen Bond
Pi-Cation
Pi-Sigma
Pi-Alkyl

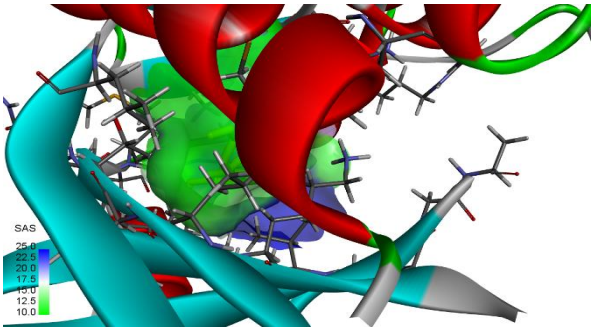
SAS

M

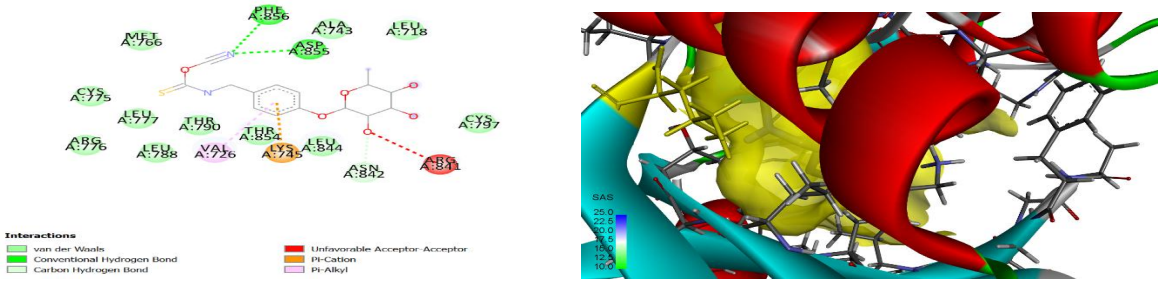

N

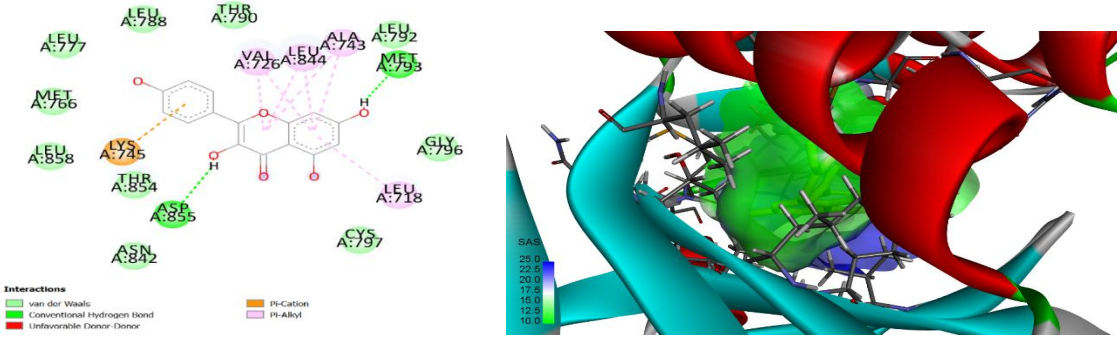

O

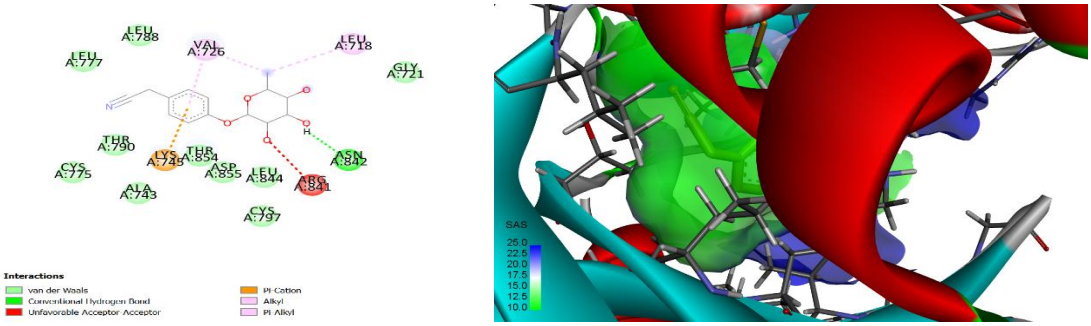

P

Fig. 3.1: 2D (left) and 3D (right) views of the molecular interactions of amino-acid residues of Epidermal Growth Factor Receptor (EGFR), 1XKK, with (A) Diadzein (B) Apigenin (C) Ellagic acid (D)Isorhamnetin (E) O-methyl N-[[4-(3,4,5-trihydroxy-6-methyloxan-2-yl)oxyphenyl]methyl]carbamothioate (F) O-Ethyl N-((4-((6-deoxy-alpha-L-mannopyranosyl)oxy)phenyl)methyl)carbamothioate (G) Niazicin A (H) Niazicinin A (I)

Carbonimidothioic acid, [[4-[(4-O-acetyl-6-deoxy-I+/--L-mannopyranosyl)oxy]phenyl]methyl]-, O-ethyl ester, (E)- (J) Rhamnetin (K) O-Coumaric Acid (L) [(2S,3R,4R,5S,6S)-2-[4-(cyanomethyl)phenoxy]-3,5-dihydroxy-6-methyloxan-4-yl] acetate (M) Luteolin (N)Niazidin (O) Kaempferol (P) Niazirin

in *Moringa oleifera.*

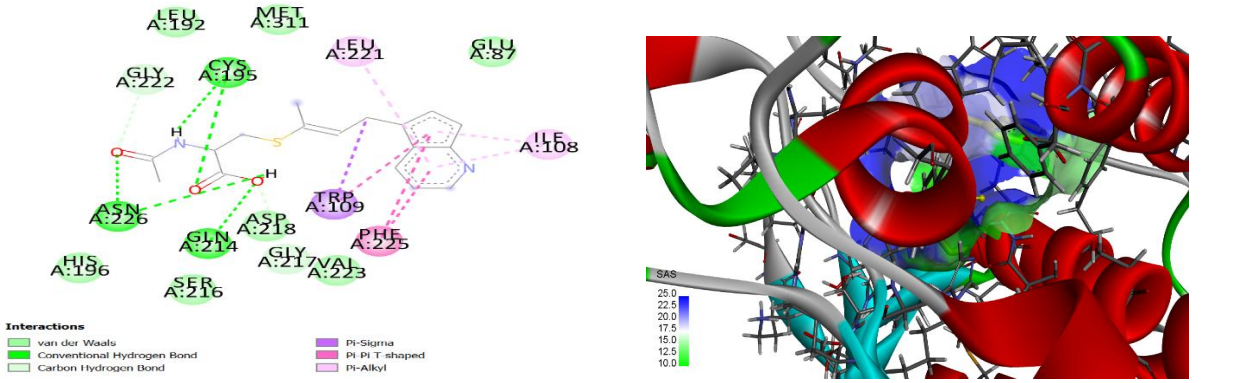

A

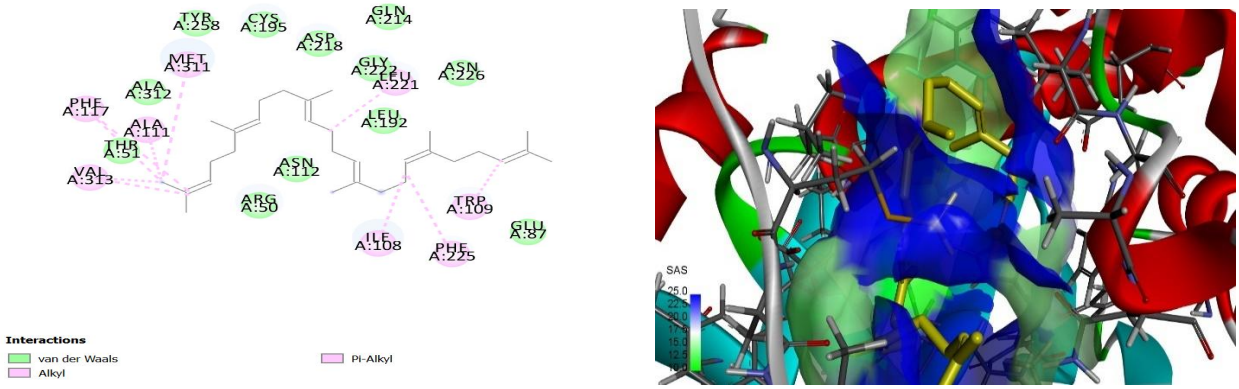

B

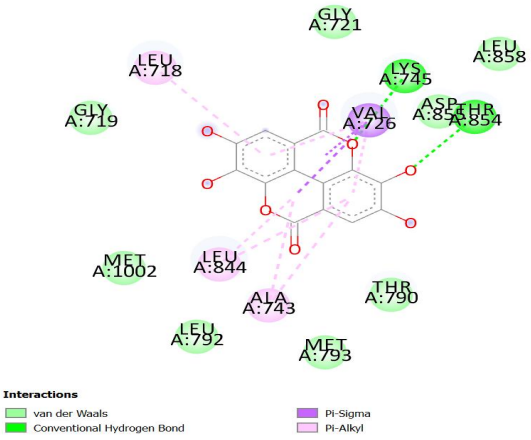
GLY A:721
LEU A:718
LEU A:858
LYS A:745
GLY A:719
VAL A:726
ASP A:855
THR A:854
MET A:1002
LEU A:844
ALA A:743
THR A:790
LEU A:792
MET A:793
Interactions
van der Waals
Conventional Hydrogen Bond
Pi-Sigma
Pi-Alkyl

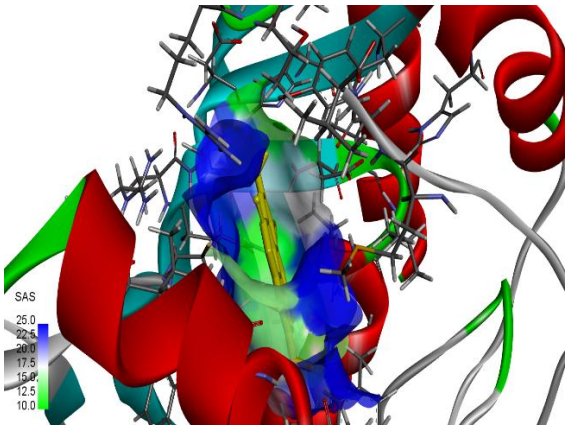
SAS
25.0
22.5
20.0
17.5
15.0
12.5
10.0

C

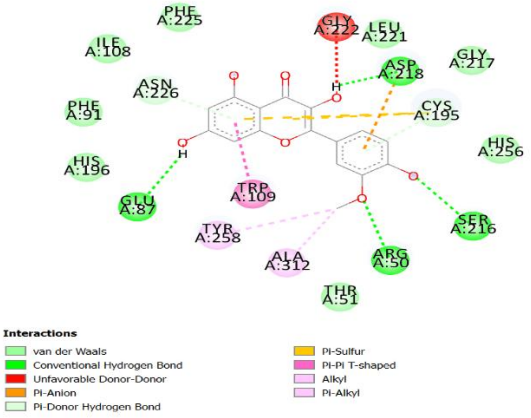
PHE A:225
GLY A:222
LEU A:221
ILE A:108
ASP A:218
GLY A:217
ASN A:226
PHE A:91
CYS A:195
HIS A:256
HIS A:196
TRP A:109
GLU A:87
SER A:216
TYR A:258
ALA A:312
ARG A:50
THR A:51
Interactions
van der Waals
Conventional Hydrogen Bond
Unfavorable Donor-Donor
Pi-Anion
Pi-Donor Hydrogen Bond
Pi-Sulfur
Pi-Pi T-shaped
Alkyl
Pi-Alkyl

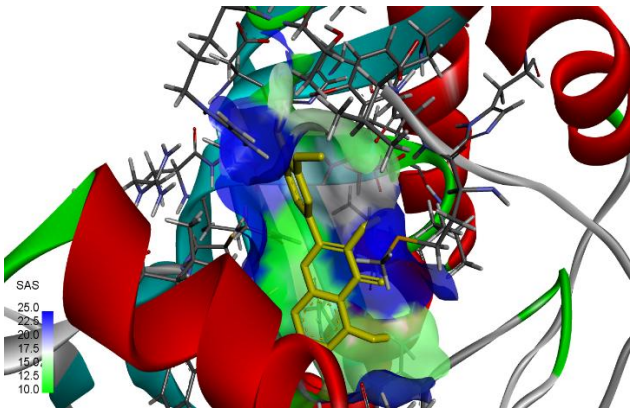
SAS
25.0
22.5
20.0
17.5
15.0
12.5
10.0

D

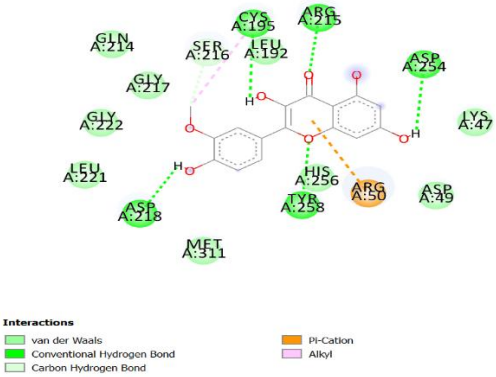
CYS A:195
ARG A:215
GLN A:214
SER A:216
LEU A:192
ASP A:254
GLY A:217
GLY A:222
LYS A:47
LEU A:221
HIS A:256
ARG A:50
ASP A:49
TYR A:258
ASP A:218
MET A:311
Interactions
van der Waals
Conventional Hydrogen Bond
Carbon Hydrogen Bond
Pi-Cation
Alkyl

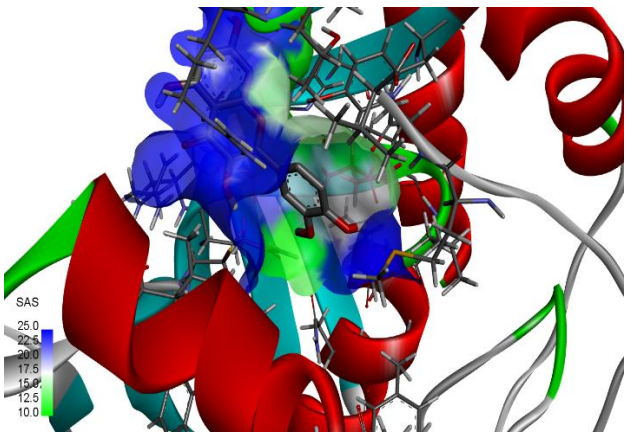
SAS
25.0
22.5
20.0
17.5
15.0
12.5
10.0

E

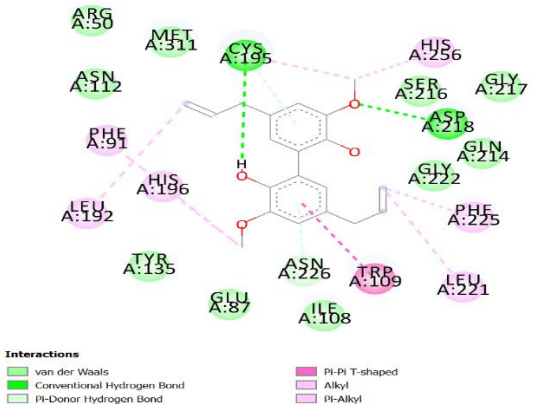
ARG A:50
MET A:311
CYS A:195
HIS A:256
ASN A:112
SER A:216
GLY A:217
ASP A:218
PHE A:91
GLN A:214
GLY A:222
HIS A:196
LEU A:192
PHE A:225
TYR A:135
ASN A:226
TRP A:109
LEU A:221
GLU A:87
ILE A:108
Interactions
van der Waals
Conventional Hydrogen Bond
Pi-Donor Hydrogen Bond
Pi-Pi T-shaped
Alkyl
Pi-Alkyl

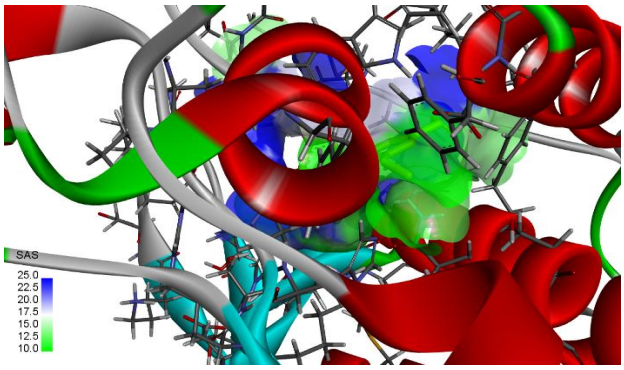
SAS
25.0
22.5
20.0
17.5
15.0
12.5
10.0

F

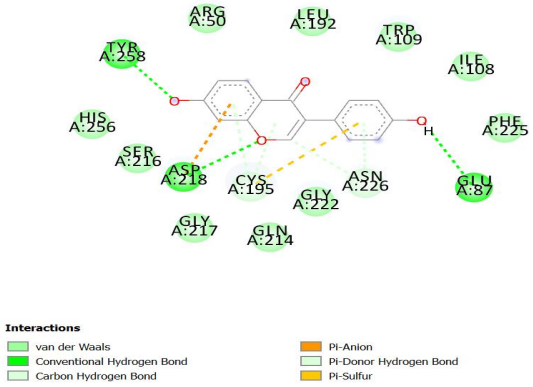
ARG A:50
LEU A:192
TRP A:109
TYR A:258
ILE A:108
HIS A:256
PHE A:225
SER A:216
ASP A:218
CYS A:195
ASN A:226
GLU A:87
GLY A:222
GLY A:217
GLN A:214
Interactions
van der Waals
Conventional Hydrogen Bond
Carbon Hydrogen Bond
Pi-Anion
Pi-Donor Hydrogen Bond
Pi-Sulfur

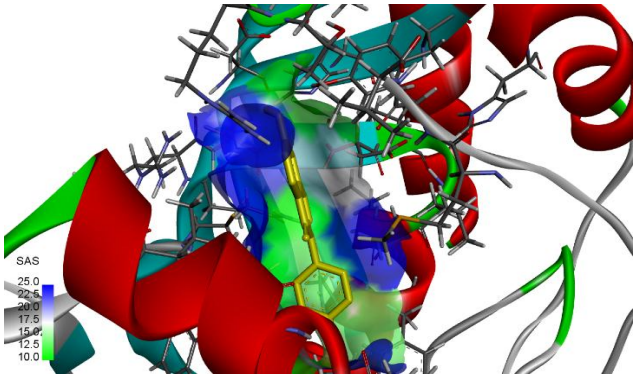
SAS
25.0
22.5
20.0
17.5
15.0
12.5
10.0

G

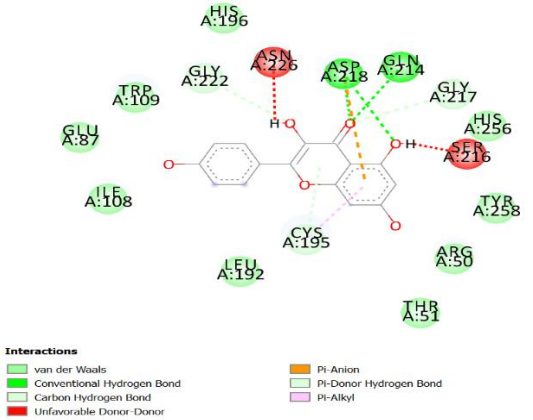
HIS A:196
ASN A:226
GLY A:222
ASP A:218
GLN A:214
TRP A:109
GLY A:217
HIS A:256
GLU A:87
SER A:216
ILE A:108
TYR A:258
CYS A:195
ARG A:50
LEU A:192
THR A:51
Interactions
van der Waals
Conventional Hydrogen Bond
Carbon Hydrogen Bond
Unfavorable Donor-Donor
Pi-Anion
Pi-Donor Hydrogen Bond
Pi-Alkyl

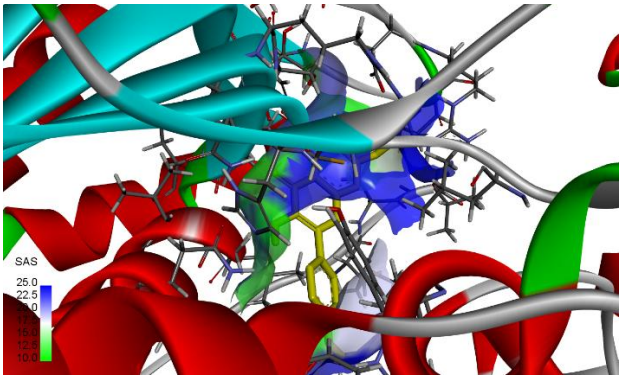
SAS
25.0
22.5
10.0

H

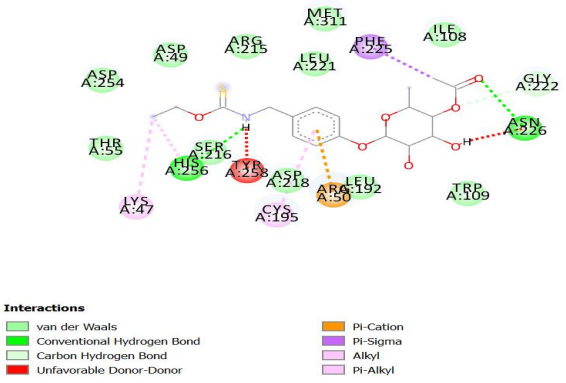
MET A:311
ILE A:108
ARG A:215
PHE A:225
ASP A:49
LEU A:221
ASP A:254
GLY A:222
ASN A:226
THR A:55
SER A:216
HIS A:256
TYR A:258
ASP A:218
LEU A:192
TRP A:109
LYS A:47
CYS A:195
Interactions
van der Waals
Conventional Hydrogen Bond
Carbon Hydrogen Bond
Unfavorable Donor-Donor
Pi-Cation
Pi-Sigma
Alkyl
Pi-Alkyl

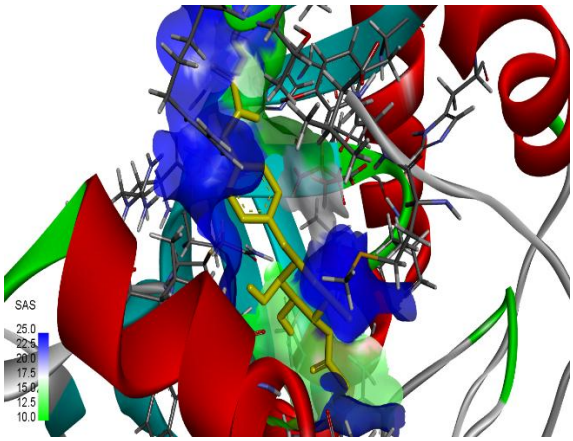
SAS
25.0
22.5
20.0
17.5
15.0
12.5
10.0

I

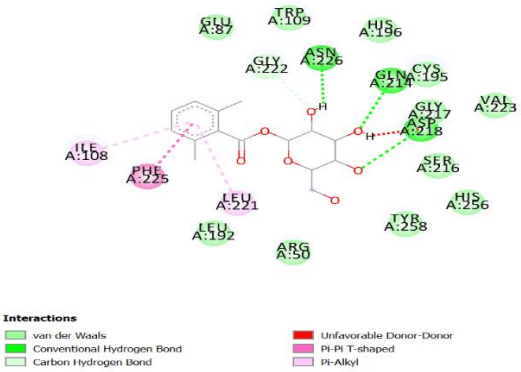
GLU A:87
TRP A:109
HIS A:196
ASN A:226
GLY A:222
GLN A:214
CYS A:195
VAL A:223
GLY A:217
ASP A:218
ILE A:108
SER A:216
PHE A:225
LEU A:221
HIS A:256
LEU A:192
TYR A:258
ARG A:50
Interactions
van der Waals
Conventional Hydrogen Bond
Carbon Hydrogen Bond
Unfavorable Donor-Donor
Pi-Pi T-shaped
Pi-Alkyl

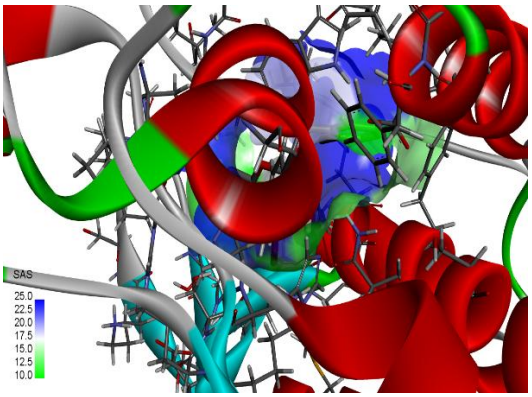
SAS
25.0
22.5
20.0
17.5
15.0
12.5
10.0

J

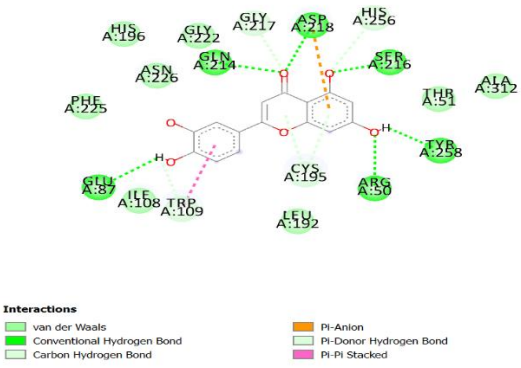
HIS A:196
GLY A:222
GLY A:217
ASP A:218
HIS A:256
GLN A:214
SER A:216
ASN A:226
ALA A:312
PHE A:225
THR A:51
TYR A:258
CYS A:195
GLU A:87
ARG A:50
ILE A:108
TRP A:109
LEU A:192
Interactions
van der Waals
Conventional Hydrogen Bond
Carbon Hydrogen Bond
Pi-Anion
Pi-Donor Hydrogen Bond
Pi-Pi Stacked

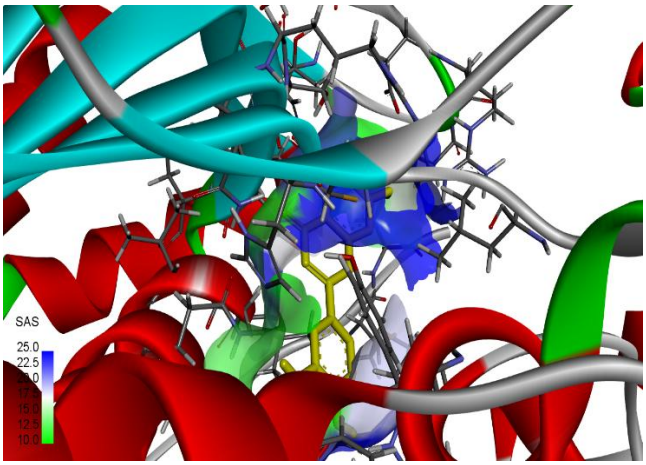
SAS
25.0
22.5
20.0
17.5
15.0
12.5
10.0

K

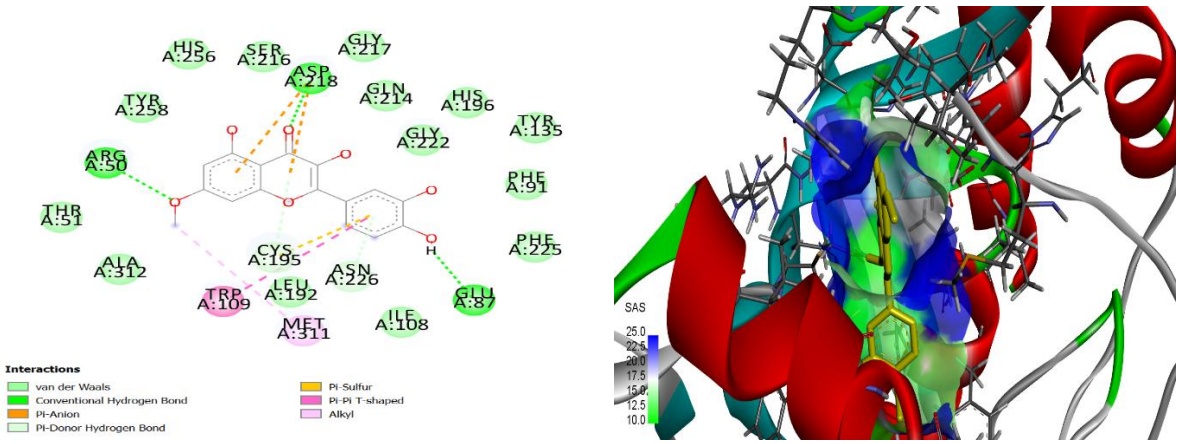
HIS A:256
SER A:216
GLY A:217
ASP A:218
GLN A:214
HIS A:196
TYR A:258
TYR A:135
GLY A:222
ARG A:50
PHE A:91
THR A:51
PHE A:225
CYS A:195
ALA A:312
ASN A:226
LEU A:192
TRP A:109
GLU A:87
ILE A:108
MET A:311
Interactions
van der Waals
Conventional Hydrogen Bond
Pi-Anion
Pi-Donor Hydrogen Bond
Pi-Sulfur
Pi-Pi T-shaped
Alkyl
SAS
25.0
22.5
20.0
17.5
15.0
12.5
10.0

L

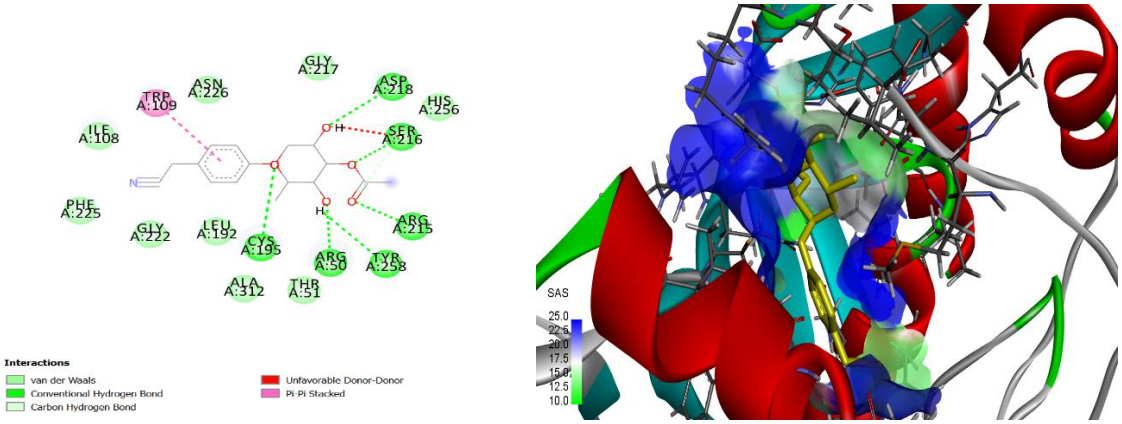
GLY A:217
ASP A:218
HIS A:256
ASN A:226
TRP A:109
SER A:216
ILE A:108
PHE A:225
ARG A:215
GLY A:222
LEU A:192
CYS A:195
ARG A:50
TYR A:258
ALA A:312
THR A:51
Interactions
van der Waals
Conventional Hydrogen Bond
Carbon Hydrogen Bond
Unfavorable Donor-Donor
Pi-Pi Stacked
SAS
25.0
22.5
20.0
17.5
15.0
12.5
10.0

M

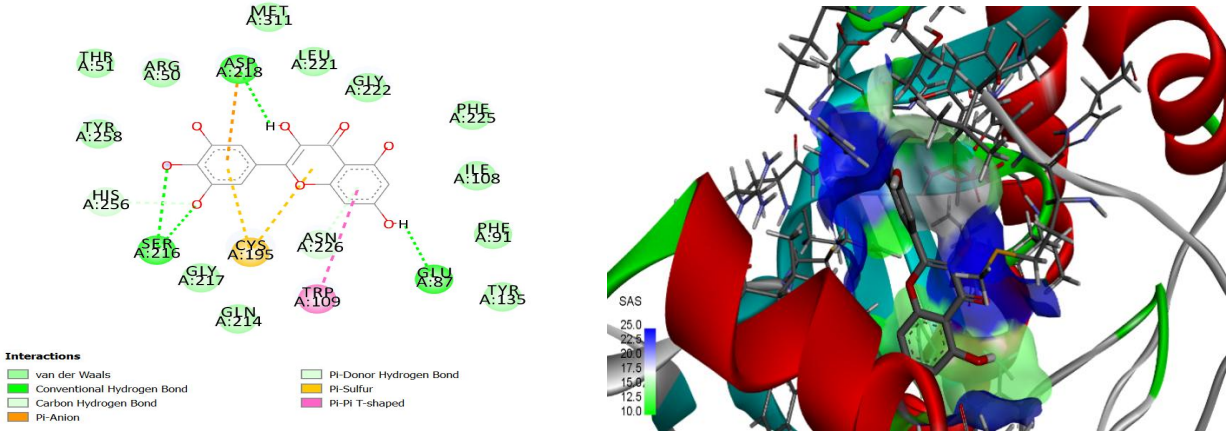
MET A:311
THR A:51
ARG A:50
ASP A:218
LEU A:221
GLY A:222
PHE A:225
TYR A:258
ILE A:108
HIS A:256
PHE A:91
SER A:216
CYS A:195
ASN A:226
GLY A:217
GLU A:87
TYR A:135
TRP A:109
GLN A:214
Interactions
van der Waals
Conventional Hydrogen Bond
Carbon Hydrogen Bond
Pi-Anion
Pi-Donor Hydrogen Bond
Pi-Sulfur
Pi-Pi T-shaped
SAS
25.0
22.5
20.0
17.5
15.0
12.5
10.0

N

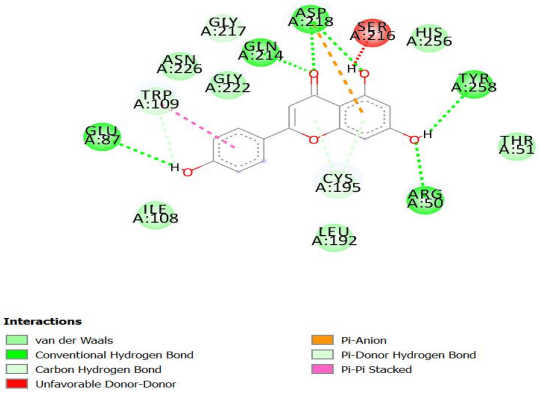
ASP A:218
GLY A:217
SER A:216
HIS A:256
GLN A:214
ASN A:226
GLY A:222
TYR A:258
TRP A:109
GLU A:87
THR A:51
CYS A:195
ARG A:50
ILE A:108
LEU A:192
Interactions
van der Waals
Conventional Hydrogen Bond
Carbon Hydrogen Bond
Unfavorable Donor-Donor
Pi-Anion
Pi-Donor Hydrogen Bond
Pi-Pi Stacked

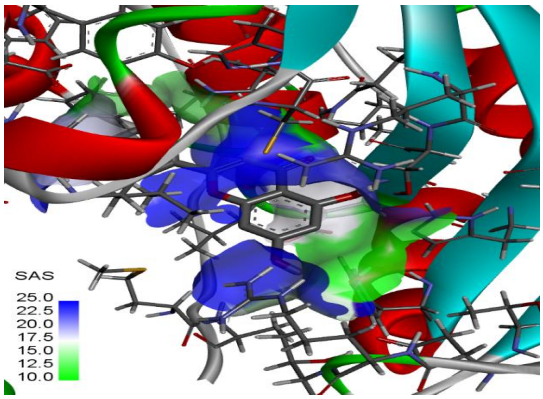
SAS
25.0
22.5
20.0
17.5
15.0
12.5
10.0

O

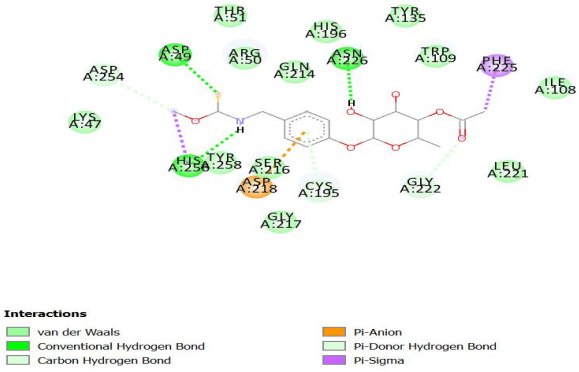
THR A:51
HIS A:196
TYR A:155
ASP A:49
ARG A:50
GLN A:214
ASN A:226
TRP A:109
PHE A:225
ASP A:254
ILE A:108
LYS A:47
HIS A:256
TYR A:258
SER A:216
ASP A:218
CYS A:195
GLY A:222
LEU A:221
GLY A:217
Interactions
van der Waals
Conventional Hydrogen Bond
Carbon Hydrogen Bond
Pi-Anion
Pi-Donor Hydrogen Bond
Pi-Sigma

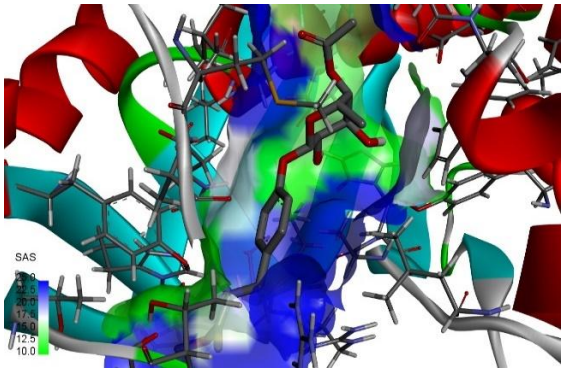
SAS

P

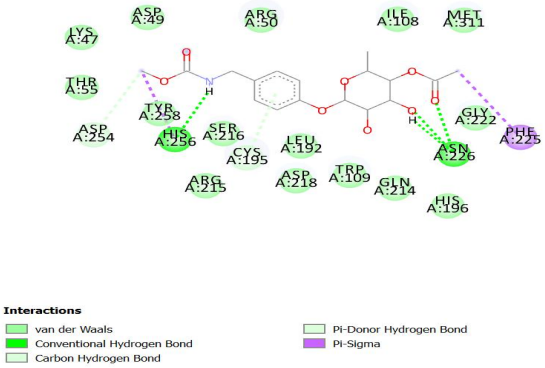
ASP A:49
ARG A:50
ILE A:108
MET A:311
LYS A:47
THR A:155
TYR A:258
GLY A:222
ASP A:254
HIS A:256
SER A:216
PHE A:225
CYS A:195
LEU A:192
ASN A:226
ARG A:215
ASP A:218
TRP A:109
GLN A:214
HIS A:196
Interactions
van der Waals
Conventional Hydrogen Bond
Carbon Hydrogen Bond
Pi-Donor Hydrogen Bond
Pi-Sigma

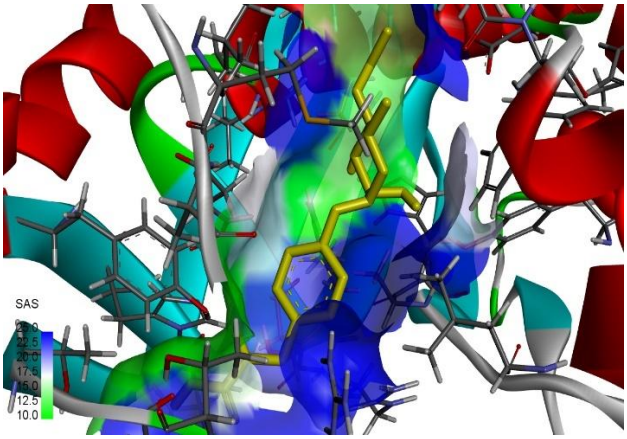
SAS

Q

Fig. 3.2 : 2D (left) and 3D (right) views of the molecular interactions of amino-acid residues of human thymidylate synthase enzyme, 1HVY, with (A) (2S)-2-acetamido-3-[(Z,4Z)-4-cyclopenta[b]pyridin-5-ylidenebut-2-en-2-yl]sulfanylpropanoic acid (B) (6Z,10E,14E,18E)-2,6,10,15,19,23-hexamethyltetracosa-2,6,10,14,18,22-hexaene (C) Ellagic acid (D) Isorhamnetin (E) Genistein (F) Dehydroeugenol (G) Diadzein (H) Kaempferol (I) Carbonimidothioic acid, [[4-[(4-O-acetyl-6-deoxy-I+/--L-mannopyranosyl)oxy]phenyl]methyl]-, O-ethyl ester, (E)- (J) I(2)-D-Glucopyranose, 1-(2,6-dimethylbenzoate) (K) Luteolin (L) Rhamnetin (M) 4-[(3-O-Acetyl-6-deoxy-I+/--L-mannopyranosyl)oxy]benzeneacetonitrile (N)Myricetin (O) Apigenin (P) Niazicin A (Q) Niazicinin A

in *Moringa oleifera.*

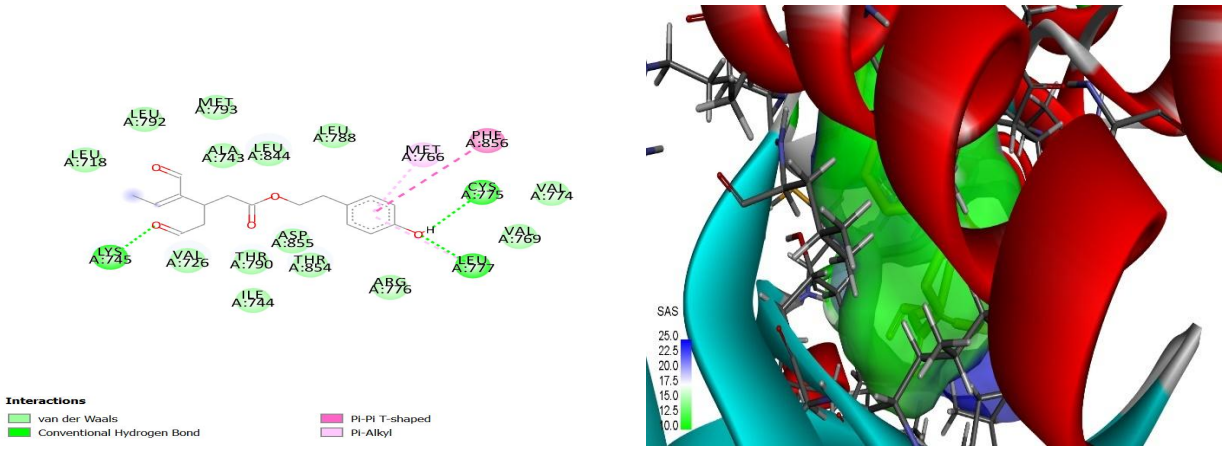

A

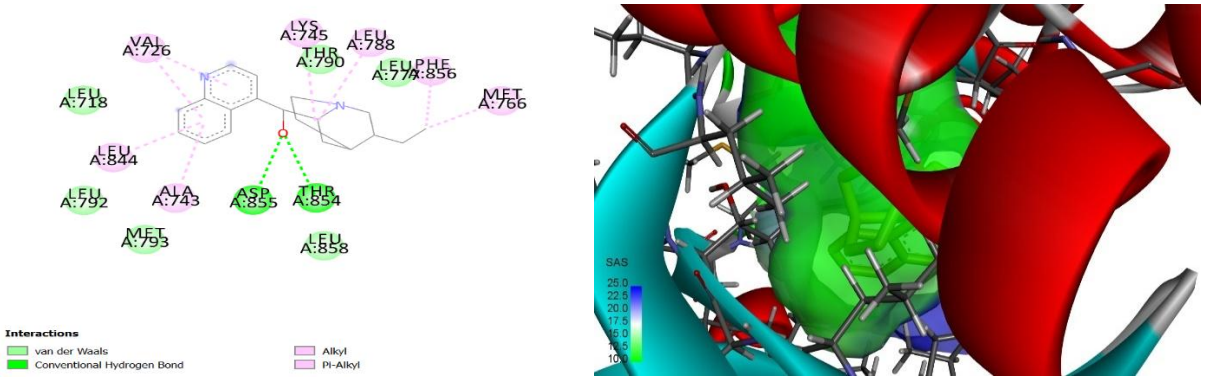

B

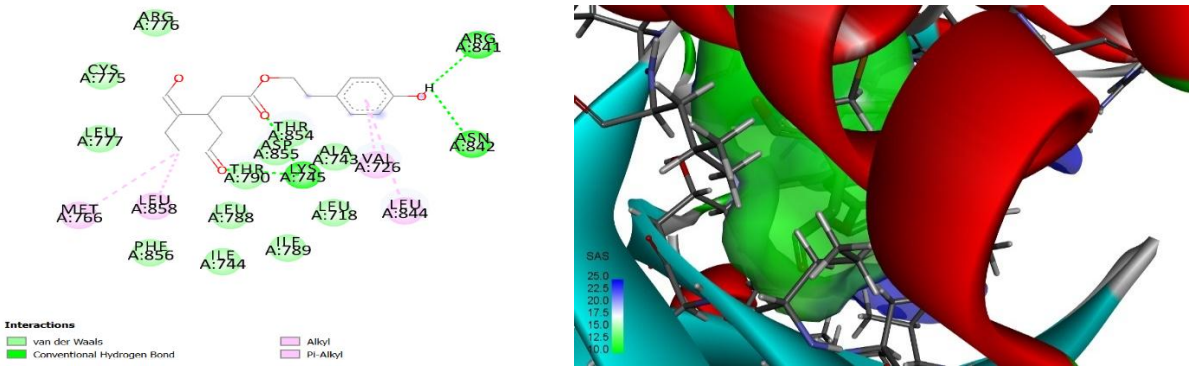

C

Fig. 3.3: 2D (left) and 3D (right) views of the molecular interactions of amino-acid residues of Epidermal Growth Factor Receptor (EGFR), 1XKK, with (A) Oleocanthal (B) Hydrocinchonine (C) Oleacin 90% in *Olea europaea.*

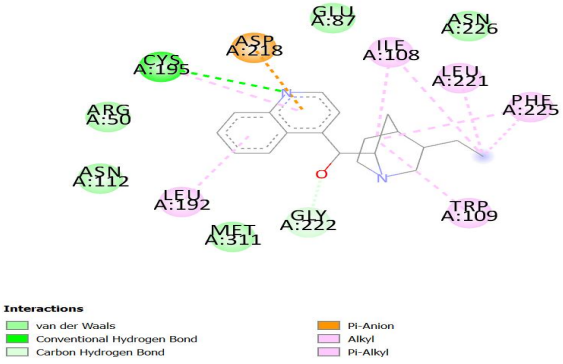
GLU A:87
ASN A:226
ASP A:218
ILE A:108
CYS A:195
LEU A:221
PHE A:225
ARG A:50
ASN A:112
LEU A:192
TRP A:109
GLY A:222
MET A:311
Interactions
van der Waals
Conventional Hydrogen Bond
Carbon Hydrogen Bond
Pi-Anion
Alkyl
Pi-Alkyl

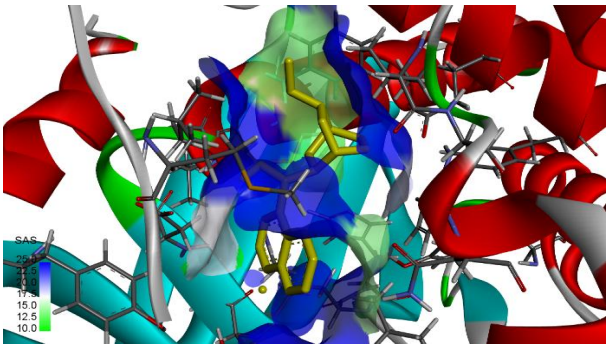

A

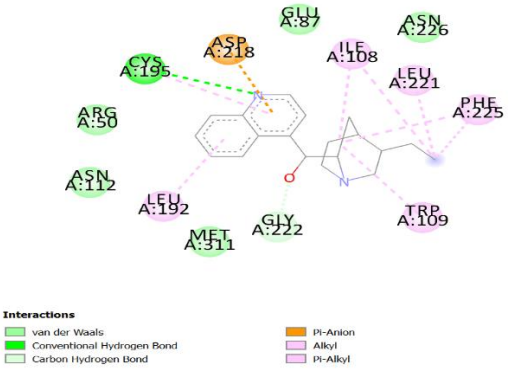
GLU A:87
ASN A:226
ASP A:218
ILE A:108
CYS A:195
LEU A:221
PHE A:225
ARG A:50
ASN A:112
LEU A:192
TRP A:109
GLY A:222
MET A:311
Interactions
van der Waals
Conventional Hydrogen Bond
Carbon Hydrogen Bond
Pi-Anion
Alkyl
Pi-Alkyl

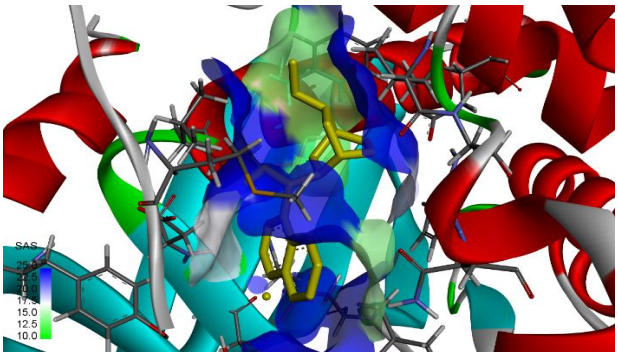

B

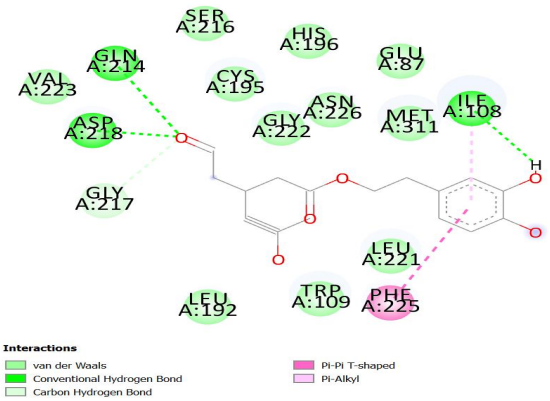
SER A:216
HIS A:196
GLN A:214
GLU A:87
VAL A:223
CYS A:195
ASN A:226
ILE A:108
ASP A:218
GLY A:222
MET A:311
GLY A:217
LEU A:221
TRP A:109
PHE A:225
LEU A:192
Interactions
van der Waals
Conventional Hydrogen Bond
Carbon Hydrogen Bond
Pi-Pi T-shaped
Pi-Alkyl

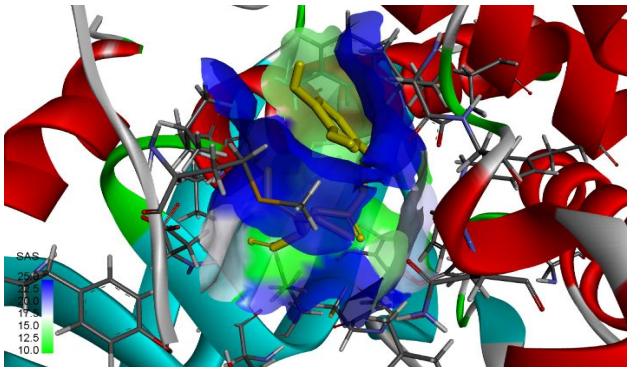

C

Fig. 3.4: 2D (left) and 3D (right) views of the molecular interactions of amino-acid residues of Human Thymidylate Synthase enzyme, 1HVY, with (A) Oleocanthal (B) Hydrocinchonine (C) Oleacin 90% in *Olea europaea.*

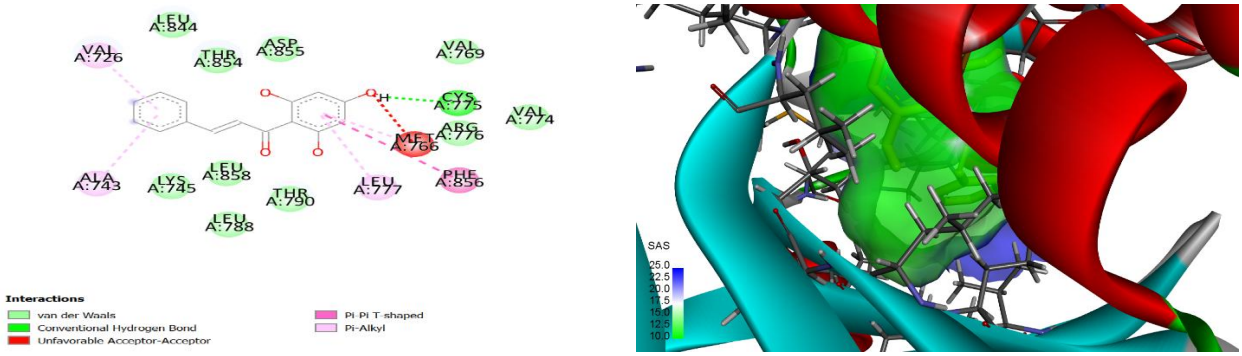

A

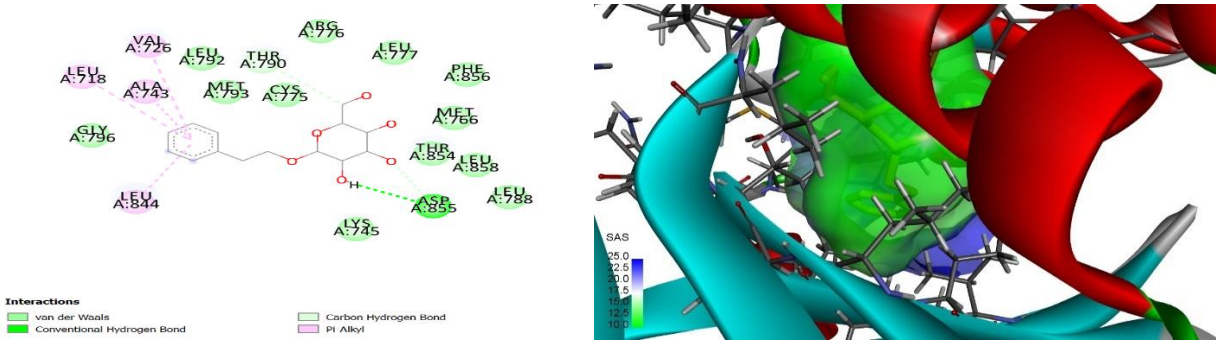

B

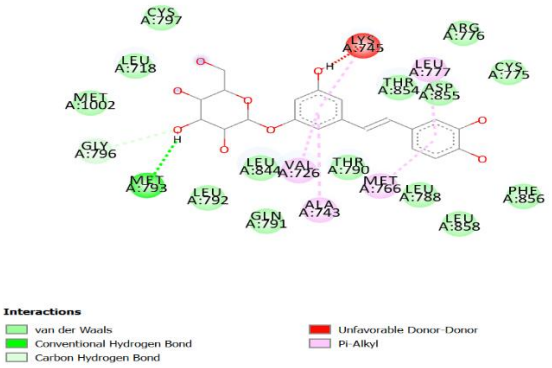
CYS A:797
ARG A:776
LYS A:745
LEU A:718
LEU A:777
CYS A:775
THR A:854
ASP A:855
MET A:1002
GLY A:796
LEU A:844
VAL A:726
THR A:790
MET A:766
LEU A:788
PHE A:856
MET A:793
LEU A:792
GLN A:791
ALA A:743
LEU A:858
Interactions
van der Waals
Conventional Hydrogen Bond
Carbon Hydrogen Bond
Unfavorable Donor-Donor
Pi-Alkyl

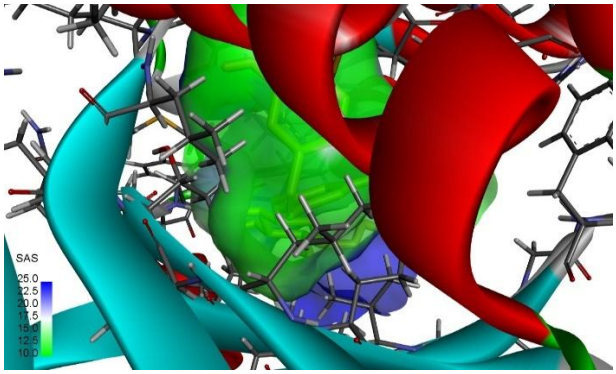
SAS

C

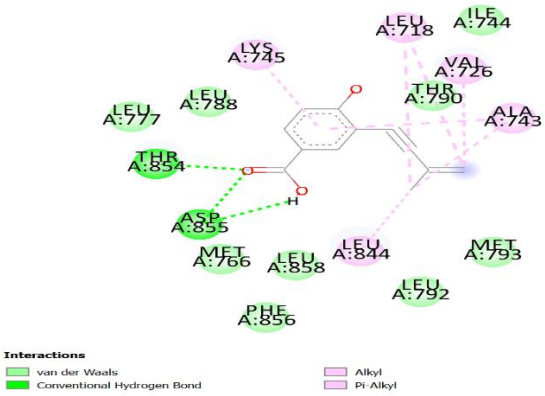
LEU A:718
ILE A:744
LYS A:745
VAL A:726
THR A:790
LEU A:788
LEU A:777
ALA A:743
THR A:854
ASP A:855
MET A:766
LEU A:858
LEU A:844
MET A:793
LEU A:792
PHE A:856
Interactions
van der Waals
Conventional Hydrogen Bond
Alkyl
Pi-Alkyl

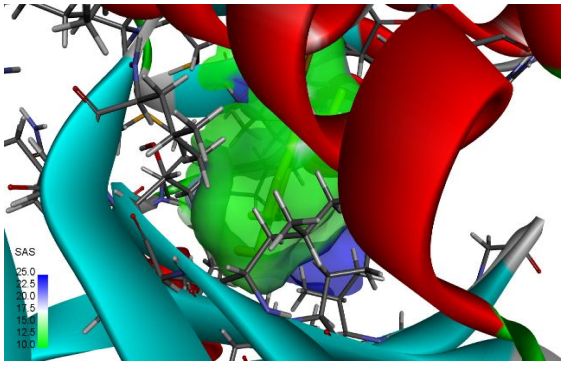
SAS

D

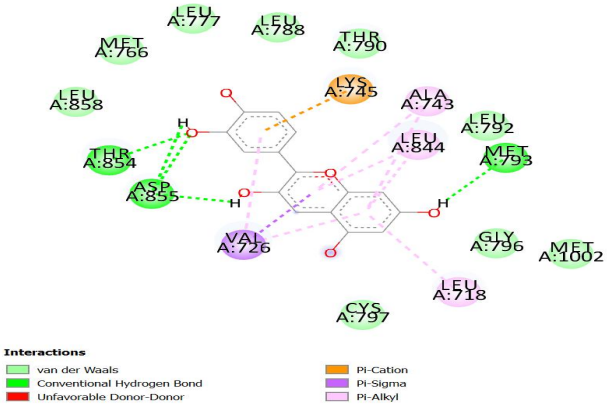
LEU A:777
LEU A:788
MET A:766
THR A:790
LYS A:745
LEU A:858
ALA A:743
LEU A:792
LEU A:844
THR A:854
MET A:793
ASP A:855
VAL A:726
GLY A:796
MET A:1002
LEU A:718
CYS A:797
Interactions
van der Waals
Conventional Hydrogen Bond
Unfavorable Donor-Donor
Pi-Cation
Pi-Sigma
Pi-Alkyl

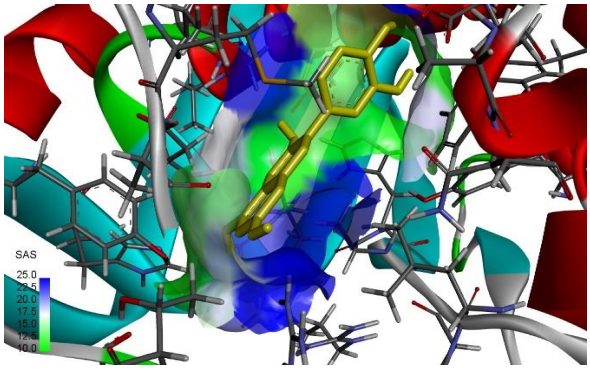
SAS

E

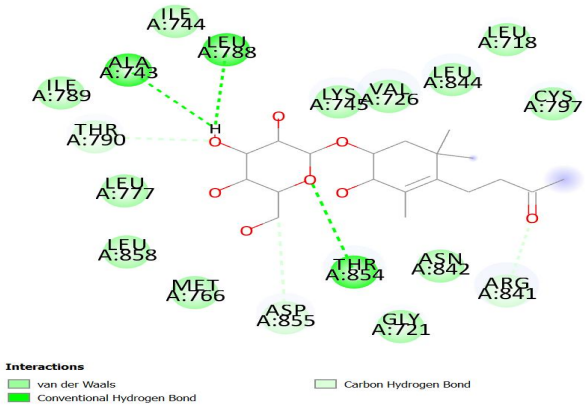
ILE A:744
LEU A:788
ALA A:743
ILE A:789
THR A:790
LEU A:777
LEU A:858
MET A:766
ASP A:855
THR A:854
ASN A:842
ARG A:841
GLY A:721
LYS A:745
VAL A:726
LEU A:844
CYS A:797
LEU A:718
Interactions
van der Waals
Conventional Hydrogen Bond
Carbon Hydrogen Bond

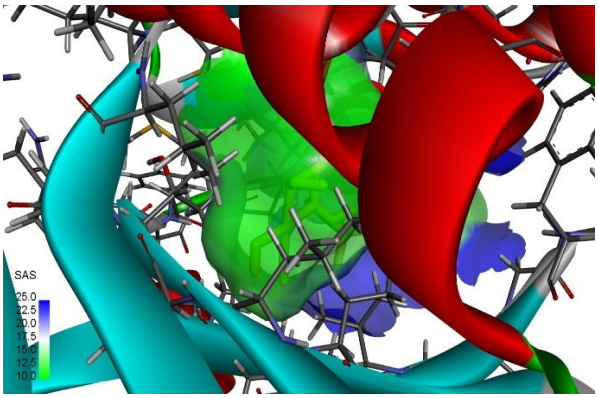
SAS

F

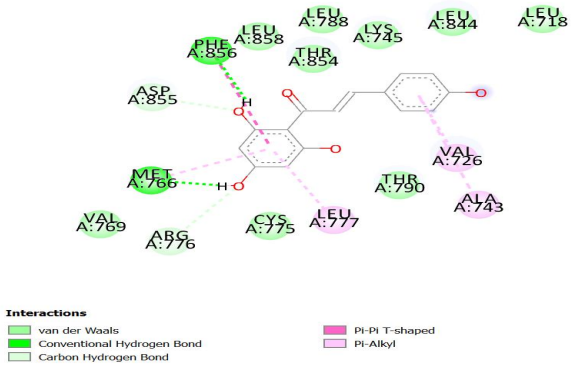
LEU A:788
LEU A:858
LYS A:745
LEU A:844
LEU A:718
PHE A:856
THR A:854
ASP A:855
VAL A:726
MET A:766
THR A:790
ALA A:743
VAL A:769
ARG A:776
CYS A:775
LEU A:777
Interactions
van der Waals
Conventional Hydrogen Bond
Carbon Hydrogen Bond
Pi-Pi T-shaped
Pi-Alkyl

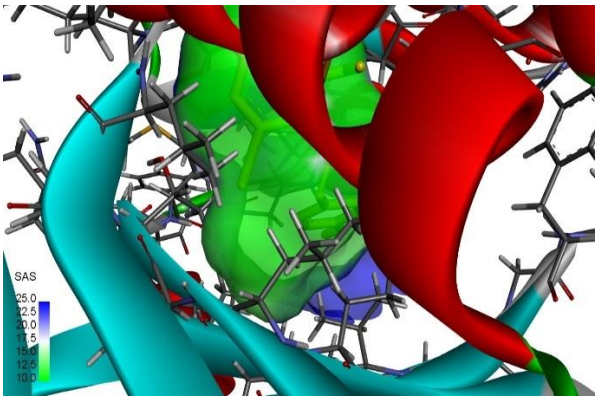
SAS

G

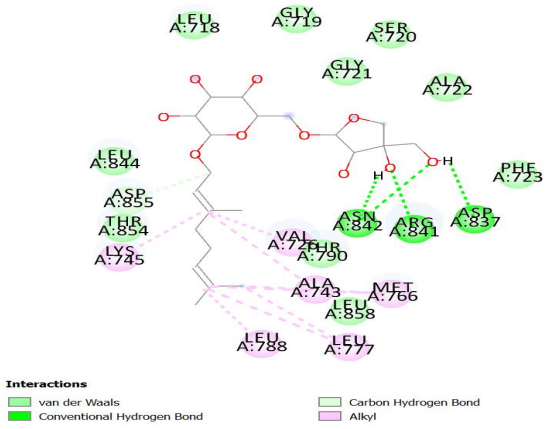
LEU A:718
GLY A:719
SER A:720
GLY A:721
ALA A:722
LEU A:844
ASP A:855
THR A:854
LYS A:745
PHE A:723
ASN A:842
ARG A:841
ASP A:837
VAL A:726
THR A:790
ALA A:743
MET A:766
LEU A:858
LEU A:788
LEU A:777
Interactions
van der Waals
Conventional Hydrogen Bond
Carbon Hydrogen Bond
Alkyl

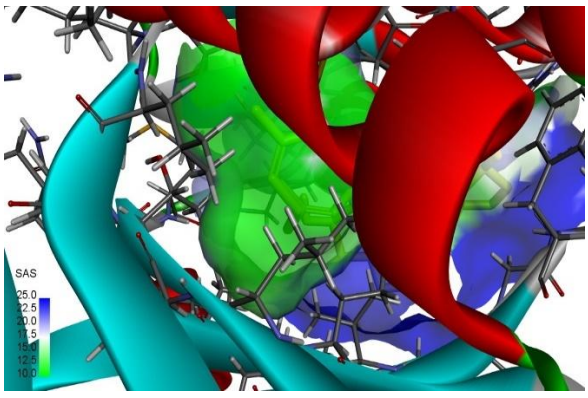
SAS

H

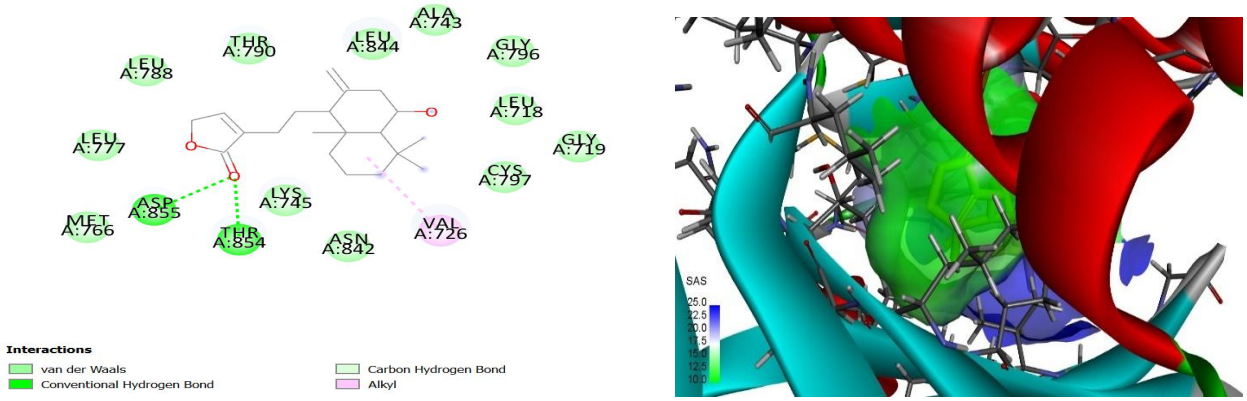

I

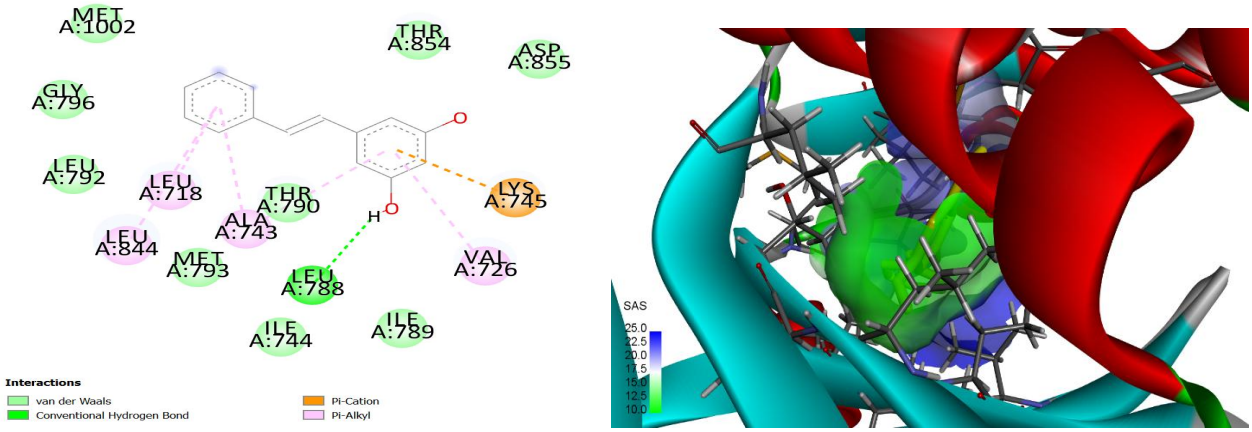

J

Figure 3.5: 2D (left) and 3D (right) views of the molecular interactions of amino-acid residues of Epidermal Growth Factor Receptor (EGFR) , 1XKK, with (A) Pinocembrin Chalcone (B) 2-Phenylethyl beta-D-galactopyranoside (C) cis-Astringin (D) 4-Hydroxy-3-(3-methylbut-3-en-1-ynyl)benzoic acid (E) Cyanidin (F) Icariside B8 (G) Naringenin Chalcone (H) Acuminoside (I) (3E)-3-[2-[(1S,4R,4aS,8aR)-4-hydroxy-5,5,8a-trimethyl-2-methylidene-3,4,4a,6,7,8-hexahydro-1H-naphthalen-1-yl]ethylidene]oxolan-2-one (J) Pinosylvin in *Vitis vinifera*.

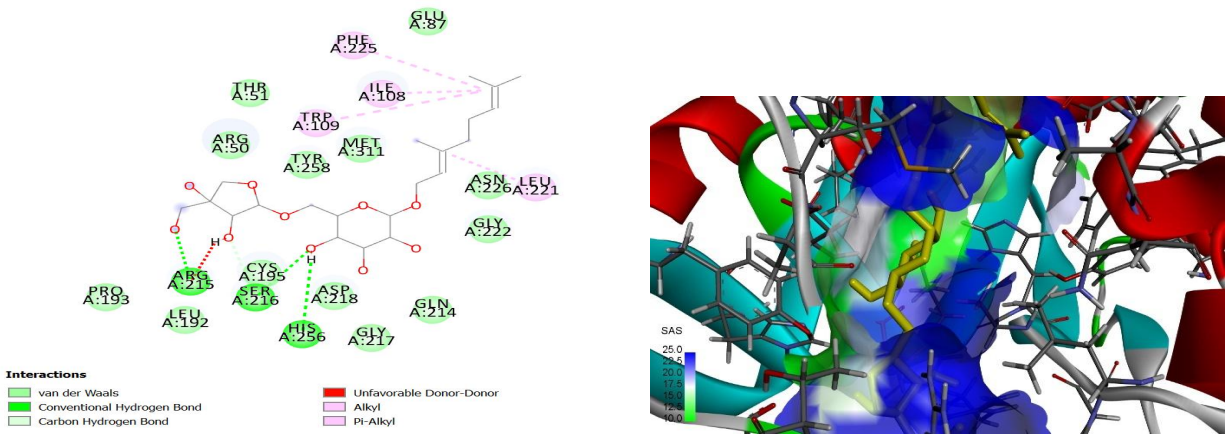
GLU A:87
PHE A:225
THR A:51
ILE A:108
TRP A:109
ARG A:50
MET A:311
TYR A:258
ASN A:226
LEU A:221
GLY A:222
ARG A:215
CYS A:195
PRO A:193
SER A:216
ASP A:218
GLN A:214
LEU A:192
HIS A:256
GLY A:217
Interactions
van der Waals
Conventional Hydrogen Bond
Carbon Hydrogen Bond
Unfavorable Donor-Donor
Alkyl
Pi-Alkyl
SAS
25.0
20.0
17.5
15.0
10.0

A

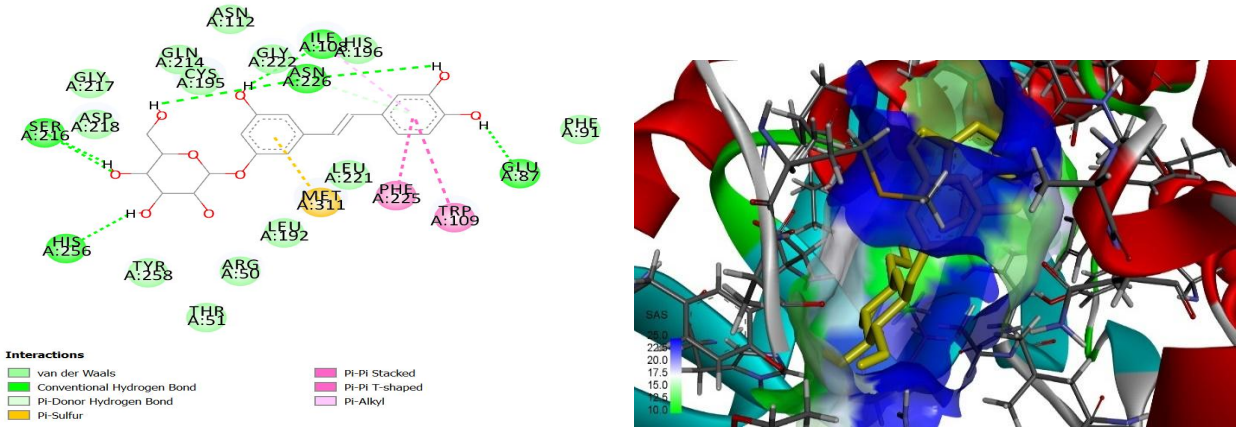
ASN A:112
GLN A:214
ILE A:108
HIS A:196
GLY A:222
GLY A:217
CYS A:195
ASN A:226
SER A:216
ASP A:218
PHE A:91
LEU A:221
GLU A:87
MET A:311
PHE A:225
TRP A:109
LEU A:192
HIS A:256
TYR A:258
ARG A:50
THR A:51
Interactions
van der Waals
Conventional Hydrogen Bond
Pi-Donor Hydrogen Bond
Pi-Sulfur
Pi-Pi Stacked
Pi-Pi T-shaped
Pi-Alkyl
SAS
20.0
17.5
15.0
10.0

B

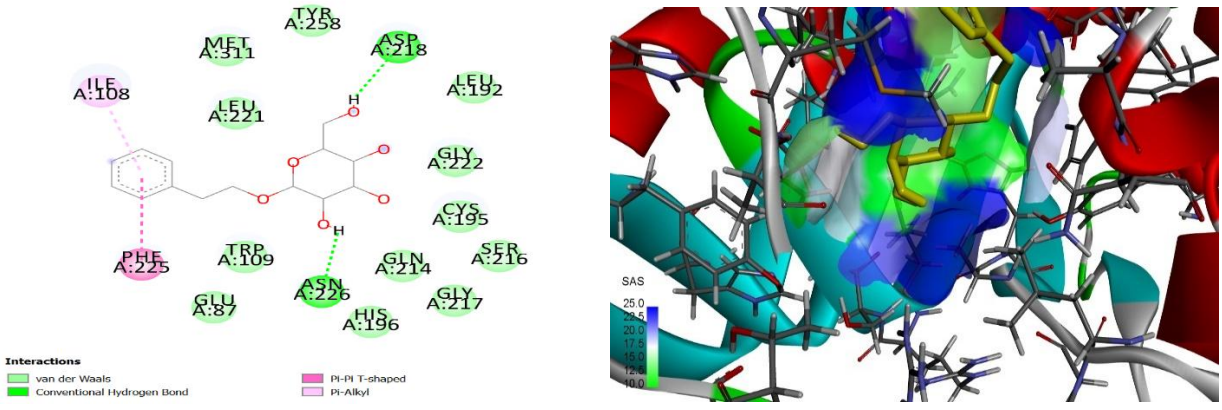
TYR A:258
MET A:311
ASP A:218
ILE A:108
LEU A:192
LEU A:221
GLY A:222
CYS A:195
PHE A:225
TRP A:109
GLN A:214
SER A:216
ASN A:226
GLU A:87
GLY A:217
HIS A:196
Interactions
van der Waals
Conventional Hydrogen Bond
Pi-Pi T-shaped
Pi-Alkyl
SAS
25.0
20.0
17.5
15.0
10.0

C

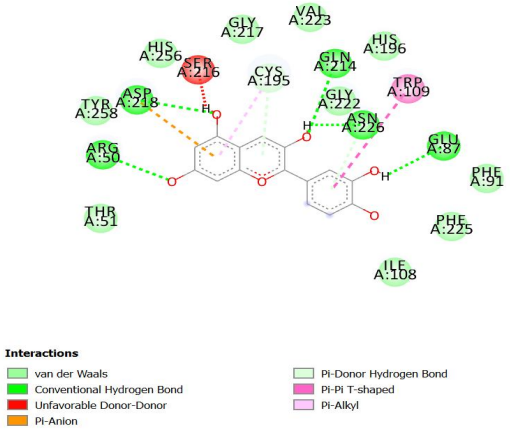
VAL A:223
GLY A:217
HIS A:256
SER A:216
CYS A:195
HIS A:196
GLN A:214
TRP A:109
GLY A:222
ASP A:218
TYR A:258
ASN A:226
GLU A:87
ARG A:50
PHE A:51
THR A:51
PHE A:225
ILE A:108
Interactions
van der Waals
Conventional Hydrogen Bond
Unfavorable Donor-Donor
Pi-Anion
Pi-Donor Hydrogen Bond
Pi-Pi T-shaped
Pi-Alkyl

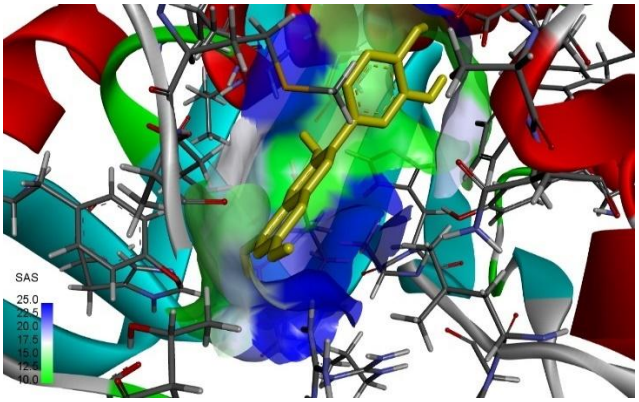
SAS
25.0
20.0
17.5
15.0
10.0

D

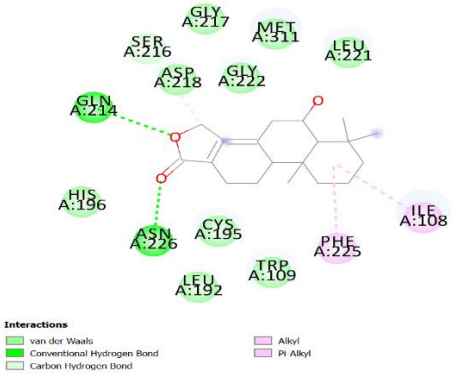
GLY A:217
MET A:311
SER A:216
LEU A:221
ASP A:218
GLY A:222
GLN A:214
HIS A:196
ILE A:108
CYS A:195
ASN A:226
PHE A:225
TRP A:109
LEU A:192
Interactions
van der Waals
Conventional Hydrogen Bond
Carbon Hydrogen Bond
Alkyl
Pi Alkyl

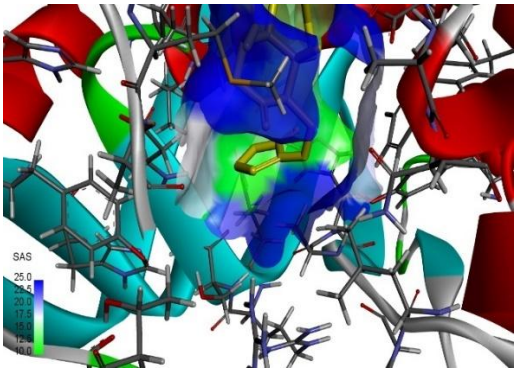
SAS
25.0
20.0
17.5
15.0
10.0

E

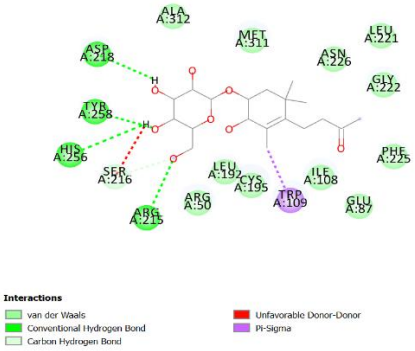
ALA A:312
MET A:311
LEU A:221
ASP A:218
ASN A:226
GLY A:222
TYR A:258
HIS A:256
PHE A:225
SER A:216
LEU A:192
CYS A:195
ILE A:108
ARG A:50
TRP A:109
GLU A:87
ARG A:215
Interactions
van der Waals
Conventional Hydrogen Bond
Carbon Hydrogen Bond
Unfavorable Donor-Donor
Pi-Sigma

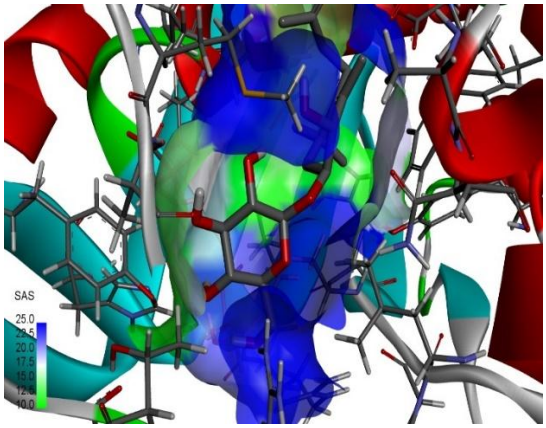
SAS
25.0
20.0
17.5
15.0
10.0

F

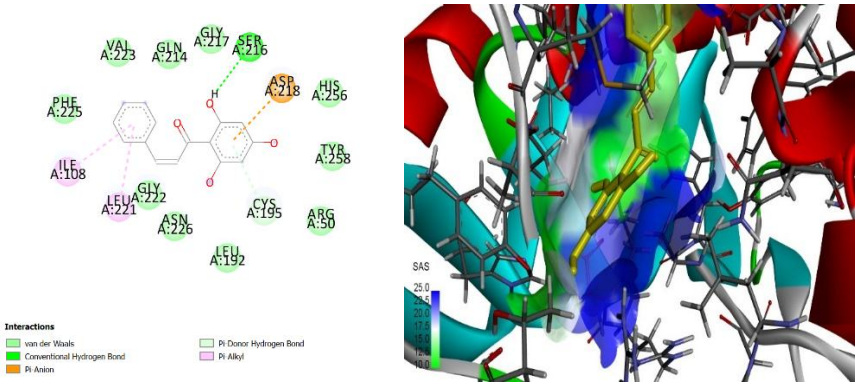

G

Fig. 3.6: 2D (left) and 3D (right) views of the molecular interactions of amino-acid residues of Human Thymidylate Synthase enzyme, 1HVY, with (A) Acuminoside (B) cis-Astringin (C) 2-Phenylethyl beta-D-galactopyranoside (D) Cyanidin (E) (3E)-3-[2-[(1S,4R,4aS,8aR)-4-hydroxy-5,5,8a-trimethyl-2-methylidene-3,4,4a,6,7,8-hexahydro-1H-naphthalen-1-yl]ethylidene]oxolan-2-one

(F) Icariside B8 (G) Pinocembrin Chalcone in *Vitis vinifera.*

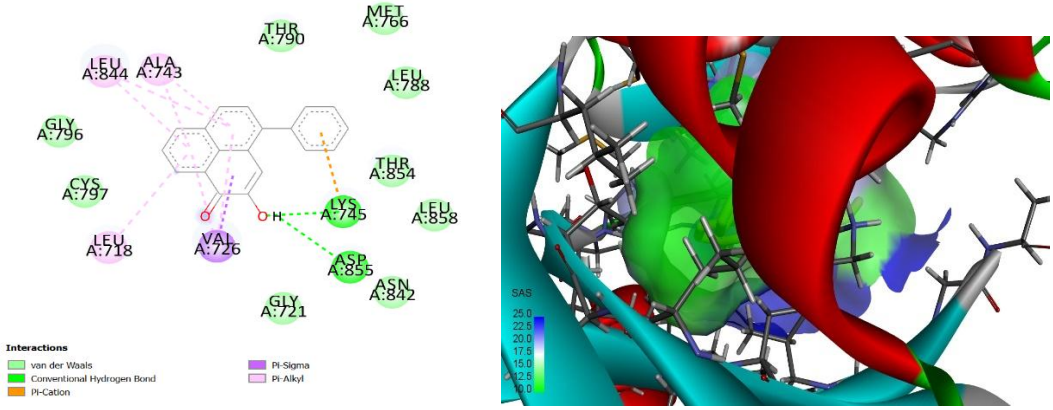

A

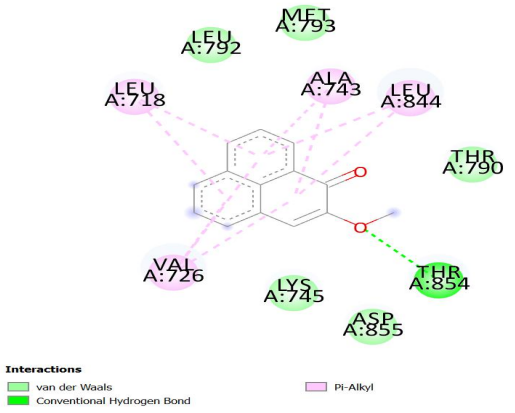
MET A:793
LEU A:792
LEU A:718
ALA A:743
LEU A:844
THR A:790
VAL A:726
LYS A:745
THR A:854
ASP A:855
Interactions
van der Waals
Conventional Hydrogen Bond
Pi-Alkyl

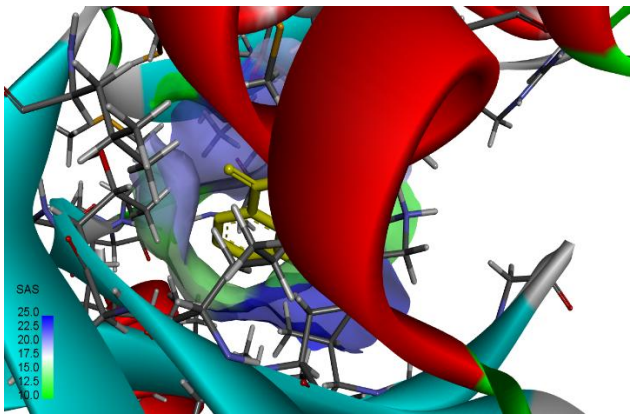
SAS
25.0
22.5
20.0
17.5
15.0
12.5
10.0

B

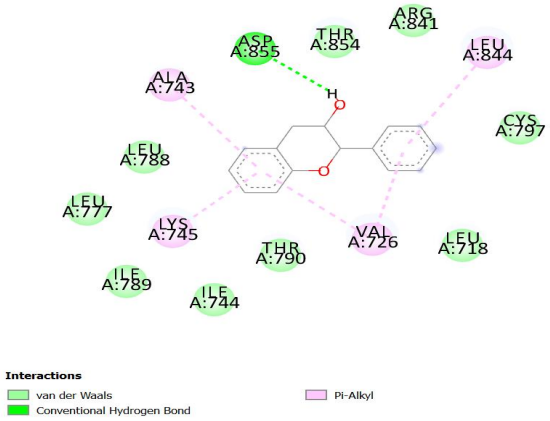
ARG A:841
ASP A:855
THR A:854
LEU A:844
ALA A:743
H
CYS A:797
LEU A:788
LEU A:777
LYS A:745
VAL A:726
LEU A:718
THR A:790
ILE A:789
ILE A:744
Interactions
van der Waals
Conventional Hydrogen Bond
Pi-Alkyl

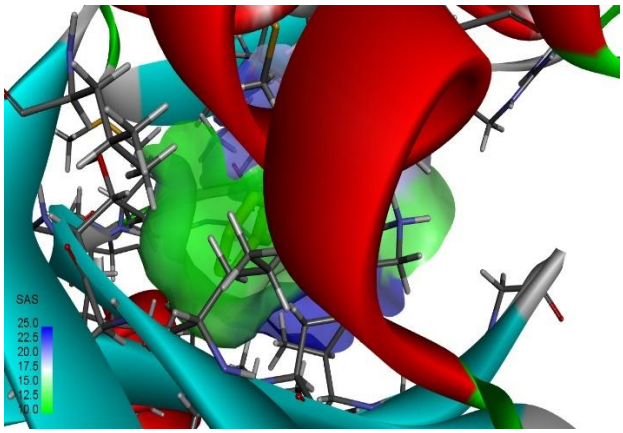
SAS
25.0
22.5
20.0
17.5
15.0
12.5
10.0

C

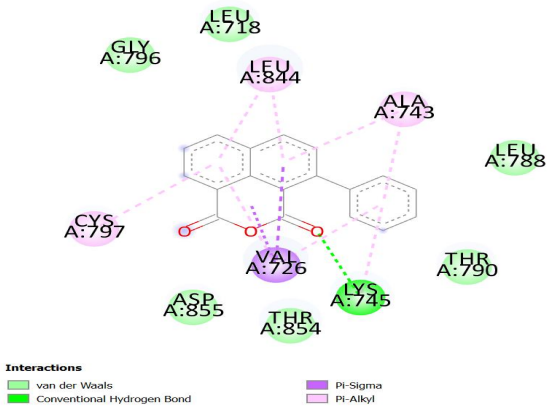
LEU A:718
GLY A:796
LEU A:844
ALA A:743
LEU A:788
CYS A:797
VAL A:726
THR A:790
LYS A:745
ASP A:855
THR A:854
Interactions
van der Waals
Conventional Hydrogen Bond
Pi-Sigma
Pi-Alkyl

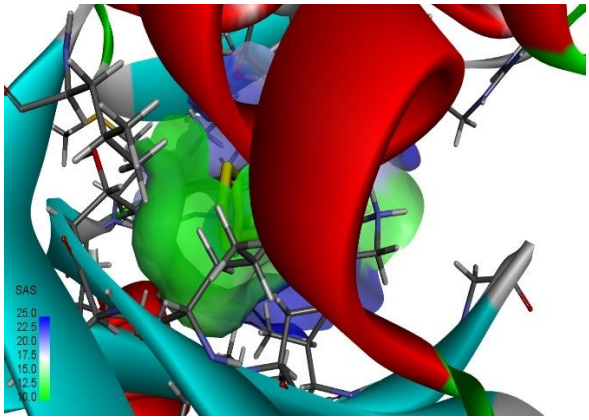
SAS
25.0
22.5
20.0
17.5
15.0
12.5
10.0

D

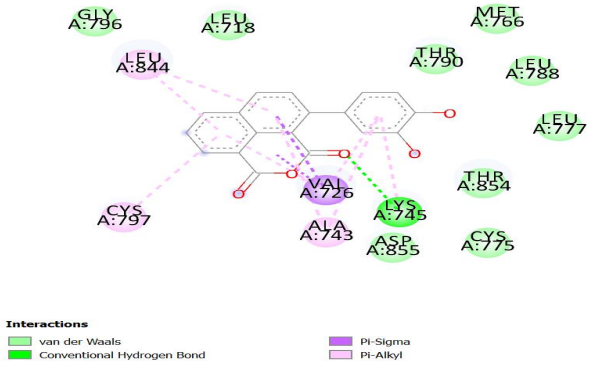
GLY A:796
LEU A:718
MET A:766
LEU A:844
THR A:790
LEU A:788
LEU A:777
THR A:854
VAL A:726
LYS A:745
CYS A:797
ALA A:743
ASP A:855
CYS A:775
Interactions
van der Waals
Conventional Hydrogen Bond
Pi-Sigma
Pi-Alkyl

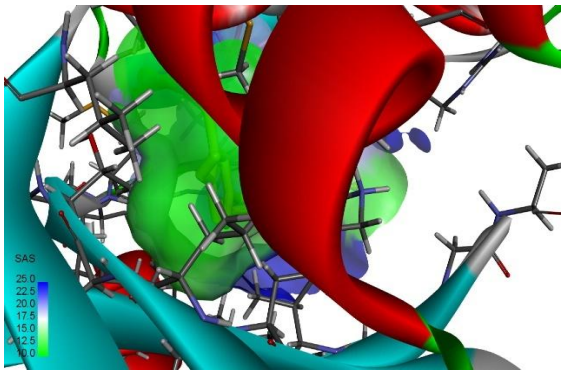
SAS
25.0
22.5
20.0
17.5
15.0
12.5
10.0

E

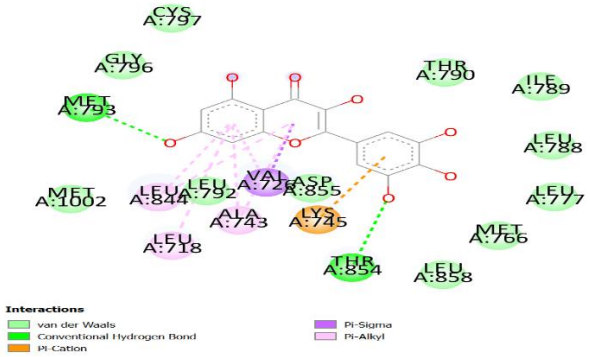
CYS A:797
GLY A:796
THR A:790
ILE A:789
MET A:793
LEU A:788
MET A:1002
LEU A:844
LEU A:792
VAL A:726
ASP A:855
LEU A:777
ALA A:743
LYS A:745
MET A:766
LEU A:718
THR A:854
LEU A:858
Interactions
van der Waals
Conventional Hydrogen Bond
Pi-Cation
Pi-Sigma
Pi-Alkyl

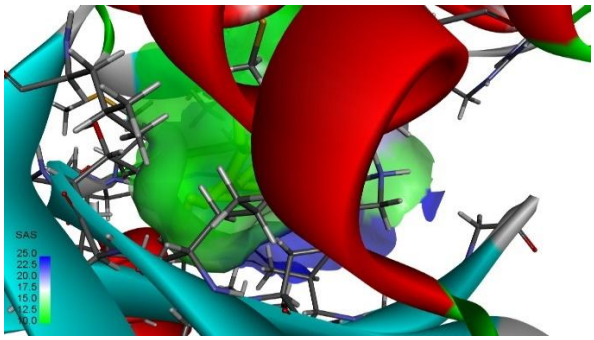
SAS
25.0
22.5
20.0
17.5
15.0
12.5
10.0

F

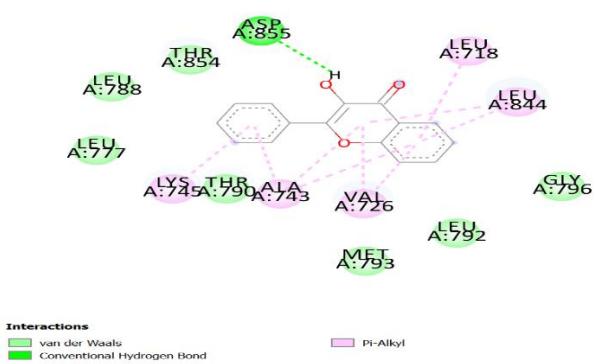
ASP A:855
THR A:854
LEU A:718
LEU A:788
LEU A:844
LEU A:777
LYS A:745
THR A:790
ALA A:743
VAL A:726
GLY A:796
LEU A:792
MET A:793
Interactions
van der Waals
Conventional Hydrogen Bond
Pi-Alkyl

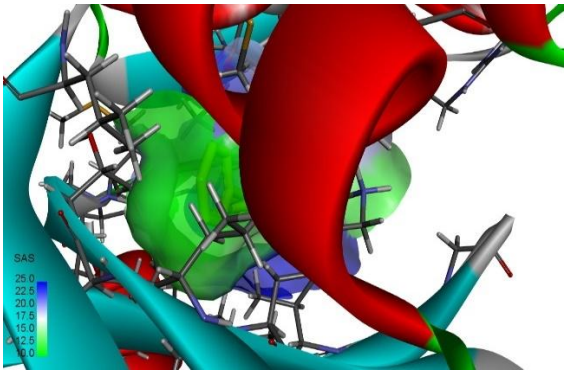
SAS
25.0
22.5
20.0
17.5
15.0
12.5
10.0

G

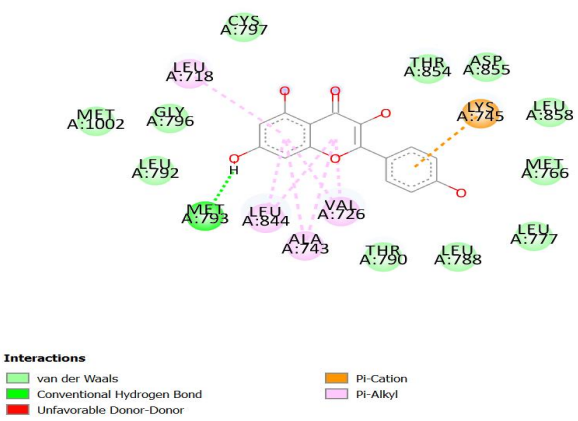
CYS A:797
LEU A:718
THR A:854
ASP A:855
MET A:1002
GLY A:796
LYS A:745
LEU A:858
LEU A:792
MET A:766
MET A:793
LEU A:844
VAL A:726
ALA A:743
LEU A:777
THR A:790
LEU A:788
Interactions
van der Waals
Conventional Hydrogen Bond
Unfavorable Donor-Donor
Pi-Cation
Pi-Alkyl

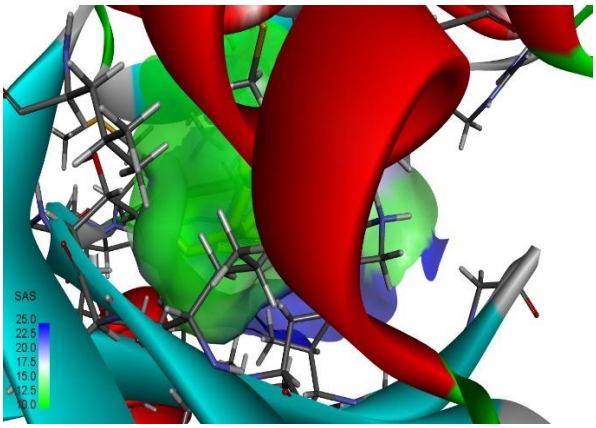
SAS
25.0
22.5
20.0
17.5
15.0
12.5
10.0

H

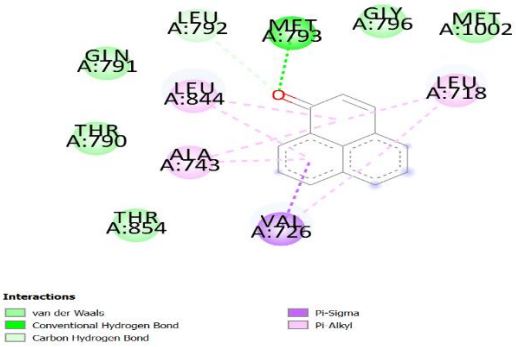
LEU A:792
MET A:793
GLY A:796
MET A:1002
GLN A:791
LEU A:844
LEU A:718
THR A:790
ALA A:743
THR A:854
VAL A:726
Interactions
van der Waals
Conventional Hydrogen Bond
Carbon Hydrogen Bond
Pi-Sigma
Pi Alkyl

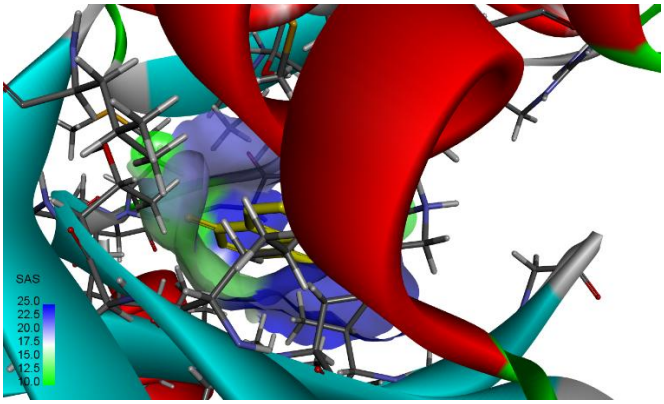
SAS
25.0
22.5
20.0
17.5
15.0
12.5
10.0

I

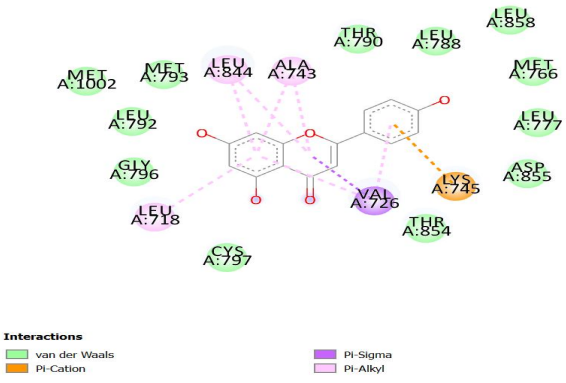
LEU A:858
THR A:790
LEU A:788
MET A:1002
MET A:793
LEU A:844
ALA A:743
MET A:766
LEU A:792
LEU A:777
GLY A:796
LYS A:745
ASP A:855
VAL A:726
LEU A:718
THR A:854
CYS A:797
Interactions
van der Waals
Pi-Cation
Pi-Sigma
Pi-Alkyl

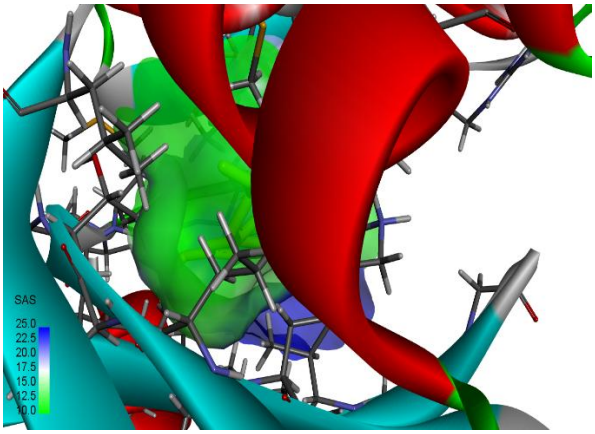
SAS
25.0
22.5
20.0
17.5
15.0
12.5
10.0

J

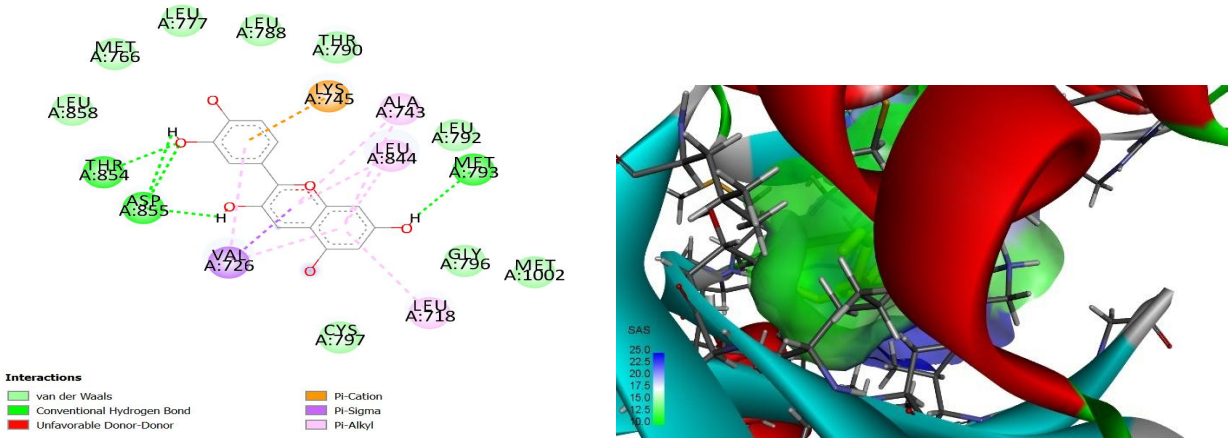

K

Fig. 3.7: 2D (left) and 3D (right) views of the molecular interactions of amino-acid residues of Epidermal Growth Factor Receptor (EGFR) , 1XKK, with (A) 2-hydroxy-4-phenylphenalen-1-one (B) 2-methoxyphenalen-1-one (C) 3-Flavanol (D) 4-Phenyl-1H,3H-naphtho(1,8-cd)pyran-1,3-dione (E) 2-(3,4-Dihydroxyphenyl)naphthalic anhydride (F) Myricetin (G) Flavonol (H) Kaempferol (I) Phenalenone (J) Quercetin (K) Cyanidin in *Brassica oleracaea*.

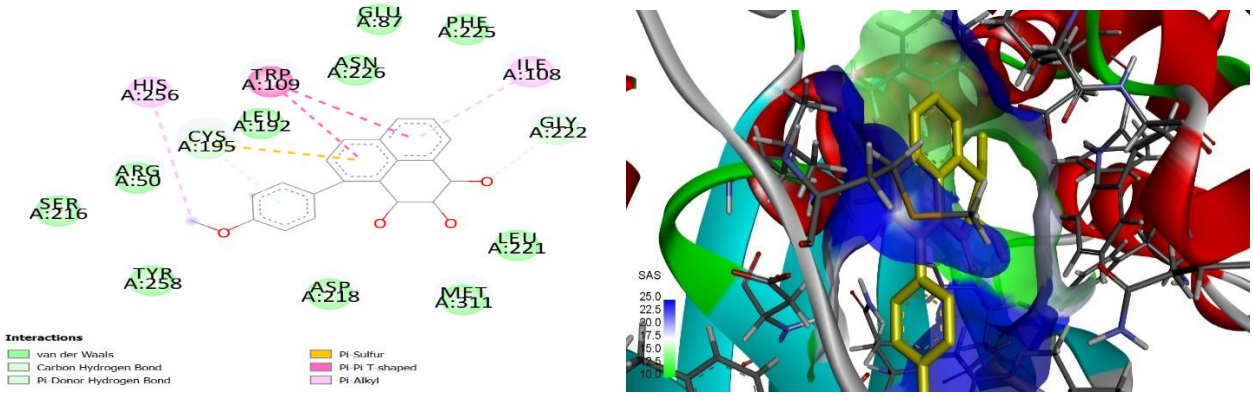

A

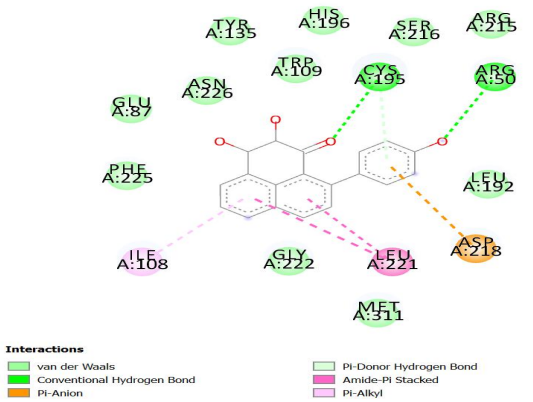
TYR A:135
HIS A:196
SER A:216
ARG A:215
TRP A:109
CYS A:195
ARG A:50
ASN A:226
GLU A:87
PHE A:225
LEU A:192
ASP A:218
ILE A:108
GLY A:222
LEU A:221
MET A:311
Interactions
van der Waals
Conventional Hydrogen Bond
Pi-Anion
Pi-Donor Hydrogen Bond
Amide-Pi Stacked
Pi-Alkyl

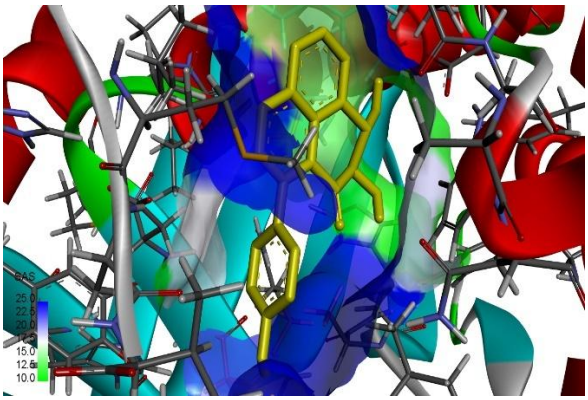
SAS
25.0
22.5
20.0
15.0
12.5
10.0

B

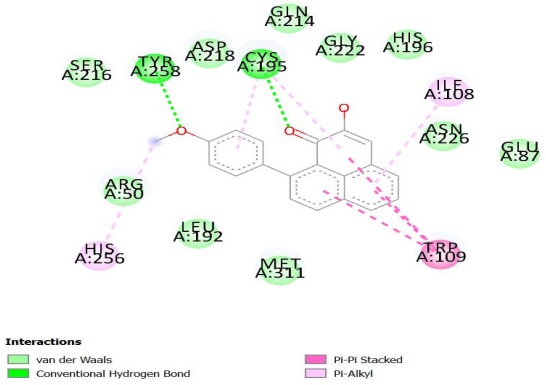
GLN A:214
ASP A:218
GLY A:222
HIS A:196
SER A:216
TYR A:258
CYS A:195
ILE A:108
ASN A:226
GLU A:87
ARG A:50
LEU A:192
HIS A:256
MET A:311
TRP A:109
Interactions
van der Waals
Conventional Hydrogen Bond
Pi-Pi Stacked
Pi-Alkyl

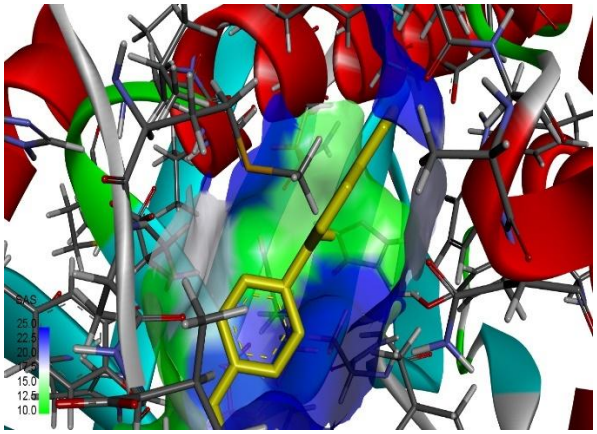
SAS
25.0
22.5
20.0
15.0
12.5
10.0

C

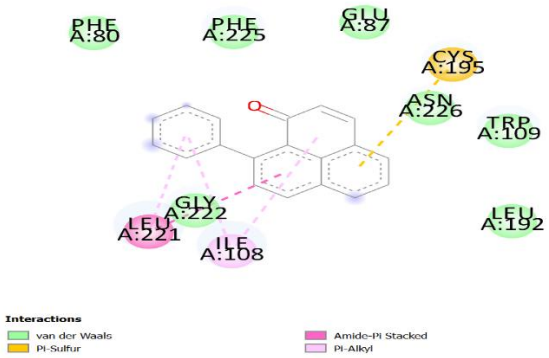
PHE A:80
PHE A:225
GLU A:87
CYS A:195
ASN A:226
TRP A:109
GLY A:222
LEU A:221
LEU A:192
ILE A:108
Interactions
van der Waals
Pi-Sulfur
Amide-Pi Stacked
Pi-Alkyl

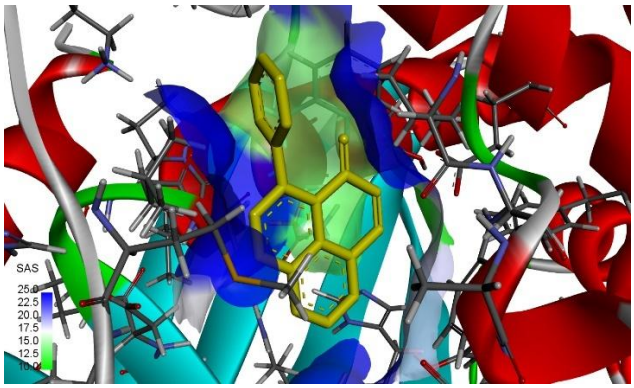
SAS
25.0
22.5
20.0
17.5
15.0
12.5

D

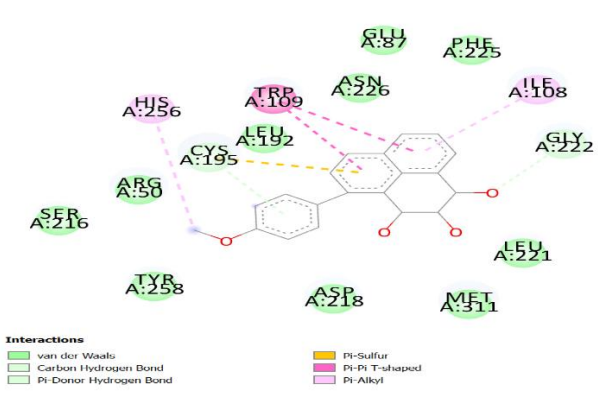
GLU A:87
PHE A:225
ASN A:226
ILE A:108
HIS A:256
TRP A:109
LEU A:192
GLY A:222
CYS A:195
ARG A:50
SER A:216
LEU A:221
TYR A:258
ASP A:218
MET A:311
Interactions
van der Waals
Carbon Hydrogen Bond
Pi-Donor Hydrogen Bond
Pi-Sulfur
Pi-Pi T-shaped
Pi-Alkyl

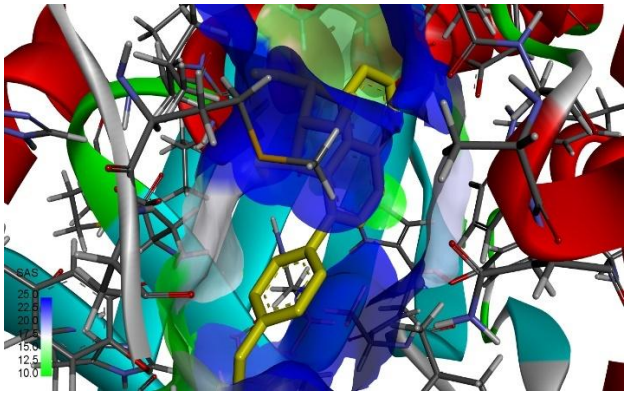

E

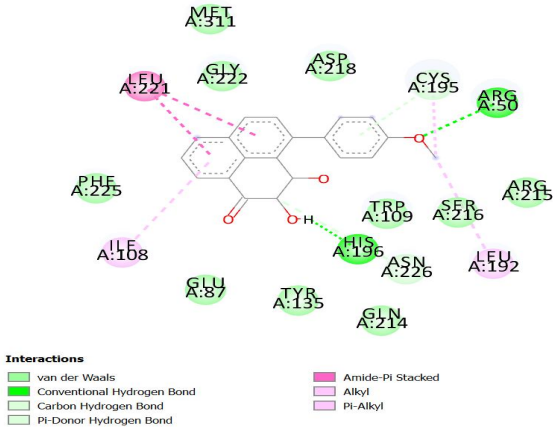
MET A:311
GLY A:222
ASP A:218
LEU A:221
CYS A:195
ARG A:50
PHE A:225
ARG A:215
TRP A:109
SER A:216
ILE A:108
HIS A:196
ASN A:226
LEU A:192
GLU A:87
TYR A:135
GLN A:214
Interactions
van der Waals
Conventional Hydrogen Bond
Carbon Hydrogen Bond
Pi-Donor Hydrogen Bond
Amide-Pi Stacked
Alkyl
Pi-Alkyl

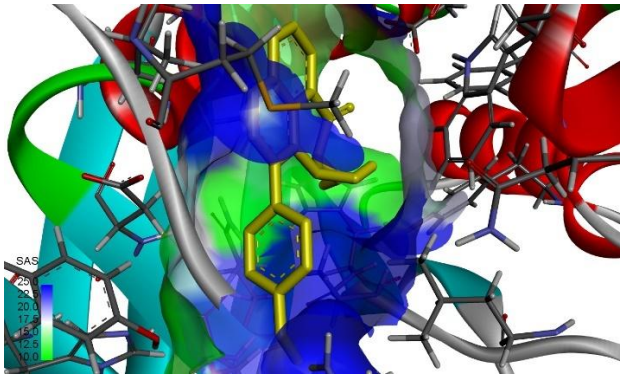

F

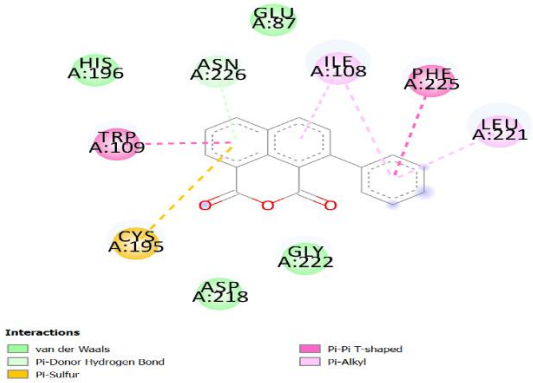
GLU A:87
HIS A:196
ASN A:226
ILE A:108
PHE A:225
TRP A:109
LEU A:221
CYS A:195
GLY A:222
ASP A:218
Interactions
van der Waals
Pi-Donor Hydrogen Bond
Pi-Sulfur
Pi-Pi T-shaped
Pi-Alkyl

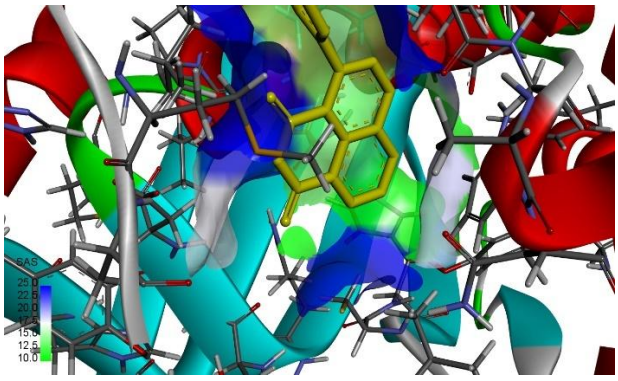

G

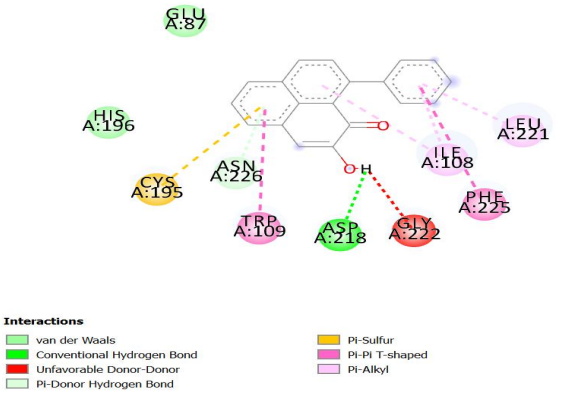
GLU A:87
HIS A:196
LEU A:221
ILE A:108
ASN A:226
CYS A:195
PHE A:225
TRP A:109
ASP A:218
GLY A:222
Interactions
van der Waals
Conventional Hydrogen Bond
Unfavorable Donor-Donor
Pi-Donor Hydrogen Bond
Pi-Sulfur
Pi-Pi T-shaped
Pi-Alkyl

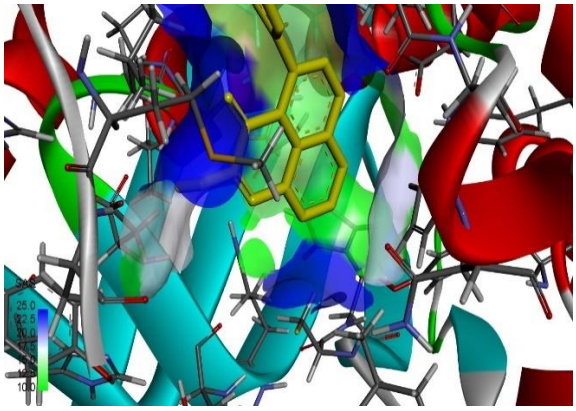

H

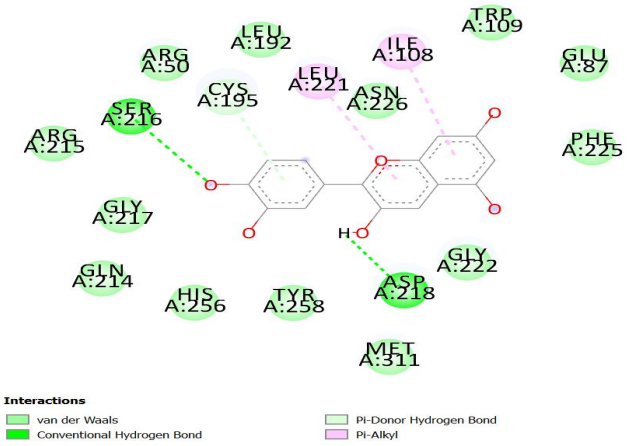
TRP A:109
LEU A:192
ILE A:108
ARG A:50
GLU A:87
CYS A:195
LEU A:221
ASN A:226
SER A:216
ARG A:215
PHE A:225
GLY A:217
GLY A:222
GLN A:214
ASP A:218
HIS A:256
TYR A:258
MET A:311
Interactions
van der Waals
Conventional Hydrogen Bond
Pi-Donor Hydrogen Bond
Pi-Alkyl

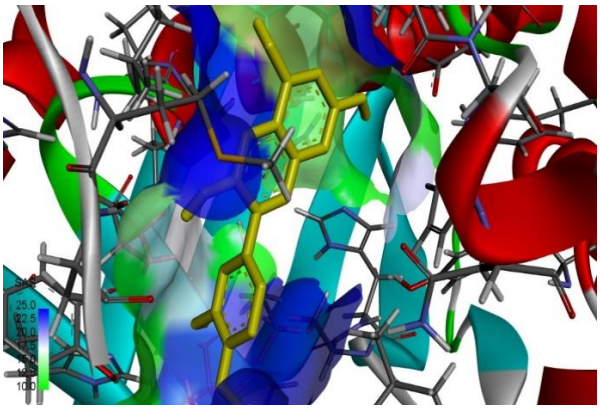

I

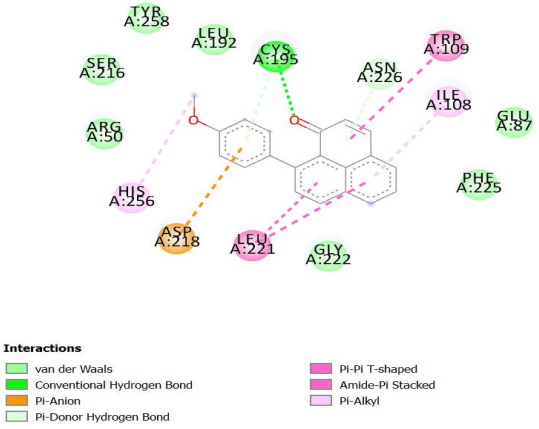
TYR A:258
LEU A:192
CYS A:195
TRP A:109
SER A:216
ASN A:226
ILE A:108
GLU A:87
ARG A:50
PHE A:225
HIS A:256
ASP A:218
LEU A:221
GLY A:222
Interactions
van der Waals
Conventional Hydrogen Bond
Pi-Anion
Pi-Donor Hydrogen Bond
Pi-Pi T-shaped
Amide-Pi Stacked
Pi-Alkyl

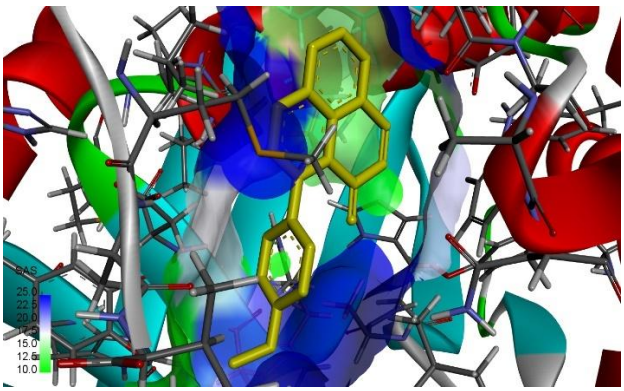

J

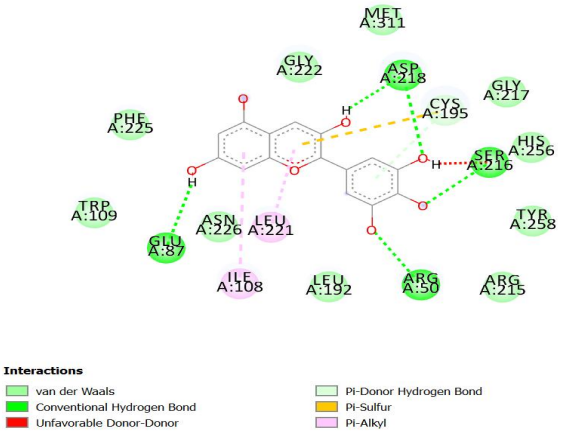
MET A:311
GLY A:222
ASP A:218
GLY A:217
CYS A:195
PHE A:225
HIS A:256
SER A:216
TRP A:109
ASN A:226
LEU A:221
TYR A:258
GLU A:87
ILE A:108
LEU A:192
ARG A:50
ARG A:215
Interactions
van der Waals
Conventional Hydrogen Bond
Unfavorable Donor-Donor
Pi-Donor Hydrogen Bond
Pi-Sulfur
Pi-Alkyl

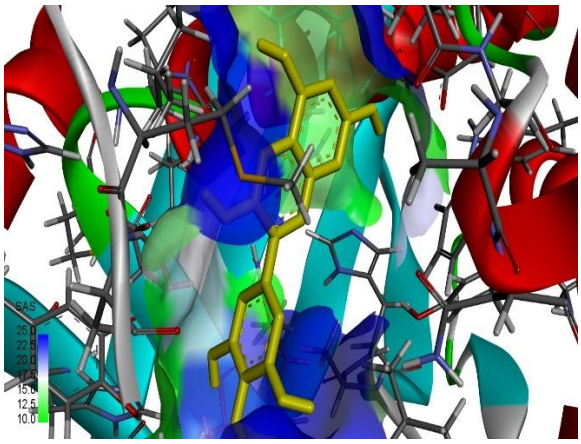
SAS

K

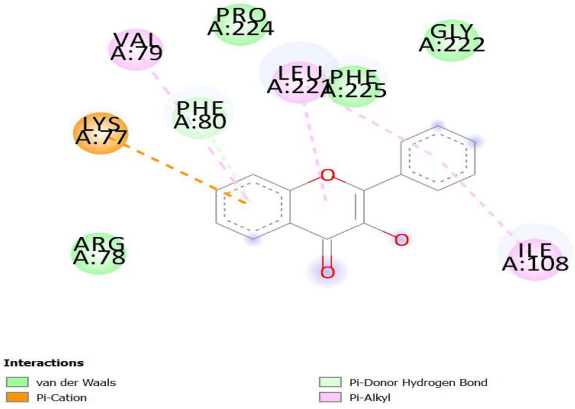
PRO A:224
VAL A:79
GLY A:222
LEU A:224
PHE A:225
PHE A:80
LYS A:77
ARG A:78
ILE A:108
Interactions
van der Waals
Pi-Cation
Pi-Donor Hydrogen Bond
Pi-Alkyl

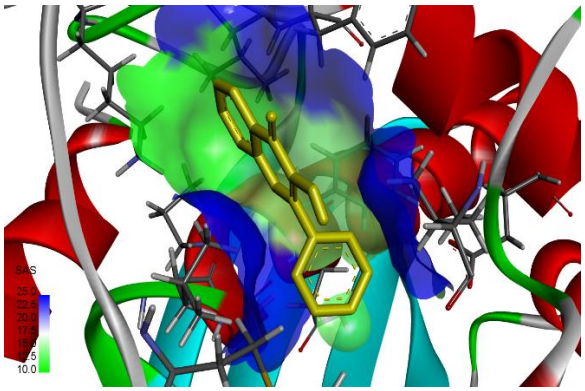
SAS

L

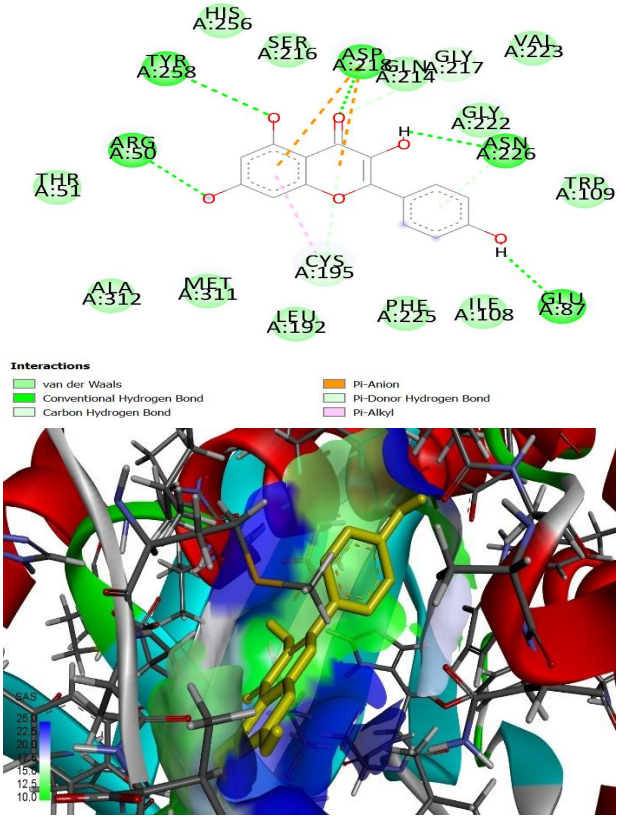
HIS A:256
SER A:216
ASP A:218
GLN A:214
GLY A:217
VAL A:223
TYR A:258
GLY A:222
ARG A:50
ASN A:226
THR A:51
TRP A:109
CYS A:195
ALA A:312
MET A:311
LEU A:192
PHE A:225
ILE A:108
GLU A:87
Interactions
van der Waals
Conventional Hydrogen Bond
Carbon Hydrogen Bond
Pi-Anion
Pi-Donor Hydrogen Bond
Pi-Alkyl

M

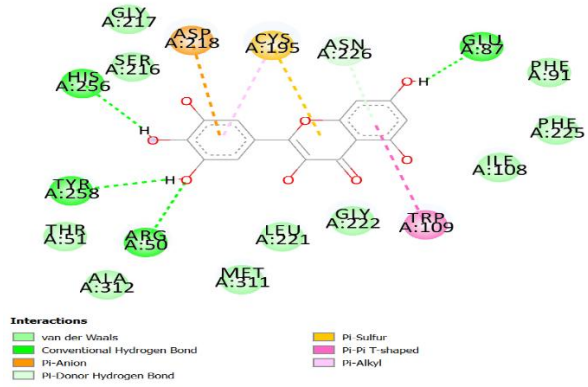
GLY A:217
ASP A:218
CYS A:195
ASN A:226
GLU A:87
SER A:216
PHE A:91
HIS A:256
PHE A:225
ILE A:108
TYR A:258
GLY A:222
TRP A:109
THR A:51
ARG A:50
LEU A:221
ALA A:312
MET A:311
Interactions
van der Waals
Conventional Hydrogen Bond
Pi-Anion
Pi-Donor Hydrogen Bond
Pi-Sulfur
Pi-Pi T-shaped
Pi-Alkyl

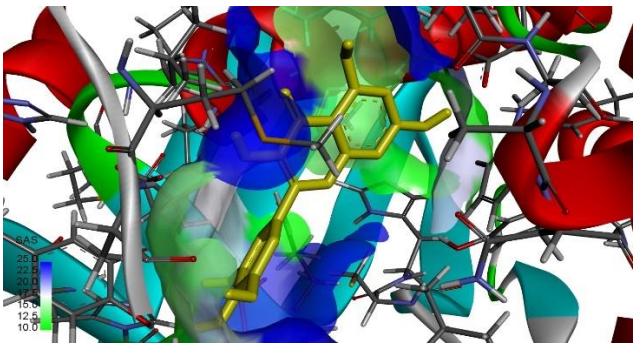

N

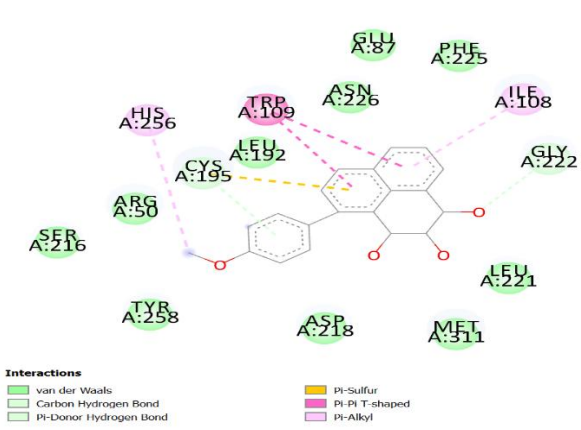
GLU A:87
PHE A:225
ASN A:226
ILE A:108
HIS A:256
TRP A:109
LEU A:192
GLY A:222
CYS A:195
ARG A:50
SER A:216
LEU A:221
TYR A:258
ASP A:218
MET A:311
Interactions
van der Waals
Carbon Hydrogen Bond
Pi-Donor Hydrogen Bond
Pi-Sulfur
Pi-Pi T-shaped
Pi-Alkyl

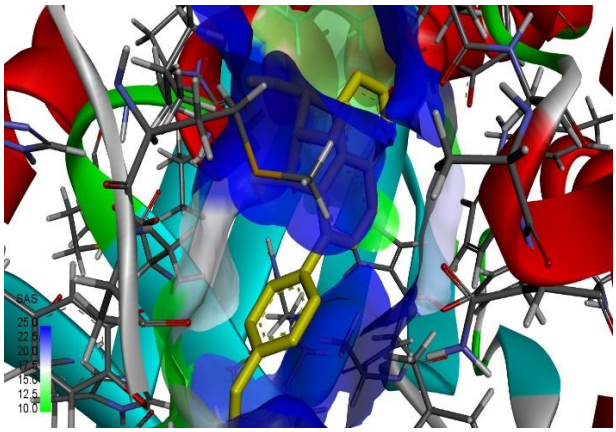
SAS
25.0
22.5
20.0
17.5
15.0
12.5
10.0

O

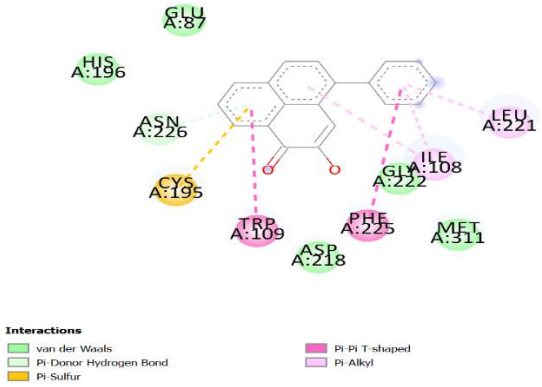
GLU A:87
HIS A:196
ASN A:226
LEU A:221
ILE A:108
GLY A:222
CYS A:195
TRP A:109
PHE A:225
MET A:311
ASP A:218
Interactions
van der Waals
Pi-Donor Hydrogen Bond
Pi-Sulfur
Pi-Pi T-shaped
Pi-Alkyl

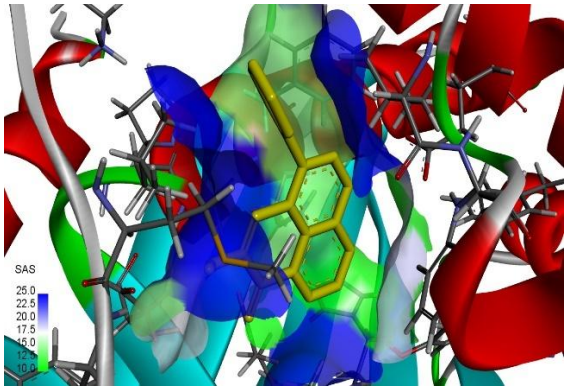
SAS
25.0
22.5
20.0
17.5
15.0
12.5
10.0

P

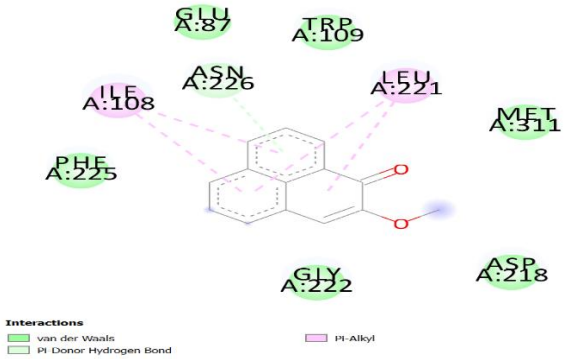
GLU A:87
TRP A:109
ASN A:226
ILE A:108
LEU A:221
MET A:311
PHE A:225
GLY A:222
ASP A:218
Interactions
van der Waals
Pi-Donor Hydrogen Bond
Pi-Alkyl

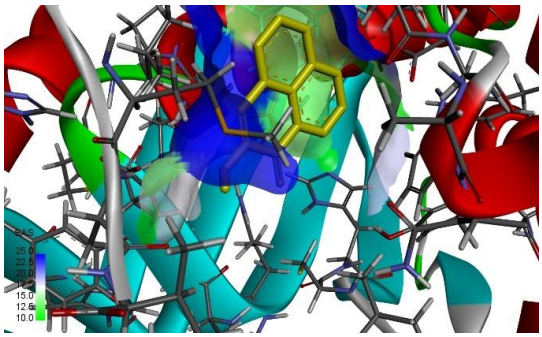
SAS
25.0
22.5
20.0
17.5
15.0
12.5
10.0

Q

Fig. 3.8: 2D (left) and 3D (right) views of the molecular interactions of amino-acid residues of Human Thymidylate Synthase enzyme, 1HVY, with (A) (2R,S)-2,3-dihydroxy-9-(4-hydroxyphenyl)-2,3-dihydrophenalen-1-one

(B) (2R,3S)-2,3-dihydroxy-9-(4-hydroxy-3-methoxyphenyl)-2,3-dihydrophenalen-1-one (C) 2-hydroxy-9-(4-methoxyphenyl)phenalen-1-one (D) 9-phenylphenalen-1-one (E) 2-(3,4-Dihydroxyphenyl)naphthalic anhydride (F) (2S,3S)-2,3-dihydroxy-4-(4-methoxyphenyl)-2,3-dihydrophenalen-1-one (G) 4-Phenyl-1H,3H-naphtho(1,8-cd)pyran-1,3-dione (H) Anigofurone (I) Cyanidin (J) 9-(4-methoxyphenyl)phenalen-1-one (K) Delphinidin (L) Flavonol (M) Kaempferol (N) Myricetin (O) 2,3-Dihydro-4-(4-methoxyphenyl)-1H-phenalene-1,2,3-triol (P) 2-hydroxy-4-phenylphenalen-1-one (Q) 2-methoxyphenalen-1-one in *Brassica oleracaea.*

3.2 ADME Profiling

Table 3.5 ADME Profiling of ligands from *M. oleifera*

Compound Name	**Bioavailabilty score**	**Molecular Weight (g/mol)**	**No. of Hydrogen Acceptors**	**No. of Hydrogen Donors**	**Consensus Log $P_{O/W}$**	**Lipinski**
Niazicin A	0.55	385.12	8	3	1.00	Yes
Niazicinin A	0.55	369.14	9	3	0.45	Yes
4-[(3-O-Acetyl-6-deoxy-I+/--L-mannopyranosyl)oxy]benzeneacetonitrile	0.55	385.12	8	3	1.00	Yes
O-Coumaric acid	0.55	164.05	3	2	1.9	Yes
(6Z,10E,14E,18E)-2,6,10,15,19,23-hexamethyltetracosa-2,6,10,14,18,22-hexaene	0.55	321.12	7	2	0.45	Yes
Ellagic acid	0.11	302.01	8	4	1.31	Yes

Carbonimidothioic acid, [[4-[(4-O-acetyl-6-deoxy-I+/--L-mannopyranosyl)oxy]phenyl]methyl]-, O-ethyl ester, (E)-	0.17	399.14	8	3	1.6	Yes
Dehydrodieugenol	0.56	326.15	4	2	2.82	Yes
I(2)-D-Glucopyranose, 1-(2,6-dimethylbenzoate)	0.17	312.12	7	4	2.88	Yes
(2S)-2-acetamido-3-[(Z,4Z)-4-cyclopenta[b]pyridin-5-ylidenebut-2-en-2-yl]sulfanylpropanoic acid	0.56	330.1	5	2	1.54	Yes
Kaempferol	0.17	286.23	6	4	1.82	Yes
Isorhamnetin	0.55	316.06	7	4	1.6	Yes
Myricetin	0.55	318.04	8	6	1.38	Yes

Rhamnetin	0.55	316.06	7	4	2.88	Yes
Diadzein	0.55	254.06	4	2	1.54	Yes
Apigenin	0.55	270.05	5	3	3.02	Yes
Luteolin	0.55	286.05	6	4	1.73	Yes
Genistein	0.55	270.05	5	3	3.04	Yes
[(2S,3R,4R,5S,6S)-2-[4-(cyanomethyl)phenoxy]-3,5-dihydroxy-6-methyloxan-4-yl] acetate	0.56	357.12	7	2	1.82	Yes
O-Ethyl N-((4-((6-deoxy-alpha-L-mannopyranosyl)oxy)phenyl)methyl)carbamothioate	0.55	357.12	7	4	1.64	Yes
O-methyl N-[[4-(3,4,5-trihydroxy-6-methyloxan-2-yl)oxyphenyl]methyl]carbamothioate	0.17	343.11	7	4	1.54	Yes

Table 3.6 ADME Profiling of ligands from *Olea europaea*

Compound name	**Bioavailabilty score**	**Molecular Weight (g/mol)**	**No. of Hydrogen Acceptors**	**No. of Hydrogen Donors**	**Consensus Log $P_{O/W}$**	**Lipinski**
Hydrocinchonine	0.55	296.19	3	1	2.1	Yes
Oleacin90%	0.55	320.13	6	2	1.6	Yes
Oleocanthal	0.55	304.13	5	1	1.53	Yes

Table 3.7 ADME Profiling of ligands from *V. vinifera*

Compound Name	**Bioavailability score**	**Molecular Weight (g/mol)**	**No. of Hydrogen Acceptors**	**No. of Hydrogen Donors**	**Consensus Log $P_{O/W}$**	**Lipinski**
Naringenin chalcone	0.55	272.25	5	4	1.83	Yes
Pinosylvin	0.55	212.24	2	2	4.63	Yes
Pinocembrin chalcone	0.55	256.25	4	3	2.6	Yes
2-Phenylethyl beta-D-galactopyranoside	0.55	284.31	6	4	1,39	Yes

Acuminoside	0.55	448.5	10	6	-0.54	Yes
Cyanidin	0.55	287.24	6	5	-0.8	Yes
4-Hydroxy-3-(3-methylbut-3-en-1-ynyl)benzoic acid	0.56	202.21	3	2	6.98	Yes
Icariside B8	0.55	388.45	8	5	-0.8	Yes
Cis-Astringin	0.55	406.38	9	7	4.75	Yes
(3E)-3-[2-[(1S,4R,4aS,8aR)-4-hydroxy-5,5,8a-trimethyl-2-methylidene-3,4,4a,6,7,8-hexahydro-1H-naphthalen-1-yl]ethylidene]oxolan-2-one	0.56	318.22	3	2	1.48	Yes

Table 3.8 ADME Profiling of ligands from *B. oleracaea*

Compound name	**Bioavailabilty score**	**Molecular Weight (g/mol)**	**No. of Hydrogen Acceptors**	**No. of Hydrogen Donors**	**Consensus Log $P_{O/W}$**	**Lipinski**
Flavonol	0.55	238.06	3	1	1.82	Yes
4-Phenyl-1H,3H-naphtho(1,8-cd)pyran-1,3-dione	0.55	274.06	3	0	3.33	Yes
Cyanidin	0.55	287.06	6	5	-0.8	Yes
2-hydroxy-4-phenylphenalen-1-one	0.55	250.11	2	1	-3.33	Yes

2-methoxyphenalen-1-one	0.55	210.07	2	0	6.96	Yes
Quercetin	0.55	302.04	7	5	6.98	Yes
Kaempferol	0.17	286.05	6	4	3.11	Yes
Myricetin	0.55	226.1	8	6	1.82	Yes
3-Flavanol	0.55	318.04	2	1	3.5	Yes
Phenalenone	0.55	180.06	0	0	1.48	Yes

3.3 Toxicity Prediction

Table 3.9 Toxicity prediction of Ligands from *M. oleifera*

Molecule	Carcinogenicity	Genotoxicity	Hematotoxicity	Nephrotoxicity	Neurotoxicity	Ototoxicity	Respiratory Toxicity

niazicin a	0.2985	0.947422	0.280298	0.528075	0.040869	0.76901	0.019957
niazicinin a	0.793352	0.987231	0.043182	0.684665	0.062957	0.813086	0.007512
Apigenin	0.689341	0.985828	0.028543	0.021411	0.060597	0.067824 0.153195	0.777349 0.729025
Luteolin	0.715984	0.977028	0.04458	0.009917	0.011588	0.074518	0.712718
Kaempferol	0.6695	0.976706	0.062082	0.018629	0.038669	0.160497	0.766274
Genistein	0.681567	0.916841	0.077119	0.101285	0.244354	0.089983 0.473624	0.796159 0.652478
Isorhamnetin	0.501712 0.62863	0.99463 0.85864 0.918908	0.014666 0.084678 0.092247	0.038753 0.00311	0.032162 0.000877	0.209626 0.184821 0.371613	0.67324 0.695835 0.277328

	0.744253			0.027516	0.015721	0.744211	0.073707
Myricetin	0.666365	0.953363	0.153735	0.112577	0.479183		
Rhamnetin	0.503221	0.958866	0.053742	0.038952	0.002699	0.693659	0.962325
Daidzein	0.118495	0.900754	0.101617	0.140964	0.332663	0.862923	0.045039
Ellagic acid	0.475413	0.334686	0.434504	0.42409	0.020665	0.249347 0.767658	0.957483 0.346106
Carbonimidothioic acid, [[4-[(4-O-acetyl-6-deoxy-I+/--L-mannopyranosyl)oxy]phenyl]methyl]-, O-ethyl ester, (E)-	0.505787	0.412152	0.121534	0.846129	0.112607	0.367563	0.965058
4-[(3-O-Acetyl-6-deoxy-I+/--L-mannopyranosyl)oxy]benzeneacetonitrile	0.551224	0.999746	0.155629	0.149557	0.635213		
I(2)-D-Glucopyranose, 1-(2,6-dimethylbenzoate)	0.025853	0.00096	0.28052	0.991354	0.668957		

Dehydrodieugenol						
(2S)-2-acetamido-3-[(Z,4Z)-4-cyclopenta[b]pyridin-5-ylidenebut-2-en-2-yl]sulfanylpropanoic acid	0.053439	0.00765	0.131756	0.523391	0.63568	
(6Z,10E,14E,18E)-2,6,10,15,19,23-hexamethyltetracosa-2,6,10,14,18,22-hexaene						

Table 3.10 Toxicity prediction of Ligands from *V. vinifera*

Molecule	**Carcinogenicity**	**Genotoxicity**	Nephrotoxicity	Neurotoxicity	Ototoicity	Respiratory toxicity
Naringenin	0.229	0.257	0.127	0.868	0.135	0.731

chalcone						
Pinosylvin	0.363	0.834	0.114	0.525	0.134	0.396
Pinocembrin chalcone	0.157	0.719	0.202	0.345	0.115	0.718
2-Phenylethyl beta-D-galactopyranoside	0.079	0.006	0.783	0.017	0.914	0.006
Acuminoside	0.209	0.123	0.157	0.547	0.924	0.093
Cyanidin	0.001	1.0	0	0	1.0	0.996
4-Hydroxy-3-(3-methylbut-3-en-1-ynyl)benzoic acid	0.413	0.198	0.504	0.242	0.376	0.79
Icariside B8	0.169	0.094	0.24	0.584	0.937	0.054
Cis-Astringin	0.035	0.112	0.683	0.014	0.96	0.004
(3E)-3-[2-[(1S,4R,4aS,8aR)-4-hydroxy-5,5,8a-trimethyl-2-methylidene-3,4,4a,6,7,8-hexahydro-1H-naphthalen-1-yl]ethylidene]oxolan-2-one	0.703	0.281	0.674	0.295	0.706	0.579

Table 3.11 Toxicity prediction of Ligands from *O. europaea*

Molecule	Carcinogenicity	Hematotoxicity	Genotoxicity	Nephrotoxicity	Neurotoxicity	Otoxicity	Respiratory toxicity
Hydrocinchonine	0.61267	0.354386	0.184403	0.870133	0.713456	0.654764	0.940536
Oleacin 90%	0.359079	0.13628	0.927325	0.38963	0.728638	0.346616	0.186661
Oleocanthal	0.292419	0.099088	0.961585	0.194641	0.254566	0.617047	0.173435

Table 3.12 Toxicity prediction of Ligands from *B. oleracaea*

Molecule	**Carcinogenicity**	**Genotoxicity**	**Hematotoxicity**	**Nephrotoxicity**	**Neurotoxicity**	**Ototoxicity**	**Respiratory toxicity**
2-methoxy-9-phenalene-1-one	0.913552	0.61365	0.756171	0.754804	0.893236	0.39217	0.83122
(2R,3S)-2,3-dihydroxy-9-(4-hydroxyphenyl)-2,3-dihydrophenalen-1-one	0.72836	0.936455	0.513942	0.83272	0.601309	0.546775	0.770697
(2S,3S)-2,3-dihydroxy-4-(4-methoxyphenyl)-2,3-dihydrophenalen-1-one	0.955031	0.790067	0.890941	0.982549	0.778193	0.628231	0.93923
Flavonol	0.728702	0.597948	0.219576	0.113023	0.246868	0.113812	0.608326
4-Phenyl-1H,3H-naphtho(1,8-cd)pyran-1,3-dione	0.468088	0.406968	0.731227	0.965361	0.401339	0.234885	0.139719
Cyanidin	0.999995	1	0.002264	1.01E-05	2.13E-09	0.000808	0.989198

Delphinidin	0.999998	1	0.004048	1.67E-05	6.54E-09	0.000917	0.995746
(2R,3S)-2,3-dihydroxy-9-(4-hydroxy-3-methoxyphenyl)-2,3-dihydrophenalen-1-one	0.676292	0.640768	0.55176	0.936781	0.707242	0.71363	0.764953
2-(3,4-Dihydroxyphenyl)naphthalic anhydride	0.332174	0.698805	0.500982	0.891984	0.065062	0.453007	0.764953
9-phenylphenalen-1-one	0.887546	0.446468	0.664135	0.728629	0.893209	0.328078	0.104636
9-(4-methoxyphenyl) phenalen-1-one	0.923733	0.400162	0.728883	0.827494	0.905271	0.411154	0.933837
2-hydroxy-9-(4-methoxyphenyl) phenalen-1-one	0.892273	0.299533	0.695107	0.803922	0.795241	0.420822	0.958057
2-methoxyphenalen-1-one	0.856688	0.311591	0.538938	0.738705	0.735497	0.361334	0.962688
		0.416834					
Kaempferol	0.715984	0.977028	0.659712	0.539008	0.788259	0.29285	0.932265
Myricetin	0.501712	0.99463	0.04458	0.018629	0.038669	0.074518	0.836615

Anigofurone	0.842305	0.343134	0.014666	0.00311	0.000877	0.473624	0.712718
2,3-Dihydro-4-(4-methoxyphenyl)-1H-phenalene-1,2,3-triol	0.728948	0.141728	0.626361	0.696543	0.77521	0.807005	0.652478
Quercetin	0.600177	0.974866	0.0325	0.010642	0.008594	0.163676	0.163676
Phenalenone	0.836053	0.385075	0.606793	0.46653	0.859175	0.271714	0.946574

CHAPTER FOUR

DISCUSSION AND CONCLUSION

4.0 DISCUSSION

Regorafenib is a multikinase inhibitor used as an antineoplastic agent with activity in several cancers, notably metastatic colorectal cancer, advanced gastrointestinal stromal tumors (GIST), and hepatocellular carcinoma. It inhibits multiple kinases involved in tumor angiogenesis, oncogenesis, and the tumor microenvironment, particularly targeting mutated KIT, VEGFRs, PDGFR, FGFR, and RAF kinases, which suppresses tumor proliferation, angiogenesis, and metastasis. Regorafenib is approved for use mainly in colorectal cancer, GIST, and liver cancer patients refractory to other treatments (Strumberg D. *et al*, 2012).

Tipifarnib is a selective inhibitor of farnesyltransferase, targeting the post-translational farnesylation of HRAS and other proteins. It has shown promise particularly as a precision therapy for HRAS-mutant head and neck squamous cell carcinoma (HNSCC), where it inhibits tumor cell proliferation, survival, and neovascularization, inducing apoptosis and tumor regression in HRAS-mutant models. Its effectiveness is primarily linked to cancers harboring HRAS mutations (Gilardi M, Wang Z. *et al*, 2020).

Osimertinib is a third-generation irreversible epidermal growth factor receptor (EGFR) inhibitor used primarily for non-small cell lung cancer (NSCLC) with specific EGFR mutations including T790M, L858R, and exon 19 deletions. It selectively inhibits mutant EGFR forms, blocking EGFR-mediated signaling, tumor growth, and proliferation while reducing toxicity compared to earlier EGFR inhibitors (Lamb YN, 2021).

Tipiracil is used in combination with trifluridine in cancer therapy. This combination, known as trifluridine-tipiracil, is approved for metastatic colorectal cancer and metastatic gastric or gastroesophageal junction adenocarcinoma after failure of multiple prior chemotherapies. Tipiracil prevents the degradation of trifluridine, allowing its incorporation into DNA, thereby inhibiting tumor cell division (Kish T. *et al*, 2016).

Capecitabine is a nucleoside metabolic inhibitor used primarily for various gastrointestinal cancers, including colorectal cancer, locally advanced rectal cancer, pancreatic adenocarcinoma, and also breast cancer. It is used as monotherapy or part of combination chemotherapy regimens for adjuvant or metastatic disease settings. Its mechanism involves incorporation into DNA, disrupting DNA synthesis and tumor cell proliferation. (Seyedi S. *et al*, 2023).

Regorafenib, capecitabine, tipifarnib, tipiracil, and Osimertinib, all well known antineoplastic agents, were docked against the target proteins 1HVY and 1XKK to evaluate their binding affinities and potential as drug molecules. Molecular docking produced binding scores that predict the interaction strength between each ligand and the target proteins. Against both receptors, regorafenib exhibited a strong binding affinity of approximately -9 kcal/mol, forming multiple interactions including Pi-Alkyl, Pi-Pi stacked, and conventional hydrogen bonds with key active site amino acids. This suggests high potential for biological activity. Capecitabine showed a moderate binding affinity around -7.7 kcal/mol, but lacked significant conventional hydrogen bonds, indicating lower efficacy. Tipifarnib and tipiracil bound with affinities of approximately -8.6 kcal/mol and -7.6 kcal/mol, respectively, showing several conventional hydrogen bonds and Pi-Donor hydrogen bonds that enhance stability, further establishing them as standard therapeutic agents. Osimertinib demonstrated a strong binding affinity of approximately

-8.2 kcal/mol forming extensive conventional hydrogen bonds and hydrophobic interactions indicative of robust binding.

4.0.1 *Moringa oleifera*

Twenty three (23) and twenty two (22) compounds including the standard/control ligands (Regorafenib, Tipifarnib, Osimertinib, Tipiracil and Capecitabine) bound with different affinities to the target proteins, 1XKK and 1HVY, respectively as can be seen in **Table 3.1.1** and **3.1.2**; binding affinities ranged from -7.1 to -9.2 kcal/mol for 1XKK and -7.2 to -9.7 kcal/mol for 1HVY with Regorafenib, Tipifarnib, Osimertinib, Capecitabine and Tipiracil having binding affinities of -9, -7, -7.4, -7.5, and -7.7 kcal/mol for 1XKK and -9.7, -9, -8, -7.8, and -7.2 kcal/mol for 1HVY. Myricetin had the highest binding affinity of -9.2 kcal/mol while O-Coumaric acid had the least binding affinity of -7.1kcal/mol for 1XKK. Ellagic acid had the highest binding affinity of -9.5 kcal/mol while Carbonimidothioic acid, [[4-[(4-O-acetyl-6-deoxy-I+/--L-mannopyranosyl)oxy]phenyl]methyl]-, O-ethyl ester, (E)- and 4-[(3-O-Acetyl-6-deoxy-I+/--L-mannopyranosyl)oxy]benzeneacetonitrile had the lowest binding affinity of -7.4kcal/mol.

For 1HVY, a remarkable number of ligands interacted with the active sites amino acid of the receptor with strong hydrogen bond, namely; Luteolin, which interacted with six (6) amino acids ($_{50}$ARG, $_{258}$TYR, $_{216}$SER, $_{218}$ASP, $_{214}$GLN, $_{87}$GLU), Cis-Astringin, which interacted with five (5) amino acids ($_{216}$SER, $_{256}$HIS, $_{87}$GLU, $_{226}$ASN, $_{108}$ILE), Apigenin, which interacted with five (5) amino acids($_{50}$ARG, $_{87}$GLU, $_{214}$GLN, $_{218}$ASP, $_{258}$TYR), Genistein, which interacted with five (5) amino acids ($_{218}$ASP, $_{254}$ASP, $_{258}$TYR, $_{215}$ARG, $_{195}$CYS), Ellagic acid, which interacted with five (5) amino acids ($_{218}$ ASP, $_{108}$ILE, $_{226}$ASN, $_{218}$ASP, $_{50}$ARG), 4-[(3-O-Acetyl-6-deoxy-I+/--L-mannopyranosyl)oxy]benzeneacetonitrile, which interacted with six (6) amino acids ($_{195}$CYS, $_{50}$ARG, $_{258}$TYR, $_{215}$ARG, $_{216}$SER, $_{218}$ASP) but had the lowest binding affinity of -7.4kcal/mol,

Isorhamnetin, which interacted with four (4) amino acids ($_{50}$ARG, $_{218}$ASP, $_{216}$SER, $_{87}$GLU), Niazicin A, which interacted with three (3) amino acids ($_{256}$HIS, $_{49}$ASP, $_{226}$ASN), Myricetin, which interacted with three (3) amino acids ($_{218}$ASP, $_{216}$SER, $_{87}$GLU), Rhamnetin, which interacted with three (3) amino acids ($_{87}$GLU, $_{87}$GLU, $_{50}$ARG), (2S)-2-acetamido-3-[(Z,4Z)-4-cyclopenta[b]pyridin-5-ylidenebut-2-en-2-yl]sulfanylpropanoic acid, which interacted with three (3) amino acids ($_{195}$CYS, $_{226}$ASN, $_{214}$GLN), Diadzein, which interacted with three (3) amino acids ($_{87}$GLU, $_{218}$ASP, $_{258}$TYR), and I(2)-D-Glucopyranose, 1-(2,6-dimethylbenzoate), which interacted with three (3) amino acids ($_{226}$ASN, $_{214}$GLN, $_{218}$ASP).

For 1XKK, not as many ligands interacted with the active sites amino acid of the receptor with strong hydrogen bond. O-methyl N-[[4-(3,4,5-trihydroxy-6-methyloxan-2-yl)oxyphenyl]methyl]carbamothioate interacted with four (4) amino acids ($_{842}$ASP, $_{841}$ARG, $_{855}$ASP, $_{854}$THR), Myricetin interacted with three (3) amino acids ($_{788}$LEU, $_{793}$MET, $_{855}$ASP) Niazidin, Kaempferol, Carbonimidothioic acid, [[4-[(4-O-acetyl-6-deoxy-I+/--L-mannopyranosyl)oxy]phenyl]methyl]-, O-ethyl ester, (E)-, and

O-Ethyl N-((4-((6-deoxy-alpha-L-mannopyranosyl)oxy)phenyl)methyl)carbamothioate all interacted with two (2) amino acids each.

The docking was done at an exhaustiveness of 8 and the autogrid measurement was:

1HVY

	X	Y	Z
Measurement	-1.2061	5.0424	15.8569
Dimensions	13.8706	20.0624	22.4571

(Angstrom)

1XKK

	X	Y	Z
Measurement Dimensions (Angstrom)	15.8832	31.3028	43.1587
	12.7802	18.2059	7.7861

4.0.2 Olea europaea

Six (6) compounds including the standard/control ligands (Regorafenib, Capecitabine and Tipiracil) bound with different affinities to each target protein as can be seen in **Table 3.1.3** and **3.1.4**. For 1XKK, binding affinities ranged from -7.1kcal/mol to -8.6kcal/mol while Regorafenib, Capecitabine and Tipiracil had binding affinities of -8.5, -7.1 and -7.7kcal/mol respectively. Hydrocinchonine had the highest binding affinity of -8.6kcal/mol, Oleacin 90% had a binding affinity of -8kcal/mol and Oleocanthal had a binding affinity of -7.5kcal/mol. For 1HVY, binding affinities ranged from -7.7 kcal/mol to -9.8kcal/mol while Regorafenib, Capecitabine and Tipiracil had binding affinities of -9.8, -7.8 and -7.7kcal/mol respectively. Hydrocinchonine and Oleocanthal both had binding affinity of -7.9, while Oleacin 90% had a binding affinity of -7.8kcal/mol. All three ligands interacted with the active sites amino acid of both receptors with strong hydrogen bond. Against 1XKK, Oleacin 90% had the highest interaction with 3 of the active/binding site amino acids ($_{841}$ARG, $_{745}$LYS, $_{842}$ASN) through hydrogen bonding. Hydrocinchonine and Oleocanthal each had 2 interactions, ($_{777}$LEU, $_{775}$CYS) and ($_{855}$ASP, $_{854}$THR) respectively. Against 1HVY, Oleacin 90% had the highest interaction with 2 of the active/binding site amino acids ($_{218}$ASP, $_{108}$ILE) through hydrogen bonding. Hydrocinchonine and Oleocanthal each had 1 interaction, ($_{195}$CYS).

The docking was done at an exhaustiveness of 8 and the autogrid measurement was:

1HVY

	X	Y	Z
Measurement	-3.065	6.3046	12.6345

Dimensions (Angstrom)	13.6243	21.4324	25.5423

1XKK

	X	Y	Z
Measurement	13.2114	33.2136	39.5924
Dimensions (Angstrom)	11.8213	14.5121	7.3412

4.0.3 Brassica oleracaea

Sixteen (16) and twenty three (23) compounds including the standard/control ligands (Regorafenib, Tipifarnib, Osimertinib, Tipiracil and Capecitabine) bound with different affinities to the target proteins, 1XKK and 1HVY, respectively as can be seen in **Table 3.1.5** and **3.1.6**; binding affinities ranged from -7kcal/mol to -8.2kcal/mol for 1XKK and from -7.3 to -9.6kcal/mol for 1HVY. For 1XKK, 3-Flavanol had the highest binding affinity of -8.2kcal/mol while Quercetin had the lowest binding affinity of -7kcal/mol. For 1HVY, (2S,3S)-2,3-dihydroxy-4-(4-methoxyphenyl)-2,3-dihydrophenalen-1-one Trans-11-octadecenoic acid had the highest binding affinity of -9.4kcal/mol (second only to Regorafenib (-9.6kcal/mol)) while 2-methoxyphenalen-1-one had the lowest binding affinity of -7.4 kcal/mol (second only to Tipiracil (-7.3kcal/mol)).

Against 1HVY, Kaempferol had the highest interaction with 5 of the active/binding site amino acids through hydrogen bonding (218 ASP, 226 ASN, 87GLU, 50ARG, 258TYR), Myricetin ($_{87}$GLU, $_{50}$ARG, $_{258}$TYR, $_{256}$HIS) and Delphinidin ($_{87}$GLU, $_{216}$SER, $_{218}$ASP, $_{50}$ARG) each had 4 interactions. Against 1XKK, Cyanidin had 3 interactions ($_{854}$THR, $_{855}$ASP, $_{793}$MET). Myricetin

(793MET, 854THR) and 2-hydroxy-4-phenylphenalen-1-one (745LYS, 855ASP) each had 2 interactions.

Docking was done at an exhaustiveness of 8 and the autogrid measurement was:

1HVY

	X	Y	Z
Measurement	-1.890	9.08251	17.8864
Dimensions (Angstrom)	14.4480	24.9133	27.0386

1XKK

	X	Y	Z
Measurement	13.8706	30.8749	35.8883
Dimensions (Angstrom)	11.7513	20.0624	22.4571

4.0.4 Vitis vinifera

Fifteen (15) and twelve (12) compounds including the standard/control ligands (Regorafenib, Tipifarnib, Osimertinib, Tipiracil and Capecitabine) bound with different affinities to the target proteins, 1XKK and 1HVY, respectively as seen in **Table 3.1.7** and **3.1.8**. The standard ligands (Regorafenib, Tipifarnib, Osimertinib, Tipiracil and Capecitabine) had binding affinities of -9.7, -9.3, -8.7, -7.7 and -7.3kcal/mol for 1HVY and -8.3, -8, -7.4, -7.8 and -7.7kcal/mol for 1XKK. For

the other ligands, binding affinity ranged from -7.4 to -8.7 kcal/mol for 1HVY, with Cis-Astringin having the highest binding affinity and 2-Phenylethyl beta-D-galactopyranoside and Pinocembrin chalcone both having the lowest binding affinity, and from -7.4 to -9.1kcal/mol for 1XKK, with Cis-Astringin having the highest binding affinity and 4-Hydroxy-3-(3-methylbut-3-en-1-ynyl)benzoic acid and Icariside B8 both having the lowest binding affinity.

For 1XKK, Cyanidin ($_{854}$THR, $_{855}$ASP, $_{793}$MET), Icariside B8 ($_{854}$THR, $_{788}$ LEU, $_{743}$ALA) and Acuminoside ($_{842}$ASN, $_{841}$ARG, $_{837}$ASP) each had interactions with 3 of the active/binding site amino acids through hydrogen bonding.

For 1HVY, Cis-Astringin ($_{226}$ASN, $_{87}$GLU, $_{108}$ILE, $_{216}$SER, $_{256}$HIS) and Cyanidin ($_{214}$GLN, $_{87}$GLU, $_{226}$ASN, $_{50}$ARG, $_{218}$ASP) each interacted strongly (hydrogen bond) with 5 of the active site amino acids. Icariside B8 and Acuminoside had 4 ($_{256}$HIS, $_{258}$TYR, $_{218}$ASP, $_{215}$ARG) and 3 ($_{215}$ARG, $_{256}$HIS, $_{216}$SER) interactions respectively.

Docking was done at an exhaustiveness of 8 and the autogrid measurement was:

1HVY

	X	Y	Z
Measurement Dimensions (Angstrom)	0.019 18.6561	4.7145 24.7709	16.9733 26.0803

1XKK

	X	Y	Z

Measurement	19.8667	36.9845	45.1983
Dimensions (Angstrom)	21.2084	17.7902	9.8947

4.0.5 ADMET Profiling

Absorption Distribution Metabolism and Excretion (ADME) studies help in the estimation of drug-likeness of compounds before synthesis as this helps to decrease the occurrences of pharmacokinetic-related failure in drug development. Different rules are available which help in the prediction of drug-likeness but for this project, the Lipinski Rule of 5 was used. The Lipinski Rule of 5 states that an orally active drug must not break more than one of the following criteria: hydrogen bond donor ≤ 5; hydrogen bond acceptor ≤ 10; molecular weight ≤ 500 Daltons; octanol-water partition coefficient ≤ 5.

For each plant, ligands were selected for ADMET study based on higher binding affinity and highest hydrogen bond interaction.

Twenty two (22) compounds were selected from *Moringa oleifera* namely; Niazicin A, Niazicinin A, Apigenin, Luteolin, Kaempferol, Genistein, Isorhamnetin, Myricetin, Diadzein, Ellagic acid, Carbonimidothioic acid, [[4-[(4-O-acetyl-6-deoxy-I+/--L-mannopyranosyl)oxy]phenyl]methyl]-, O-ethyl ester, (E)-, 4-[(3-O-Acetyl-6-deoxy-I+/--L-mannopyranosyl)oxy]benzeneacetonitrile, I(2)-D-Glucopyranose, 1-(2,6-dimethylbenzoate), Dehydrodieugenol, (2S)-2-acetamido-3-[(Z,4Z)-4-cyclopenta[b]pyridin-5-ylidenebut-2-en-2-yl]sulfanylpropanoic acid, (6Z,10E,14E,18E)-2,6,10,15,19,23-hexamethyltetracosa-2,6,10,14,18,22-hexaene, O-Coumaric acid, O-Ethyl N-((4-((6-deoxy-alpha-L-

mannopyranosyl)oxy)phenyl)methyl)carbamothioate, [(2S,3R,4R,5S,6S)-2-[4-(cyanomethyl)phenoxy]-3,5-dihydroxy-6-methyloxan-4-yl] acetate, Niazidin, Niazirin, and O-methyl N-[[4-(3,4,5-trihydroxy-6-methyloxan-2-yl)oxyphenyl]methyl]carbamothioate.

ADME study was done and all compounds passed as drug-like. These compounds were then put through the toxicity test and were found not to have any toxicity on any major organ, thus qualifying as potential drug molecules.

For *Olea europaea*, Hydrocinchonine, Oleacin 90%, and Oleocanthal were the only compound selected and after ADME profiling, the compounds passed as drug-like and all passed toxicity testing.

For *Brassica oleracae*, twenty (20) compounds were selected namely; 2-methoxy-9-phenyl-1H-phenalen-1-one, (2R,3S)-2,3-dihydroxy-9-(4-hydroxyphenyl)-2,3-dihydrophenalen-1-one, Flavaonol, 4-Phenyl-1H,3H-naphtho(1,8-cd)pyran-1,3-dione, Delphinidin, Cyanidin, (2R,3S)-2,3-dihydroxy-9-(4-hydroxy-3-methoxyphenyl)-2,3-dihydrophenalen-1-one, 2-(3,4-Dihydroxyphenyl)naphthalic anhydride, 9-phenylphenalen-1-one, 9-(4-methoxyphenyl)phenalen-1-one, 2-hydroxy-9-(4-methoxyphenyl)phenalen-1-one, 2-hydroxy-4-phenylphenalen-1-one

2-methoxyphenalen-1-one, Kaempferol, Myricetin, Anigorufone, 2,3-Dihydro-4-(4-methoxyphenyl)-1H-phenalene-1,2,3-triol, Quercetin and Phenalenone. All compounds passed the drug-likeness test and had favorable toxicity profiles, thus qualifying as a potential drug molecules.

Vitis vinifera produced nine (9) compounds of interest, namely; Acuminoside, Cyanidin, Icariside B8, Pinocembrin chalcone, 2-Phenylethyl beta-D-galactopyranoside, (3E)-3-[2-

[(1S,4R,4aS,8aR)-4-hydroxy-5,5,8a-trimethyl-2-methylidene-3,4,4a,6,7,8-hexahydro-1H-naphthalen-1-yl]ethylidene]oxolan-2-one, Pinosylvin, Naringenin chalcone and 4-Hydroxy-3-(3-methylbut-3-en-1-ynyl)benzoic acid. All compounds passed the drug-likeliness test and had favourable ADME and toxicity properties, thus qualifying as potential drug molecules.

4.1 CONCLUSION

The phytoconstituents isolated from the plants were obtained and molecular docking was carried out against Epidermal Growth Factor Receptor (EGFR), 1XKK, and Human Thymidylate Synthase enzyme, 1HVY; post-docking analysis carried out and the ADMET properties of selected ligands determined.

The binding affinities and interaction with active site residues possessed by phytoconstituents present in *Moringa oleifera, Olea europaea, Brassica oleracaea,* and *Vitis vinifera* validates their use traditionally for the treatment and prophylaxis of colorectal cancer.

REFERENCES

Abd-Rabou AA, Abdalla AM, Ali NA, Zoheir KM. *Moringa oleifera* Root Induces Cancer Apoptosis more Effectively than Leave Nanocomposites and Its Free Counterpart. Asian Pac J Cancer Prev. 2017 Aug 27;18(8):2141-2149.

Al-Asmari AK, Albalawi SM, Athar MT, Khan AQ, Al-Shahrani H, Islam M. *Moringa oleifera* as an Anti-Cancer Agent against Breast and Colorectal Cancer Cell Lines. PLoS One. 2015 Aug 19;10(8):e0135814.

Al-Shalabi, Abdul Samad, Lim Vuanghao, Ibrahim Al Deeb, Julia Joseph., (2023), Moringa oleifera's Effect on Colorectal Cancer , Journal of Angiotherpay, 7(1)

Ami Shah, R., & Gadhvi, R. (2024). Cytotoxic Effect of *Brassica oleracea* L. var. italica Florets and Microgreens on Cancer Cell Line. CAASJK. Reports higher anticancer activity in microgreens of broccoli against cancer.

Arora, R., Kumar, R., Mahajan, J., Vig, A.P., Singh, B., Singh, B. and Arora, S. 2016. 3-Butenyl isothiocyanate: A hydrolytic product of glucosinolate as a potential cytotoxic agent against human cancer cell lines. Journal of Food Science and Technology, 53: 3437-3445

Bodoque-Villar R, Roldán-Díaz EM, Serrano-Oviedo L, Garzón-Quintero HD, Cañete-Rodríguez M, Gómez LA, Gracia I, Rodríguez JF, Bejarano-Ramírez N, Verdugo-Moreno G, Muñoz-Rodríguez JR, Redondo-Calvo FJ. Evaluating *Allium sativum* and *Vitis vinifera* Extracts as Potential Adjuvant Agents in Colorectal Cancer: Insights from HT-29 and Caco-2 Models. Biomedicines. 2025 Aug 13;13(8):1968.

Bhandari, S.R., Jo, J.S. and Lee, J.G. 2015. Comparison of glucosinolate profiles in different tissues of nine Brassica crops. Molecules, 20(9): 15827-15841.

Borzì AM, Biondi A, Basile F, Luca S, Vicari ES, Vacante M. Olive oil effects on colorectal cancer. Nutrients 11(1), 11010032–11010048 (2019).

Chauhan, E.S., Tiwari, A. and Singh, A. 2016. Phytochemical screening of red cabbage (Brassica oleracea) powder and juice - A comparative study. Journal of Medicinal Plants Studies, 4(5): 196-199.

Darzynkiewicz, Z., Juan, G., Li, X., Gorczyca, W., Murakami, T. and Traganos, F. 1997. Cytometry in cell necrobiology: Analysis of apoptosis and accidental cell death (necrosis). Cytometry, 27(1): 1-20.

De la Fuente, B., López-García, G., Máñez, V., Alegría, A., Barberá, R. and Cilla, A. 2020. Antiproliferative effect of bioaccessible fractions of four Brassicaceae microgreens on human colon cancer cells linked to their phytochemical composition. Antioxidants, 9(5): 368.

Gamli Ö. The health effects of oleuropein, one of the major phenolic compounds of olives, *Olea*

europaea L. Ital. J. Food Sci. 28(2), 355–358 (2016).

Greco, G., Schnekenburger, M., Catanzaro, E., Turrini, E., Ferrini, F., Sestili, P., Diederich, M. and Fimognari, C. 2021. Discovery of sulforaphane as an inducer of ferroptosis in U-937 leukemia cells: Expanding its anticancer potential. Cancers, 14(1): 76.

Jang, H.W., Moon, J.K. and Shibamoto, T. 2015. Analysis and antioxidant activity of extracts from broccoli (*Brassica oleracea* L.) sprouts. Journal of Agricultural and Food Chemistry, 63(4): 1169-1174.

Kiraz, Y., Adan, A., Kartal Yandim, M. and Baran, Y. 2016. Major apoptotic mechanisms and genes involved in apoptosis. Tumor Biology, 37: 8471-8486.

Kish T, Uppal P. Trifluridine/Tipiracil (Lonsurf) for the Treatment of Metastatic Colorectal Cancer. P T. 2016 May;41(5):314-25.

Koolivand, M., Ansari, M., Piroozian, F., Moein, S. and MalekZadeh, K. 2018. Alleviating the progression of acute myeloid leukemia (AML) by sulforaphane through controlling miR-155 levels. Molecular Biology Reports, 45: 2491-2499.

Kowitcharoen, L., Phornvillay, S., Lekkham, P., Pongprasert, N. and Srilaong, V. 2021. Bioactive composition and nutritional profile of microgreens cultivated in Thailand. Applied Sciences, 11(17): 7981.

Lakshmi, D.S. and Shalini, J.V. 2016. In vitro antioxidant studies of fresh *Brassica oleracea* and the characterization of its bioactive compounds using Fourier transform infrared spectroscopy (FTIR). Journal of Chemical and Pharmaceutical Research, 8(5): 900-905.

Lamb YN. Osimertinib: A Review in Previously Untreated, EGFR Mutation-Positive, Advanced NSCLC. Target Oncol. 2021 Sep;16(5):687-695. doi: 10.1007/s11523-021-00839-w. Erratum in: Target Oncol. 2021 Nov;16(6):869. doi: 10.1007/s11523-021-00853-y. PMID: 34564820; PMCID: PMC8536603.

Le, T.N., Chiu, C.H. and Hsieh, P.C. 2020a. Bioactive compounds and bioactivities of *Brassica oleracea* L. var. italica sprouts and microgreens: An updated overview from a nutraceutical perspective. Plants, 9(8): 946.

Le, T.N., Luong, H.Q., Li, H.P., Chiu, C.H. and Hsieh, P.C. 2019. Broccoli (*Brassica oleracea* L. var. italica) sprouts as the potential food source for bioactive properties: A comprehensive study on in vitro disease models. Foods, 8(11): 532.

Mahmood TH, Al-Samydai A, Sulaibi MA*et al*. Development of pegylated nano-phytosome formulation with oleuropein and rutin to compare anti-colonic cancer activity with *Olea europaea* leaves extract. Chem. Biodivers. 20(8), e202300534 (2023).

Neira-Ospina E, Rojas J, Santa-Gonzalez GA, Garzón MAG. Phenolic compounds in grapes

(genus *Vitis*): A review of their antioxidant activity, antiproliferative capacity, and cytotoxic effect on colorectal cancer. J Appl Pharm Sci. 2024;14(06):071–089.

Nsairat H, Jaber AM, Faddah H, Ahmad S. Oleuropein impact on colorectal cancer. Future Sci OA. 2024 May 23;10(1).

Seyedi S, Teo R, Foster L, Saha D, Mina L, Northfelt D, Anderson KS, Shibata D, Gatenby R, Cisneros L, Troan B, Anderson ARA, Maley CC. Testing Adaptive Therapy Protocols using Gemcitabine and Capecitabine on a Mouse Model of Endocrine-Resistant Breast Cancer. bioRxiv [Preprint]. 2023 Sep 22:2023.09.18.558136. doi: 10.1101/2023.09.18.558136. Update in: Cancers (Basel). 2024 Jan 06;16(2):257

Tajalli, F., Saeedi, M. and Malekabadi, A.V. 2020. Anticancer and antioxidant effects of red cabbage on three cancerous cell lines and comparison with a normal cell line (HFF-3). Journal of Genes and Cells, 6(1): 12-20.

Tiloke, C., Phulukdaree, A., Gengan, R. M., & Chuturgoon, A. A. (2019). *Moringa oleifera* aqueous leaf extract induces cell-cycle arrest and apoptosis in human liver hepatocellular carcinoma cells. Nutrition and cancer, 71(7), 1165-1174.

Tomas, M., Zhang, L., Zengin, G., Rocchetti, G., Capanoglu, E. and Lucini, L. 2021. Metabolomic insight into the profile, in vitro bioaccessibility and bioactive properties of polyphenols and glucosinolates from four Brassicaceae microgreens. Food Research International, 140: 110039.

Tragulpakseerojn, J., Yamaguchi, N., Pamonsinlapatham, P., Wetwitayaklung, P., Yoneyama, T., Ishikawa, N., ... & Apirakaramwong, A. (2017). Anti-proliferative effect of *Moringa oleifera* Lam (Moringaceae) leaf extract on human colon cancer HCT116 cell line. Tropical Journal of Pharmaceutical Research, 16(2), 371-378.

Vogel, J. D., Felder, S. I., Bhama, A. R., Hawkins, A. T., Langenfeld, S. J., Shaffer, V. O., ... & Paquette, I. M. (2022). The American Society of Colon and Rectal Surgeons clinical practice guidelines for the management of colon cancer. Diseases of the Colon & Rectum, 65(2), 148-177.

Vongsak, B., Mangmool, S., & Gritsanapan, W. (2015). Antioxidant activity and induction of mRNA expressions of antioxidant enzymes in HEK-293 cells of *Moringa oleifera* leaf extract. Planta Medica, 81(12/13), 1084–1089.

Zeriouh W, Nani A, Belarbi M, Dumont A, de Rosny C, *et al*. (2017) Correction: Phenolic extract from oleaster (*Olea europaea* var. *Sylvestris*) leaves reduces colon cancer growth and induces caspase-dependent apoptosis in colon cancer cells via the mitochondrial apoptotic pathway. PLOS ONE 12(4): e017657

APPENDIX

i. Olea europaea

1HVY

Compound	Hydrogen bond	Vanderwaals	Others
Hydrocinchonine	CYS 195	MET 311, GLY 222, ASN 112, ARG 50, GLU 87, ASN 226	Pi-Alkyl Alkyl Pi-Anion Carbon hydrogen bond
Oleocanthal	CYS 195	ASN 112, MET 311, GLY 222, ARG 50, GLY 87, ASN 226, MET 311, VAL 223, GLY 217	Carbon hydrogen bond Pi-Anion Alkyl Pi-Alkyl
Oleacin 90%	ASP 218, ILE 108	VAL 223, LEU 192, TRP 109, LEU 221, GLY 217, SER216 HIS 196, GLU 87, MET 311, VAL 223, GLY 217, ASN 226, CYS 195, GLY 222	Pi-PI T-shaped Pi-Alkyl Carbon hydrogen bond

1XKK

Compound	Hydrogen bond	Vanderwaals	Others
Hydrocinchonine	ASP 855, THR 854	LEU 792, MET 793, LEU 777, THR 790, LEU 718, LEU 858	Pi-Alkyl Pi-Pi T-shaped
Oleocanthal	LEU 777, CYS 775	VAL 726, 1LE 744, LEU 844, LEU788, LEU 792, LEU 718, ALA 743, THR790, ASP 855, THR 854, ARG 776, VAL 774, VAL 769	Carbon hydrogen bond Pi-Pi T-shaped Pi-Alkyl
Oleacin 90%	ARG 841, LYS 745, ASN 842	ARG 776, CYS 775, LEU 777, THR 854, ASP 855, THR 790 LEU 788, PHE 856, ILE 744, ILE 789, LEU 718, ALA 743	Alkyl Carbon hydrogen bond Pi-Alkyl

ii. Vitis vinifera

IHVY

Compound	Hydrogen bond	Vanderwaals	Others
Cis-Astringin	GLU 87, ASN 226, 1LE 108,	ASN 112, GLY 222, HIS 196, CYS195,	Pi donor hydrogen bond

	SER 216, HIS 256	GLY 217, ASP 218, PHE 91, LEU 221, LEU 192, ARG 50, THR 51, TYR 258	Carbon hydrogen bond Pi-Alkyl Pi-Pi T shaped Pi-Pi Stacked Pi-Sulfur
Acuminoside	SER 216, HIS 256, ARG 215	PRO193, LEU 192, GLY 217, ASP218, CYS 195, GLY 214, GLY 222, ASN 226, MET 311, TYR, 258, ARG 50, THR 51, GLU 87	Carbon hydrogen bond Unfavorable donor-donor Alkyl Pi-Alkyl
Cyanidin	ASP 218, ARG 50, GLU 87, ASN 226, GLN 224	THR 51, TYR 258, HIS 256, GLY 217, VAL 223, HIS 196, GLY 222, PHE 225, ILE 108	Carbon hydrogen bond Unfavorable donor-donor Pi-Anion Pi donor hydrogen bond, Pi-Pi T-Stacked Pi-Alkyl
Icariside B8	HIS 256, TYR 258, ASP 218, ARG 215	ALA 312, MET 311, ASN 226, LEU 221, GLY 222, PHE 225, GLU 87, ILE 108, CYS 195, LEU 192, ARG 50	Carbon hydrogen bond Pi-Sigma Unfavorable donor-donor

Pinocembrin chalcone	SER 216	VAL 223, GLY 217, GLN 214, HIS 256, TYR 258, ARG 50, LEU 192, ASN 226, GLY 222, PHE 225	Pi-Alkyl Pi donor hydrogen bond Pi-Anion Carbon hydrogen bond
2-Phenylethyl beta-D-galactopyranoside	ASP 218, ASN 226	LEU 221, MET 311, TYR 258, LEU 192, GLY 222, CYS 195, GLN 214, GLY 217, SER 216, HIS 196, GLY 87, TRP 109	Pi-Pi T-Stacked Pi-Alkyl Carbon hydrogen bond
(3E)-3-[2-[(1S,4R,4aS,8aR)-4-hydroxy-5,5,8a-trimethyl-2-methylidene-3,4,4a,6,7,8-hexahydro-1H-naphthalen-1-yl]ethylidene]oxolan-2-one	GLN 214, ASN 226	GLY 217, MET 311, LEU 221, GLY 222, ASP 218, HIS 196, CYS 195, TRP 109, LEU 192	Pi-Alkyl Alkyl Carbon hydrogen bond

1XKK

Compound	Hydrogen bond	Vanderwaals	Others
Cyanidin	854THR, 855ASP, 793MET	CYS 797, MET 1002, GLY 796, LEU 792, THR 790, LEU 788, LEU 777, MET 766, LEU 858	Pi-Cation Pi-Sigma Pi-Alkyl Carbon hydrogen bond Unfavorable donor-donor
Icariside B8	ALA 743, LEU 788, THR 854	ASN 842, LEU 858, MET 766, GLY 721, CYS797, LEU 718, LEU 844, VAL 726, LYS 745, ILE 744, ILE 789, LEU 777	Carbon hydrogen bond
Acuminoside	ASN 842, ARG 841, ASP 837	LEU 858, THR 790, PHE 723, ALA 722, GLY 719, LEU 718, LEU 844, ASP 855, THR 854	Carbon hydrogen bond Alkyl
Naringenin chalcone	MET 766, PHE 856	VAL 769, CYS 775, THR 790, LEU 718, LEU 844, LYS 745, LEU 788, THR 854, LEU 858	Pi-Pi T-shaped Pi-Alkyl Carbon hydrogen bond

4-Hydroxy-3-(3-methylbut-3-en-1-ynyl)benzoic acid	ASP 855, THR 854	MET766, LEU 858, PHE 856, LEU 792, MET 793, THR 790, ILE 744, LEU 788, LEU 777	Pi-Alkyl Alkyl Carbon hydrogen bond
(3E)-3-[2-[(1S,4R,4aS,8aR)-4-hydroxy-5,5,8a-trimethyl-2-methylidene-3,4,4a,6,7,8-hexahydro-1H-naphthalen-1-yl]ethylidene]oxolan-2-one	ASP855, THR 854	LYS 745, ASN 842, CYS 797, GLY 719, LEU 718, GLY 796, ALA 743, LEU 844, THR 790, LEU 788, LEU 777, MET 766	Alkyl, Carbon hydrogen bond
Pinocembrin	CYS 775	LEU 788, THR 790, LEU 858, LYS 745, ARG 776, VAL 774, VAL 769, ASP 858, THR 854, LEU 844	Carbon hydrogen bond Pi-Pi T-shaped Pi-Alkyl Unfavorable acceptor-acceptor
Pinosylvin	LEU 788	GLY 796, MET 1002, LEU 792, MET 793, ILE744, ILE 789, ASP855, THR 854, THR 790	Carbon hydrogen bond Pi-Cation Pi-Alkyl

2-Phenylethyl beta-D-galactopyranoside	ASP 855	LYS 745, LEU 858, THR 854, MET 766, PHE 856, LEU 777, ARG 776, CYS 775, MET 793, THR 790, LEU 792, GLY 796	Carbon hydrogen bond Pi-Alkyl
Cis-Astringin	MET 793	CYS 797, LEU 718, MET 1002, GLY 796, LEU 792, GLN 791, THR 790, LEU 788, PHE 856, THR 854, ASP 855, CYS 775, ARG 776,	Carbon hydrogen bond Pi-Alkyl

iii. Brassica oleracaea

1HVY

Compound	**Hydrogen bond**	**Vanderwaals**	**Others**
2-methoxy-9-phenyl-1H-phenalen-1-one	ASP 113, PHE 193	VAL 114, THR 110, TYR 316, ASN 312, TRP 109	Carbon hydrogen bond Pi-Alkyl Pi-Sigma
(2R,3S)-2,3-dihydroxy-9-(4-hydroxyphenyl)-2,3-dihydrophenalen-1-one	-	PHE 289, ASN 312, TYR 308,	Pi-Pi Stacked Pi-Anion

		TRP 109, THR 110, VAL 114	
(2S,3S)-2,3-dihydroxy-4-(4-methoxyphenyl)-2,3-dihydrophenalen-1-one	ASN 312	TYR 308, PHE 289, TRP 109, THR 110	Pi-Pi Stacked Pi-Alkyl
Flavonol	-	TYR 199	-
	-	THR 110, TYR 308, ASN 312, ASN 293, TRP 286, TYR 316, SER 204, SER 207, SER 203	Pi-Pi Stacked Pi-Alkyl
4-Phenyl-1H,3H-naphtho(1,8-cd)pyran-1,3-dione	-	TYR 199	-
Delphinidin	THR 110	TYR 308, ASN 312, VAL 114, TRP 109	Pi-Anion Pi-Pi Stacked Pi-Alkyl
Cyanidin	SER 204	TYR 308, PHE 289, ASN 293, SER 203, SER 207, THR 118, ASN 312, TRP 109, TYR 316, THR 110, VAL 117	Carbon hydrogen bond Pi-Pi Stacked Pi-Alkyl
(2R,3S)-2,3-dihydroxy-9-(4-hydroxy-3-methoxyphenyl)-2,3-dihydrophenalen-1-one	-	THR 110, VAL 117, SER 207, SER 203, SER 204, PHE 290,	Pi-sigma Pi-Alkyl
2-(3,4-Dihydroxyphenyl)naphthalic anhydride			

		TYR 308, TRP 109, ASN 312, TYR 316, ASP 113	
9-phenylphenalen-1-one	-	TRP 109, THR 110, TYR 308, ASN 312, PHE 289, TRP 286, PHE 290	Pi-Pi stacked Pi-Anion Alkyl
9-(4-methoxyphenyl)phenalen-1-one	SER 203, ASN 293	SER 204, SER 207, PHE 290, ASP 113, THR 110, ASN 312	Pi-Alkyl
2-hydroxy-9-(4-methoxyphenyl)phenalen-1-one	-	ASN 293, THR 110, TRP 109, ASN 312, TYR 308	Pi-Alkyl Pi-Pi stacked Pi-Anion
2-hydroxy-4-phenylphenalen-1-one	ASN 312	TYR 308, TRP 109, ASN 293, THR 110, VAL 114, VAL 117	Pi-Anion Pi-Alkyl Pi-Pi stacked
2-methoxyphenalen-1-one	-	THR 110, ASP 113, PHE 289, PHE 290, ASN 293, TRP 109, ASN 312, TRP 286, SER 203, SER 207, TYR 316	Pi-Alkyl
Kaempferol	SER 203	PHE 193, ASN 293, SER 204,	Pi-Pi T-shaped Pi-Alkyl

		PHE 290, TRP 286, TYR 316	Unfavorable Donor-Donor
Myricetin	VAL 114, PHE 193	THR 118, SER 207, SER 203, SER 204, PHE 290, PHE 289, TYR 308, TRP 109, TYR 316, ASP 113, ASN 312	Pi-Alkyl Pi-sigma
Anigofurone	-	SER 207, SER 204, SER 203, ASN 293, THR 110, TRP 109, TYR 308, ASP 113, ASN 312, TRP 286, TYR 316, VAL 117	Pi-Alkyl Pi-Pi stacked
2,3-Dihydro-4-(4-methoxyphenyl)-1H-phenalene-1,2,3-triol	-	ASN 312, VAL 117, TYR 308, PHE 289, THR 118, SER 203, SER 207, SER 204, PHE 290, ASP 113, THR 110	Pi-Alkyl

1XKK

Compound	Hydrogen	Vanderwaals	Others

	bond		
Flavonol	ASP 855	MET 793, LEU 792, GLY 796, LEU 788, THR 854	Carbon hydrogen bond Pi-Alkyl
4-Phenyl-1H,3H-naphtho(1,8-cd)pyran-1,3-dione	LYS 745	THR 854, ASP 855, GLY 796, LEU 718, LEU 788, THR 790	Carbon hydrogen bond Pi-Alkyl Pi-Sigma
Cyanidin	MET 793, ASP 855, THR 854	GLY 796, MET 1002, CYS 797, LEU 792, THR 790, LEU 788, LEU 777, MET 766, LEU 858	Carbon hydrogen bond Pi-Cation Unfavorable donor-donor Pi-Alkyl Pi-Sigma
2-(3,4-Dihydroxyphenyl)naphthalic anhydride	LYS 745	ASP 855, CYS 745, THR 854, LEU 777, LEU 788, MET 766, LEU 718, GLY 796	Pi-sigma Pi-Alkyl Carbon hydrogen bond

2-hydroxy-4-phenylphenalen-1-one	LYS 745, ASP 855	CYS 797, GLY 796, THR 790, MET 766, LEU 788, THR 854, LEU 858, ASN 842, GLY 721	Pi-Cation Pi-Alkyl Pi-Sigma Carbon hydrogen bond
2-methoxyphenalen-1-one	THR 854	LYS 745, ASP 855, THR 790, LEU 792, MET 793	Pi-Alkyl
Quercetin	-	CYS 797, THR 854, ASP 855, LEU 777, MET 766, LEU 858, LEU 788, MET 766, LEU 858, LEU 788, THR 790, MET 1002, MET 793, GLY 796, LEU 792	Pi-Cation Pi-Sigma Pi-Alkyl
Myricetin	THR 854	LEU 858, MET 766, LEU 777, LEU 788, ILE 789, THR 790,	Pi-Cation Pi-Sigma Pi-Alkyl

		GLY 796, MET 1002	
Kaempferol	MET 793	THR 792, MET 1002, GLY 796, CYS 797, THR 854, ASP 855, LEU 858, MET 766, LEU 777, LEU 788, THR 790	Pi-Alkyl Pi-Cation Unfavorable donor-donor
3-Flavanol	ASP 855	THR 854, ARG 841, CYS 797, LEU 718, THR 790, ILE 789, ILE 744, LEU 777, LEU 788	Pi-Alkyl
Phenalenone	MET 793	THR 854, GLY 796, THR 790, MET 1002, GLY 791,	Pi-Alkyl Pi-Sigma Carbon hydrogen bond